The discovery of several novel deflagellation genes and the identification of *ADF1*

by

Fabian Meili

B.Sc., Simon Fraser University, 2015

Thesis Submitted in Partial Fulfillment of the
Requirements for the Degree of
Master of Science

in the
Department of Molecular Biology and Biochemistry
Faculty of Science

SIMON FRASER UNIVERSITY

Fall 2015

Approval

Name:	**Fabian Meili**
Degree:	**Master of Science in Molecular Biology and Biochemistry**
Title:	***The discovery of several novel deflagellation genes and the identification of ADF1***
Examining Committee:	**Chair:** Dr. Fiona Brinkman Professor

Dr. Lynne Quarmby
Senior Supervisor
Professor

Dr. Michel Leroux
Supervisor
Professor

Dr. Michael Silverman
Supervisor
Associate Professor

Dr. Nancy Hawkins
Internal Examiner
Associate Professor

Date Defended/Approved: December 07, 2015

Abstract

Defective cilia, hair-like organelles that protrude from the cell membrane, cause diverse human diseases. The Quarmby lab previously used the unicellular alga, *Chlamydomonas reinhardtii*, to uncover three genes involved in the ciliary stress response known as deflagellation. They showed that defects in a related gene in humans underlie a severe form of juvenile onset polycystic kidney disease. We postulated that rare or subtle variants in additional disease genes could be uncovered by using a more sensitive genetic screen.

Armed with advances in whole genome sequencing and an enhanced enrichment protocol, we recovered multiple alleles of previously isolated genes and several alleles of three novel deflagellation genes. We identify the previously elusive ADF1 as TRP15, a putative cation channel activated by intracellular acidification. We also identify the novel deflagellation genes *ADF2* as a putative Ins(1,3,4)P3 5/6 Kinase, *ADF5* as FAP16 and *ADF4* as a glycosyltransferase exhibiting a novel starvation-specific deflagellation defect.

Keywords: Cilia; Flagella; Chlamydomonas reinhardtii; Deflagellation; Genetic Screen; Whole Genome Sequencing

Dedication

To my family for supporting me in seeing the world.

To my friends for making me feel at home.

Acknowledgements

I would like to thank all former members of the Quarmby Lab that helped and supported me throughout the years and provided me with a new home. This includes especially Laura Hilton, who taught me nearly everything I ended up applying in this thesis, as well as Julie Pike and Paul Buckoll who were long-term partners in crime. I would also like to thank Mette Lethan, Irene Qi, Kavisha Gunawardane, Freda Warner, Petra Szathmary, Fabian Garces, Shinako Takimoto and Evan Quon. I would also like to acknowledge all undergraduate volunteers who I've had the pleasure of supervising and who have themselves taught me a lot, namely Paul Mun, Andrea Hernández Rojas, Carmela De Jesus, Bisman Dhaliwal and Gregory Frick. I would like to thank my friends and family for their support and motivation, especially Albertina Wong, Chloe Gerak, Hailey MacDonald and Frank Lui, my father Daniel, my mother Edith and my sister Alexandra, without whom I would not be who I am today. Finally, I would like to give the biggest thank you of all to my supervisor, Lynne Quarmby. Thank you initially taking me up in your lab when I was just a green-faced 2nd-year student, thank you for fostering my scientific thinking and education and thank you for taking me then on as a Master's student and guiding me through the sometimes difficult graduate student lifestyle. I will always be grateful for the opportunities you have provided me with.

Table of Contents

List of Tables

List of Figures

List of Acronyms

At	*Arabidopsis thaliana* (mouse-ear cress, a flowering plant)
Cr/Cre	*Chlamydomonas reinhardtii*
Cv	*Chlorella variabilis* (a single-cell green alga)
Dd	*Dictyostelium discoideum* (slime mold, an amoeba)
Dm	*Drosophila Melanogaster* (fruit fly)
Dr	*Danio rerio* (zebrafish)
Gs	*Galderia sulphuraria* (a red alga)
Hs	*Homo Sapiens*
Lm	*Leishmania major* (a pathogenic protozoan)
Os	*Oryza sativa* (Asian rice)
Sb	*Sorghum bicolor* (a grass)
Sg	*Selaginella moellendorffii* (a vascular plant)
Ta	*Triticum aestivum* (wheat)
Tc	*Trypanosoma cruzi* (a parasitic protozoan)
Tv	*Trichomonas vaginalis* (a flagellated protozoan)
Zm	*Zea mays* (maize)
ADF1	The protein ADF1
ADF1	The gene *adf1*
adf1-1	The mutant strain&allele *adf1-1*
ADF	The acid-induced deflagellation phenotype, ADF

Introductory Image

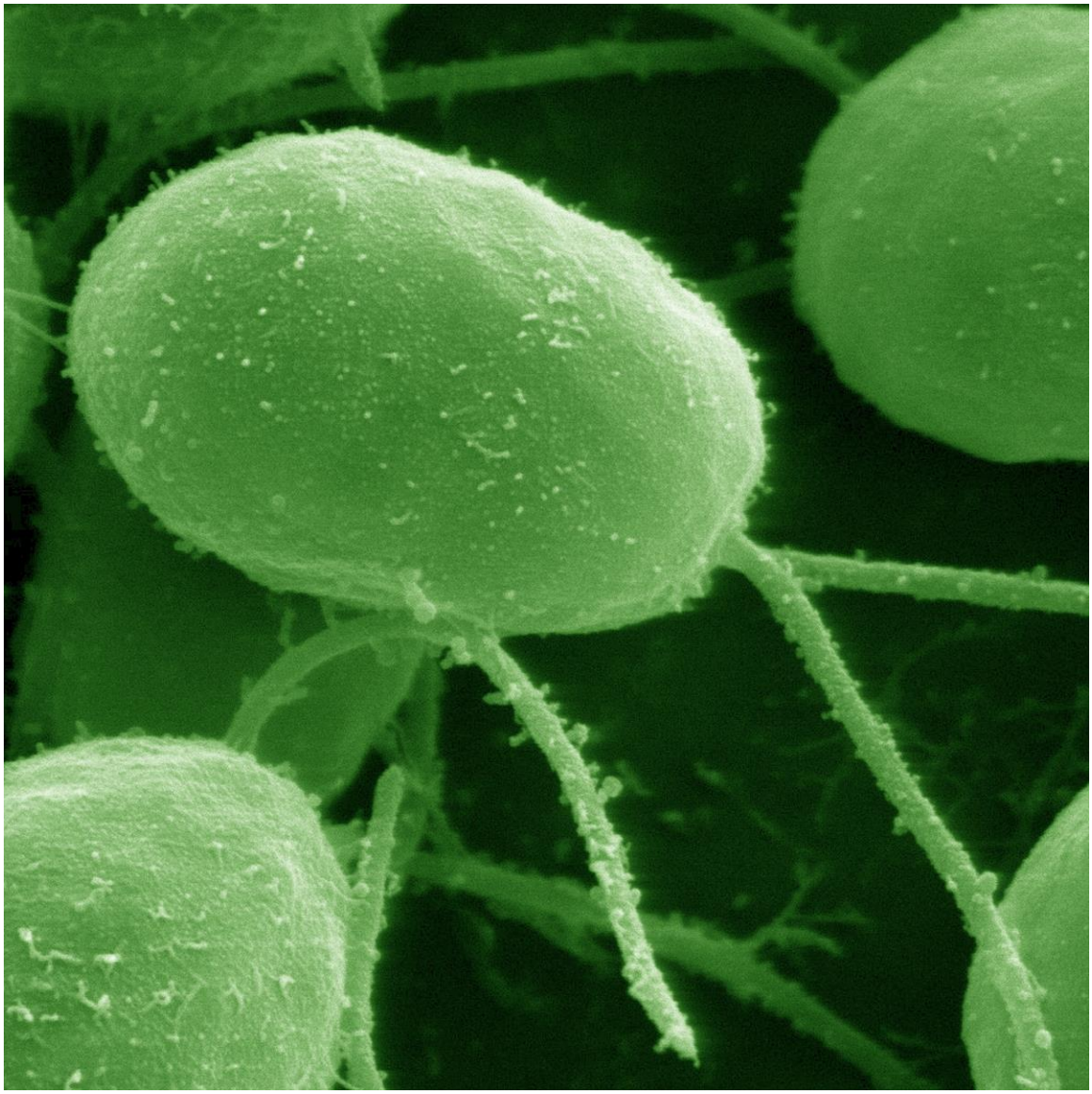

False-coloured scanning electron micrograph of *Chlamydomonas reinhardtii*
Note. Image by Louisa Howard (Dartmouth College)

Chapter 1. Introduction

1.1. Chlamydomonas reinhardtii

The unicellular eukaryotic alga *Chlamydomonas reinhardtii* is a model organism which is used for studying a variety of cellular processes. As cells can be grown in large volumes at room temperature and in a variety of simple media in only a short period of time, the organism lends itself to the study of the many cellular mechanisms and structures found to be conserved among eukaryotes. Furthermore, as the *Chlamydomonas* genome is haploid and only one fault copy of a gene needs to be present to induce a defect-dependent phenotype, it has become an established model organism for genetic studies.

Each *Chlamydomonas* cell possesses two prominent cilia, also known as flagella, which are microtubule-based organelles that protrude from the cell. The terms cilia and flagella are often used interchangeably in literature. As cilia is the more generic term for historical reasons, the term flagella will be used in this thesis when referring to *Chlamydomonas*. The cell uses its two flagella for both propelling itself forward as well as allowing rotating its cell body so photoreceptors in the *Chlamydomonas* eyespot can detect environmental light conditions (Yoshimura and Kamiya 2001; Hader and Lebert 2009). They also exhibit phototactic behaviour, as they will swim towards optimal light conditions (Nultsch 1977; Sjoblad and Frederikse 1981).

Chlamydomonas cells are able to reproduce both sexually and asexually. When cells are deprived of nitrogen, different types of the adhesion glycoprotein agglutinin are expressed on the surface of the flagella of each of two mating types called plus and minus and cells undergo gametogenesis (Quarmby 1994; Watanabe, Saijoh et al. 2003; Ferris, Waffenschmidt et al. 2005). When a plus- and minus-type gamete meet, the two flagella of each cell will adhere to each other via the agglutinins, inducing cell fusion.

During this process, a temporary quadriflagellate cell with two nuclei will form (also called a temporary dikaryon), before eventually undergoing zygote formation.

Green algae have also been of growing interest to the biofuels industry, as nitrogen-starved cells will accumulate large volumes of triacylglycerol, a biodiesel (Li, Han et al. 2010; Merchant, Kropat et al. 2012). Since cultures can be grown under fairly promiscuous liquid-media conditions and do not compete for land usage with traditional biofuel-producing plants, *Chlamydomonas* is a promising candidate to solve a looming energy crisis (Dismukes, Carrieri et al. 2008; Scranton, Ostrand et al. 2015).

Aside from its ease of culturing, *Chlamydomonas* possesses other features that make it a useful model organism. Its eyespot, which it uses to sense environmental light conditions, is one of the simplest photoreceptors and is used to study signal transmission after light detection. Channelrhodopsin-1 and -2 (ChR1 and ChR2), light-sensitive cation channels, were first isolated in *Chlamydomonas* and are at the forefront of the field of optogenetics (Nagel, Ollig et al. 2002; Nagel, Szellas et al. 2003). Nature's "Technique of the Year" 2010, this is a technique to study (often nerve) cells using light-activation. If virally delivered, Channelrhodopsins have been shown to propagate action potentials in response to light and can reinstate vision in mouse models of blindness (Doroudchi, Greenberg et al. 2011; Pulver, Hornstein et al. 2011; Tomita, Sugano et al. 2014).

Important findings in the study of flagellar microtubules have been made in *Chlamydomonas* as well. A flagellar stress response known as deflagellation (see Chapter 1.3) results in the severing and separation of flagella from the cell body, allowing the isolation of large amounts of isolated flagella. This in turn makes preparing large samples of this organelle comparatively easy. Because the structure of flagella is highly conserved amongst eukaryotes, *Chlamydomonas* is a prime model organism for studying microtubule dynamics and flagellar structure and function. If rapidly restored to normal growth conditions after deflagellation, *Chlamydomonas* cells regrow their flagella within 1-2 hours. This remarkable feat provides a unique opportunity to readily study the assembly of an organelle in a synchronized fashion on a large population of cells simultaneously. Studies of flagellar growth, also called ciliogenesis, have led to the

discovery of intraflagellar transport (IFT), the mechanism by which eukaryotic cilia are assembled, maintained and resorbed.

The uncovering of the structure of flagella in *Chlamydomonas* and the identification of a multitude of genes encoding flagellar proteins essential for proper flagellar function have also led to the discovery of homologous mammalian genes and shed light on their roles in other eukaryotes based on their role in *Chlamydomonas* (Li, Gerdes et al. 2004; Pazour 2004). Delta-tubulin, for example, was first identified in *Chlamydomonas* as the UNI3 gene and was subsequently shown to have a human homologue encoded by the TUBD1 gene, the product of which localizes to basal bodies, the microtubule-organizing centres at the base of cilia (Dutcher and Trabuco 1998; O'Toole, Giddings et al. 2003).

Studies analyzing both flagellar disassembly and assembly before and after cell division, where basal bodies transform to become nucleating centres known as centrioles, have led to a better understanding of the interaction between the cell cycle and flagella and have shown a role for flagella in its regulation (see Chapter 1.2.2).

1.2. Cilia

1.2.1. Structure

The structure of cilia is highly conserved among eukaryotes. As seen in figure 1.1, nine microtubule-doublets form a ring structure that extends to the end of a single cilium. Together with a central microtubule pair (CP), this forms a structure called the axoneme. An axonemal structure of nine doublets and a central pair is present in all motile cilia and is also referred to as the “9+2 axoneme”. This serves to distinguish it from a similar structure called the “9+0 axoneme” (Piasecki and Silflow 2009). This latter type of axoneme makes up the structure of non-motile or primary cilia, which often have a more sensory role than motile cilia. Figure 1.2 shows that these axonemes also consist of nine doublet microtubules forming an outer ring, but they do not possess a central pair. The structure at the base of the cilium is called the basal body (BB), which consists of nine microtubule triplets. Connecting the basal body and the 9+2 axoneme is an

electron-dense structure called the transition zone (TZ, Figure 1.3). This region forms a solid base for axonemal growth to occur. Strong connections between microtubule doublets and the cell membrane called Y-linkers also serve as a selective barrier between the flagellum and the cytosol. Because the flagellum is a highly specialized organelle, this barrier, also called the ciliary necklace, furthermore organizes which proteins are allowed to enter and leave the flagellum (Garcia-Gonzalo, Corbit et al. 2011; Reiter, Blacque et al. 2012). Connecting the outer microtubules of the 9+2 axoneme serve proteins called Nexins, while Radial Spoke Proteins are responsible for linking the central pair to the outer doublets. Because turnover at the plus-tip of a cilium is constantly ongoing, a process called intraflagellar transport (IFT) serves to transport tubulin and other cargo to and from the end at the tip (Marshall and Rosenbaum 2001).

1.2.2. Function of Motile and Primary Cilia

As the name suggests, one of the major roles of motile cilia is to provide a cell with the ability to swim towards a specific direction, be it a human sperm swimming towards an ovum or a *Chlamydomonas reinhardtii* cell looking for optimal light conditions. In the human lung, the beating of motile cilia does not move the cell, but serves to move the fluid overlying the cells, thereby clearing the lungs of particles. Studies have shown a correlation between ciliary dysfunction and moderate to severe asthma, where the cilia of asthma patients show structural defects (Thomas, Rutman et al. 2010; Jain, Javidan-Nejad et al. 2012). Mammalian cilia also possess some signaling capability. One example are the polycystin-1 and -2 proteins, which are responsible for sensing liquid flow in the human kidney and if defective can lead to the development of autosomal dominant polycystic kidney disease (Pazour, San Agustin et al. 2002; Wang, Zhang et al. 2007).

The discovery of the association between ciliary defects and kidney disease was one of the early driving forces that prompted further study of this previously poorly characterized organelle. Another factor was the discovery of their important role in signaling. Primary or sensory cilia host a wide range of important receptors and cell signaling molecules. The platelet-derived growth factor receptor (PDGFR), mutations in which can lead to cancer, components of the hedgehog pathway essential for proper

embryonic development such as Smoothened (SMO) or suppressor of fused (SUFU) are just some examples (May, Ashique et al. 2005; Schneider, Clement et al. 2005; Kim, Kato et al. 2009). The well-studied Hedgehog-signaling pathway as well as the regulation of the canonical WNT pathway, which is an important regulator of gene transcription, require an intact ciliary machinery (Rohatgi, Milenkovic et al. 2007; Lal, Song et al. 2008). In bones, cilia convert mechanical stress signals into appropriate anabolic metabolism responses to regulate skeletal development through a process called mechanosensation (Yuan, Serra et al. 2015).

Rod cells in the mammalian eye have a specialized non-motile cilium which hosts the photoreceptor protein rhodopsin (Imai, Kefalov et al. 2007). Bardet-Biedl syndrome, a type of congenital blindness with a variety of other symptoms, is caused by defects in any number of proteins that form part of a structure called the BBsome, which is a protein complex that associates at the base of cilia. Members of this complex play roles in microtubule polymerization, stability, acetylation and the export of signaling molecules out of the cilium. Mutations in *Chlamydomonas* BBS proteins lead to proper assembly of cilia but an accumulation of ciliary signaling proteins as well as the loss of phototaxis (Zaghloul and Katsanis 2009; Jin, White et al. 2010; Wiens, Tong et al. 2010; Zhang, Nishimura et al. 2013).

1.2.3. Cilia and the Cell Cycle

Cilia also play an important role in the cell cycle. When mitosis is initiated, the microtubule-organizing centre at the base of the cilium, the centriole, needs to be separated from the ciliary axoneme to transition to become a spindle pole, also known as the centrosome. The cell manages this by reabsorbing its axoneme prior to cell division. During cell division then, the centrosome is responsible for nucleating spindles and pulling apart the sister chromatids (Johnson and Porter 1968). While the effects of cell division on cilia have been known for many decades, the inverse effects of cilia on cell cycle regulation have only recently come to light. Early evidence for this came from studies performed in *Chlamydomonas*. IFT88, a component of intraflagellar transport, is necessary for proper spindle orientation and G1-S phase progression during mitosis, where it aids in transporting flagellar microtubule-binding proteins to the newly forming

spindle poles (Robert, Margall-Ducos et al. 2007; Delaval, Bright et al. 2011). Defects in the Tg737 gene, the mouse homologue of *Chlamydomonas* IFT88, have been shown to lead to the development of autosomal recessive polycystic kidney disease due to a shortening of primary cilia in the kidneys and the effect on cell cycle (Schrick, Onuchic et al. 1995; Pazour, Dickert et al. 2000). Ligand-binding to PDGFR can induce cell-division through the MAP/ERK pathway and in cells where ciliary assembly is abrogated PDGFR is localized to the cell body and ligand-binding and PDGFR-induced cell division is defective (Schneider, Clement et al. 2005).

Von-Hippel-Lindau (VHL) disease is caused by mutations in a tumour suppressor gene with the same name. Discovered as one of the rare hereditary disease known to induce cancer, kidney cells in VHL-patients often also lack functional cilia (Schermer, Ghenoiu et al. 2006; Pan, Seeger-Nukpezah et al. 2013). Evidence suggest that VHL plays a role in suppressing ciliary disassembly through the mammalian Aurora A Kinase (AURKA) and its *Chlamydomonas* homologue Aurora-like Kinase (CALK), a protein that induces disassembly. Lack of VHL activates AURKA/CALK as well suppressing Kinesin-II, both of which leads to an increase in flagellar disassembly (Pan, Wang et al. 2004; Pugacheva, Jablonski et al. 2007; Xu, Li et al. 2010). Because flagellar resorption is necessary for cell division and the absence of cilia is often a hallmark of cancer cells, activation of ciliary disassembly or inhibition of ciliary assembly may be a role in which cells regulate cell division and how ciliopathies may contribute to the development of cancer (Pan, Seeger-Nukpezah et al. 2013). The various impacts of ciliopathies then make studying microtubule dynamics in *Chlamydomonas* vital for enhancing our understanding of these processes.

1.3. Ciliary Dynamics

1.3.1. Intraflagellar Transport (IFT)

Two major families of conserved AAA-protein motors have been found to carry out the role of intraflagellar transport, which is the process that both delivers and removes tubulin-dimers and microtubule-associated proteins to and from the axonemal tip. Axonemal dynein transports its cargo from the plus tip of the flagellar microtubules

back to the minus end at the base of the cilia. *Chlamydomonas reinhardtii* possesses at least 14 different axonemal dyneins, which possess different rates of binding, affinity or speed (King and Kamiya 2009; Yagi, Uematsu et al. 2009). The selective binding of dyneins to axonemal microtubules and their movement along them also is what permits flagellar motility (Hook, Yagi et al. 2009). By regulating the location and timing of the power stroke and thus microtubule-sliding by dynein, the cell is able to introduce and resolve bends in the axoneme that serve to propel itself.

Also a type of ATP-utilizing motor protein, kinesins are essential for flagellar growth as they deliver new tubulin to the growing flagella. Depletion of the FLA10 protein, which encodes Kinesin-II, leads to no new tubulin delivered to the tip and flagella shorten and eventually disappear as a result (Kozminski, Beech et al. 1995; Scholey 2012). Recent studies have also shown that Kinesin-II is involved in the propagation of sensory signals, such as the induction of zygote formation upon agglutination through the cyclic nucleotide cAMP (Pasquale and Goodenough 1987; Johnson and Leroux 2010). Furthermore, mutations in the mammalian orthologue of *Chlamydomonas* Kinesin-II lead to apoptotic photoreceptor cell death due to the impaired transport of opsin and arrestin (Lopes, Jimeno et al. 2010).

1.3.2. Assembly

Flagellar assembly begins after a cell has exited the cell cycle (Rosenbaum and Child 1967). The first step for this is the delivery of the microtubule-organizing centre and protein components such as BBSome components of flagellar assembly to the site of the growing flagellum by components of IFT (Marshall and Rosenbaum 2001; Nachury, Loktev et al. 2007; Pedersen and Rosenbaum 2008). In *Chlamydomonas*, this growth begins from the basal body even before the daughters cells have been expulsed from the maternal cell wall (Umen and Goodenough 2001; Parker, Hilton et al. 2010). The growth of the central pair microtubules leads assembly of the flagellum, with outer microtubules only lagging shortly (~50nm) behind (Hoog, Lacomble et al. 2014). Given the average length of a fully-grown *Chlamydomonas* flagellum is 10000-14000nm (Wilson, Iyer et al. 2008), this is only a very minimal difference. The central pair at no point is in direct contact with the membrane of the growing flagellum (Hoog, Lacomble et

al. 2014) and the flagellar membrane is not structurally separated from the plasma membrane, as evidence by cell body proteins such as agglutinin being able to migrate to the flagellar membrane (Hunnicutt, Kosfiszer et al. 1990). It is thus hypothesized that the flagellar membrane extends ahead of the growing axoneme and is not pushed outwards by it directly.

Flagellar and cell body proteins, however, are separated by linkages between the basal body and the membrane to form a selective barrier and regulate entry and exit of proteins (Craige, Tsao et al. 2010). During growth, filaments link central pair, axonemal microtubules and the flagellar membrane, though clear structural components that link membrane and axoneme during flagellar growth have only been identified at the growing axonemal tip (Dentler and Rosenbaum 1977; Dentler 1980; Dentler 2013).

1.3.3. Disassembly

IFT is also required for pre-mitotic ciliary disassembly, a highly conserved process amongst eukaryotes (Plotnikova, Pugacheva et al. 2009). Cilia need to disassemble before cell division as the centriole at the base of the flagellum needs to be separated from the flagellar axoneme to become the microtubule-nucleating centre during cell division (Quarmby 2004; Parker, Hilton et al. 2010). The Quarmby lab has recently demonstrated that CNK2 provides a means for Chlamydomonas to sense flagellar length and regulate rates of disassembly, which was for a long time thought to be constant and length-independent (Marshall, Qin et al. 2005; Hilton, Gunawardane et al. 2013). CNK2, however, appears to only regulate disassembly, while not being the initial activator of it. The role of trigger in pre-mitotic resorption in *Chlamydomonas* is largely attributed to CALK, a homologue of human Aurora A kinase that is injected into the flagellum in response to mating between *Chlamydomonas* cells (Pan, Wang et al. 2004; Pugacheva, Jablonski et al. 2007). In addition to an increase in disassembly, there is also a counter-intuitive increase in the injection of IFT particles into the flagellum. Unlike being loaded with tubulin during assembly, they are, however, more often loaded empty to pick up flagellar components and transport them back to the cell body (Pan and Snell 2005).

Despite conservation of the ciliary disassembly mechanism, the timing of flagellar disassembly varies amongst organisms and cells between S-phase or G2/M transition, though the latter is more common (Rash, Shay et al. 1969; Rieder, Jensen et al. 1979). As cells progress into and through the cell cycle, the CDK2-cyclinE complex begins associating with the basal body as it is transforming and relocating into the centrosome and this linkage is thought to activate the complex and thereby DNA synthesis and centrosome duplication (Hinchcliffe and Sluder 2001). As cilia resorb, flagellar components are also recycled by being transported back into the cytoplasm for use during cell division or eventual flagellar assembly, as evidenced by the presence of endocytic transport at the base of the cilium and the localization of flagellar components at the centrosome (Coyne and Rosenbaum 1970; Robert, Margall-Ducos et al. 2007; Delaval, Bright et al. 2011; Ghossoub, Molla-Herman et al. 2011).

1.4. Deflagellation

1.4.1. Background

As mentioned previously, Chlamydomonas also possesses a second way of flagellar disassembly, the ciliary stress response called deflagellation. This mechanism has been exploited to provide science not just with an easy abundance of purified flagella to correlate structure, function and genetics, but also to study organelle assembly through ciliogenesis. In spite of its enormous contribution to ciliary biology and conservation amongst all eukaryotes in which the process has been looked at, the function and pathway of deflagellation itself is poorly understood.

In *Chlamydomonas*, deflagellation can be induced by pH-shock with a weak organic acid such as acetic acid or benzoate, which leads to a decrease in intracellular pH. Through an unknown mechanism this then mediates the influx of extracellular calcium and triggers deflagellation downstream. Alternatively, use of a membrane-permeabilizing agent such as a detergent or the anesthetic dibucaine can also trigger deflagellation, presumably by allowing the influx of extracellular calcium directly (Satir, Sale et al. 1976; Butterworth and Strichartz 1990; Quarmby and Hartzell 1994; Finst, Kim et al. 1998; Quarmby 2009; Nishikawa, Sakamoto et al. 2010). The decrease in pH

is required to occur intracellularly, as a decrease in extracellular pH by a strong acid that cannot permeate the non-polar cell membrane will not trigger deflagellation (Hartzell, Hartzell et al. 1993). This is also why only a weak, membrane-permeable acid can induce pH-shock mediated deflagellation. An unknown mechanism activated by the intracellular calcium signal then leads to the severing of the axonemal microtubules at a site distal to the transition zone called the Site of Flagellar Assembly/Autotomy, or SOFA (Figure 1.4).

Either calcium, an intermediary signal or the severing event itself then also leads to the transcriptional activation of various proteins involved in flagellar regrowth. Studies analyzing which signal is responsible to trigger the upregulation have been inconclusive (Davies and Grossman 1994; Thomas, Morle et al. 2010). Cells that are unable to shed their flagella still trigger the transcriptional upregulation of genes responsible for ciliogenesis and calcium has been implicated in transcriptional regulation of flagellar genes (Evans and Keller 1997; Liang and Pan 2013). *Chlamydomonas* however also begins reabsorbing its flagella in response to a deflagellation signal even when cells are unable to shed or in the absence of extracellular calcium (Cheshire and Keller 1991; Parker and Quarmby 2003), leaving it unclear whether it is the absence of flagella, calcium or a different signal that is responsible for transcriptional upregulation of ciliogenesis.

1-2 hours after severing, flagella will have regrown (Lefebvre, Silflow et al. 1980; Stolc, Samanta et al. 2005; Thomas, Morle et al. 2010). While deflagellation is much better studied in *Chlamydomonas* than other organisms, mainly due to being the prime model organism for the process, evidence for it also exists in other organisms. In epithelial and lung cells, cilia are shed in response to chemical stresses and associated with the increase of tight junctions and is hypothesized to be needed for increased transepithelial barrier function, while in sea urchin deflagellation induces increased thermoresistance (Casano, Roccheri et al. 2003; Quarmby 2004; Stadtlander 2006; Overgaard, Sanzone et al. 2009).

During *Chlamydomonas* cell division, we hypothesize that a similar event takes place. After cell fusion between cells of opposing mating types, flagella will begin to

shorten from the tip down by reabsorption of microtubule components. Once shortened, the Quarmby lab discovered that axonemal microtubules are severed at a different site, proximal to the transition zone, to expulse the electron-dense transition zone before mitosis (Figure 1.5) (Rasi, Parker et al. 2009; Parker, Hilton et al. 2010). This allows the centriole to transition to become a spindle pole serving cell division (Johnson and Porter 1968). Figure 1.6 schematically shows the differences between acid-induced deflagellation and pre-mitotic severing. Because both mechanisms involve microtubule severing, we hypothesize that at least some components of the flagellar severing machinery may be common to the two events. If this hypothesis holds true, this implies that discoveries made when studying deflagellation in *Chlamydomonas* may shed important insight into pre-mitotic severing and cell cycle control. While pre-mitotic severing in addition to flagellar resorption has only been shown in *Chlamydomonas*, all ciliated eukaryotic cells need to separate their transition zones from their basal bodies before cell division, a process that is not fully understood. We thus hypothesize that this pre-mitotic severing event is also required for other organism that possess as complex a ciliary transition zone as *Chlamydomonas* that cannot be disassembled as easily as the axoneme. Furthermore, cytoplasmic microtubules are also severed as cells as enter the cell cycle, and components of both axonemal and cytoplasmic microtubule severing might be shared (Shiina, Gotoh et al. 1995; McNally and Thomas 1998).

The microtubule-severing protein katanin has been implicated in both of these events, though no direct evidence exist (Lohret, McNally et al. 1998; Lohret, Zhao et al. 1999). Katanin is able to sever axonemes in vitro and microtubules in vivo. Katanin also plays a known role in cell-cycle progression where it mediates cytokinesis (Stoppin-Mellet, Gaillard et al. 2002; Panteris, Adamakis et al. 2011). As both these pathways involve a transition zone severing event, the Quarmby lab has long hypothesized that components of the deflagellation pathway also play a role in pre-mitotic resorption and the expulsion of the transition zone prior to cell division. This hypothesis is supported by immunofluorescence and axonemal severing assays experiments that show that a protein detected by an anti-human katanin antibody localizes to the *Chlamydomonas* basal body and deflagellation is impaired if the antibody is used (Lohret, McNally et al. 1998).

1.4.2. Previous Genetic Screen for Deflagellation Mutants

Twenty years ago, the Quarmby lab performed a genetic screen to isolate and identify genes involved in the deflagellation pathway (Finst, Kim et al. 1998). One mutant strain with a deflagellation defect had been isolated earlier, suggesting that the process of deflagellation was a bone fide cellular stress response. (Lewin and Burrascano 1983). *fa1-1* was discovered as a mutant that did not shed its flagella in response to ethanol, whereas wild-type cells would, though the causative gene was not identified yet (Lewin and Burrascano 1983). .

In the genetic screen published in 1998 then, mutant strains allelic to *fa1-1* were recovered, as well as alleles of two novel deflagellation genes, *ADF1* and *FA2*. The Quarmby lab also discovered that these three mutants had two distinct deflagellation-defective phenotypes. While *ADF1* mutant strains were able to shed their flagella in response to the membrane-permeabilizing detergent Triton X-100, they was unable to do so when treated with the weak organic acid sodium acetate. *FA1* and *FA2* mutants on the other hand were unable to deflagellate when treated with either agent. This difference then is also what prompted the naming of these three genes. ADF-mutants, for acid-deflagellation-mutants, do not deflagellate in response to treatment with acetic acid, whereas wild-type (WT) cells do. The second group of deflagellation-defective mutants, labelled FA for flagellar autotomy, do not deflagellate under any known condition (Figure 1.7) (Quarmby and Hartzell 1994). Treatment with detergent permeabilizes the cell membrane and allow for the influx of extracellular calcium (Hartzell, Hartzell et al. 1993). Because of this, the Quarmby lab hypothesized that ADF-genes are likely involved in initial acid-sensing or calcium-influx, a defect that can be overcome by inducing extracellular calcium influx by membrane permeabilization. FA-genes on the other hand are hypothesized to be involved in the downstream severing event, a defect which cannot be overcome the same way.

No second gene of the ADF-group was discovered and the identity of *ADF1* remained unknown. The additional discovery of *FA2* meant that there were now two genes in the group of FA-deflagellation mutants. They were later identified by the Quarmby lab as FA1, a scaffolding protein that localizes to the ciliary transition zone, and FA2, a NIMA-related kinase that localizes to the SOFA (Figure 1.8) (Finst, Kim et al.

2000; Mahjoub, Montpetit et al. 2002; Mahjoub, Rasi et al. 2004). Never In Mitosis/AuroraA (NIMA)-family members possess a role in cell cycle regulation, and *FA2 Chlamydomonas* mutants also are delayed in cell cycle progression. Evidence suggests that in addition to its essential role during axonemal severing, FA2 plays a non-essential role during G2/M-phase progression and post-mitotic flagellar assembly (Mahjoub, Montpetit et al. 2002).

1.4.3. Pathway

Figure 1.9 shows the deflagellation pathway as it was hypothesized before this thesis (Quarmby 2009).The numbers on the diagram correspond to processes as follows: First, cells are exposed to a weak organic acid, such as acetic acid (1). This weak organic acid is able to permeate the non-polar cell membrane and is protonated intracellularly, introducing an acidic intracellular pH (2). This activates the influx of extracellular calcium at the base of the cilium (3), leading to an initial increase in calcium concentration localized to the base of the flagellum (4) (Wheeler, Joint et al. 2008). This calcium-increase is a necessary step for deflagellation, as cells treated with acid in the absence of extracellular calcium fail to deflagellate (Quarmby and Hartzell 1994). Calcium-channel blockers such as cadmium (Cd^{2+}) or lanthanum (La^{3+}) prevent deflagellation upon pH-shock (4), further establishing the presence of a deflagellation-related ion channel in the pathway. The primary local increase in calcium at the base of the flagellum propagates a signal to the flagellum (5) and a secondary release of intracellular calcium stores (6). In the flagellum then, the severing event is ultimately triggered at the SOFA (7).

This severing event relies on the mobilization of calcium from intracellular storage on top of the influx of extracellular calcium. This was shown as pH-shock in the extracellular presence of the divalent cation ctrontium (Sr^{2+}) used instead of calcium can trigger acid-induced deflagellation, but permeabilization of the cell-membrane with detergent in the presence of Sr^{2+} instead of calcium cannot (Evans and Keller 1997). This suggests that pH-shock and the influx of an extracellular divalent cation (such as Ca^{2+} or Sr^{2+}) signals the release of calcium from an intracellular storage, which then in turn mediates the severing event. Without acid-induced influx of the extracellular ion, no

intracellular calcium release is triggered and no severing event occurs. Because the defect in ADF-mutants can be overcome by permeabilization of the cell membrane, which allows the influx of calcium by bypassing any hypothetical ion channel, it is thought that ADF-family members are involved in the initial steps of deflagellation, such as pH-sensing, calcium influx or localized calcium sensing (Finst, Kim et al. 1998). As even calcium influx by permeabilization of the cell membrane does not cause FA-mutants to shed their flagella at the SOFA, these proteins are thought to be components of the downstream flagellar signaling or severing apparatus.

In this thesis, I will present the design and results of a novel *Chlamydomonas reinhardtii* genetic screen for deflagellation-defective mutants. Using a high-throughput phototaxis enrichment protocol, PCR-based recombination mapping, whole genome sequencing and gene cloning, I isolated at least three novel deflagellation genes, all of which I was able to identify and rescue and will henceforth be known as *ADF2*, *ADF4* and *ADF5*. These genes encode a *Chlamydomonas* homologue of ITPK1, a predicted glycosyltransferase and the flagellar protein FAP16, respectively. After 20 years of remaining elusive, we also identify *ADF1* as TRP15, a predicted calcium-channel we hypothesize to be responsible for mediating the initial influx of calcium which triggers deflagellation. I also present evidence for a potential fourth and fifth novel deflagellation gene named *ADF3* and *ADF6*, though we were not able to identify them.

1.5. Figures

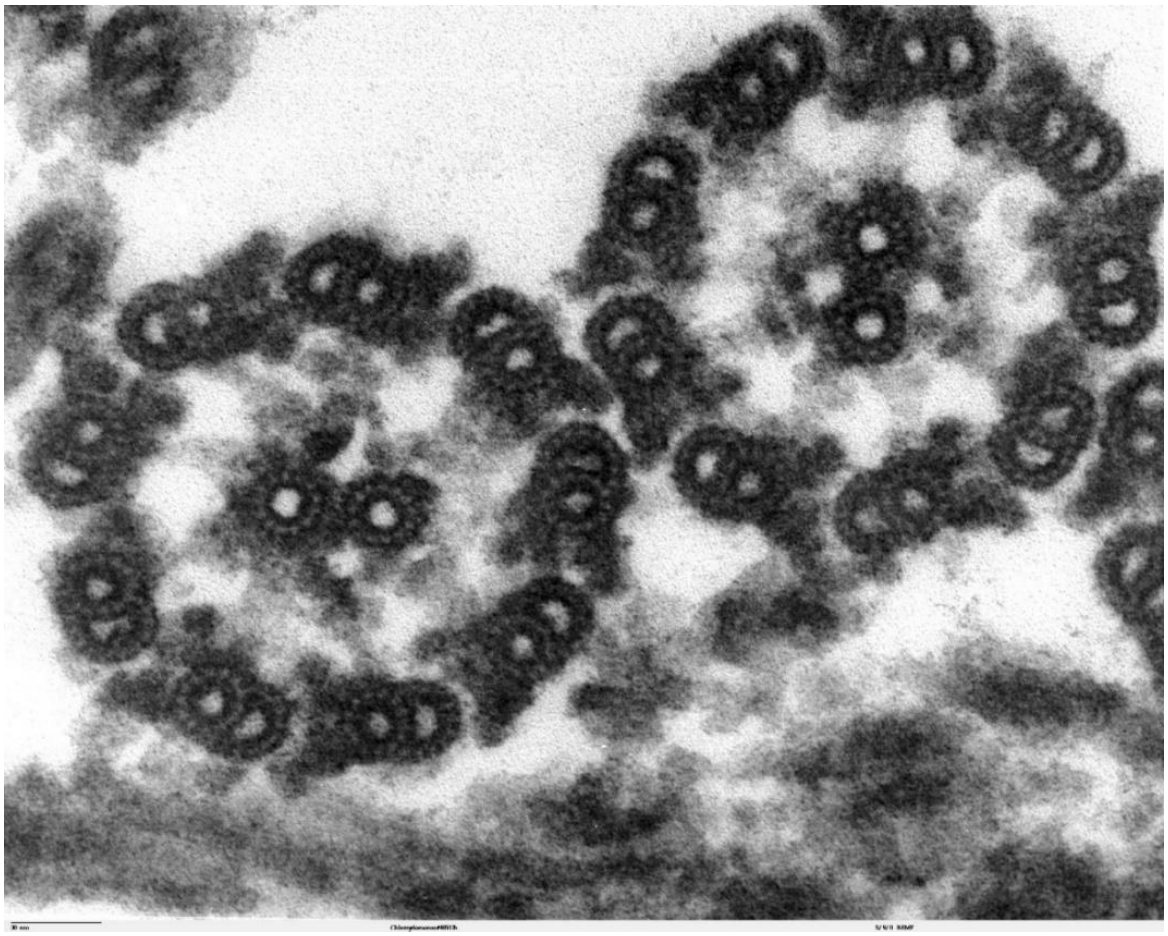

Figure 1.1. Electron micrograph of *Chlamydomonas reinhardtii* "9+2" axonemes
Note. Smith, E.F and P.A. Lefebvre (1996)

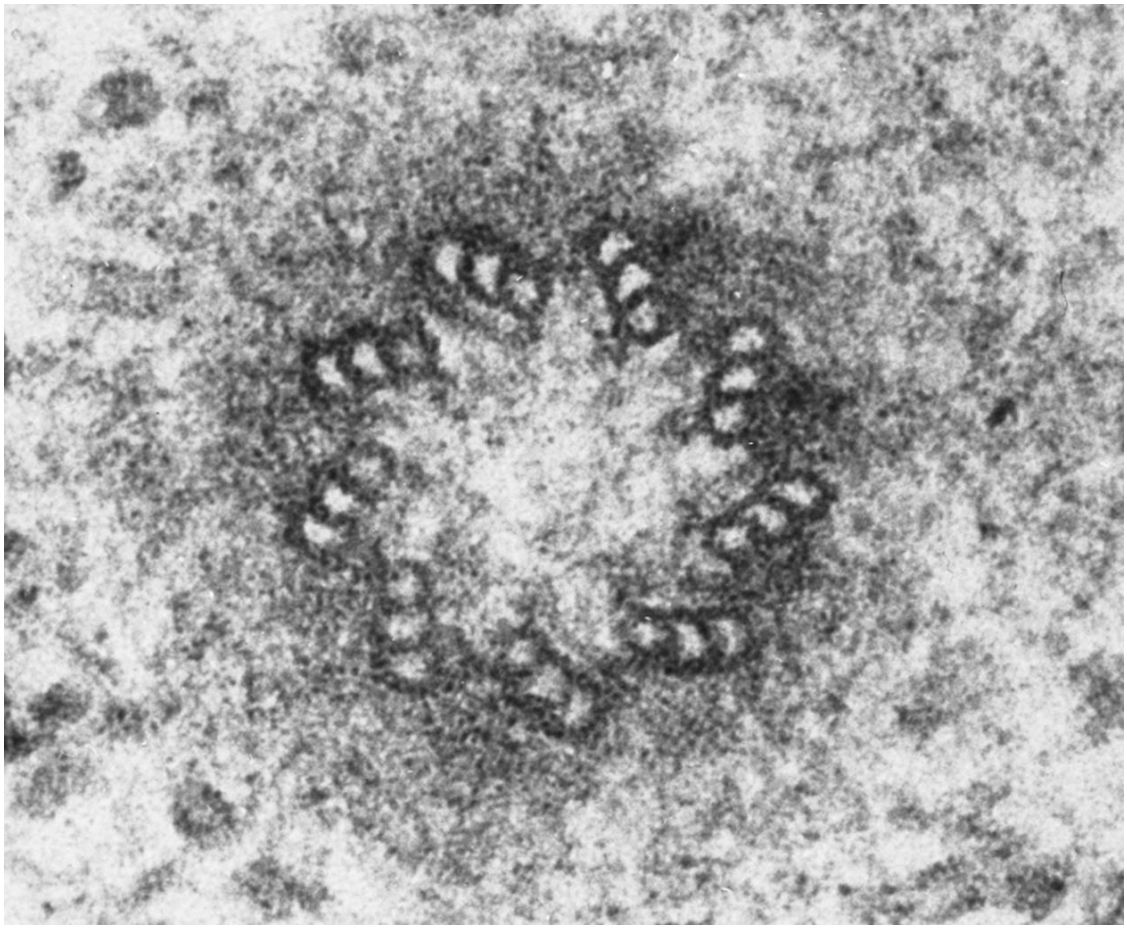

Figure 1.2. Electron micrograph of mouse epithelial cell “9+0” centriole

Note. © Breck Byers (U of Washington). Original resource Keith R Porter Archives (University of Maryland Baltimore County)

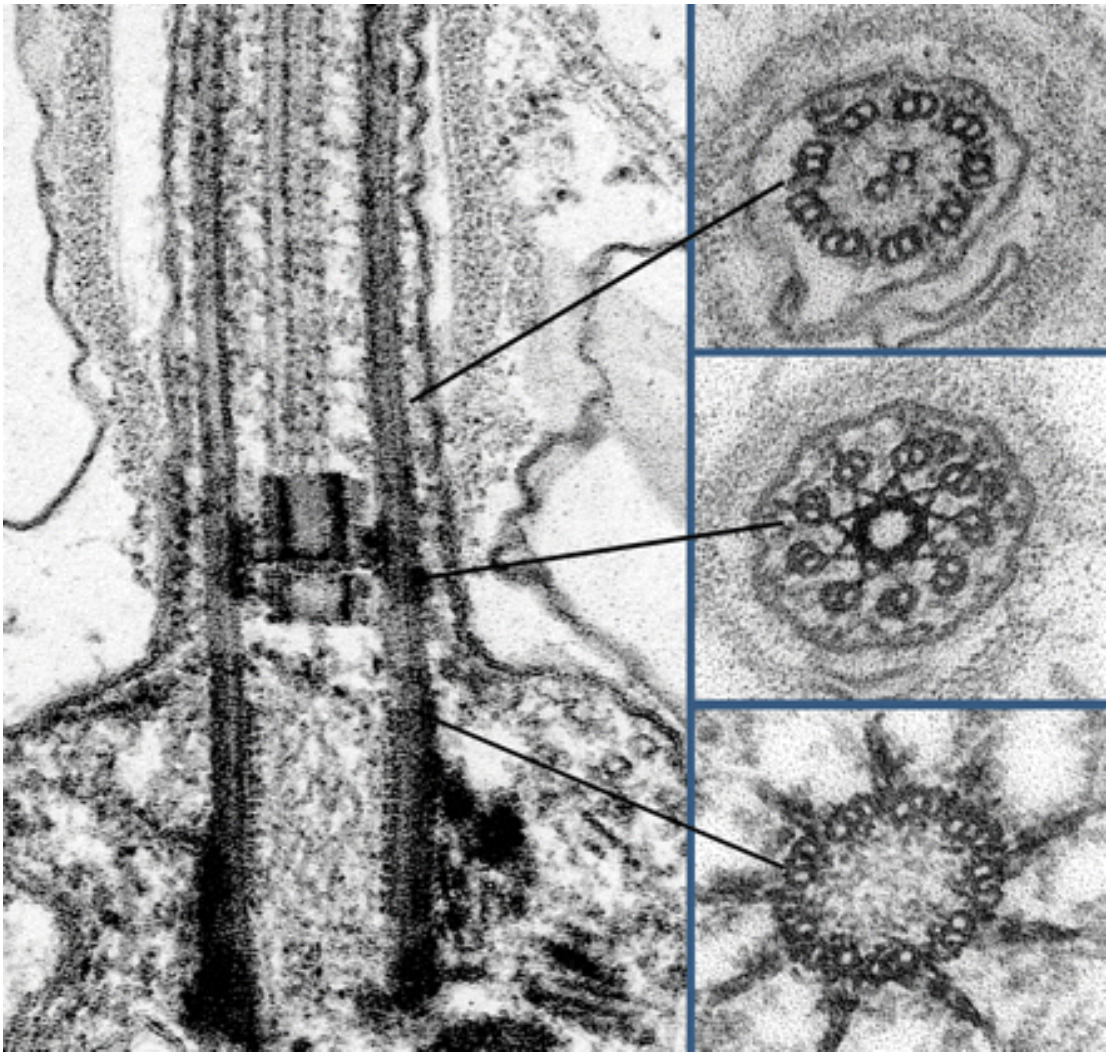

Figure 1.3. Electron micrograph of *Chlamydomonas reinhardtii* cilium

Note. Top: 9+2 axoneme. Centre: Electron-dense transition zone. Bottom: 9+0 basal body/centriole. Cover photo of Molecular Biology of the Cell, January 1, 2009, 20(1). Image by Brian P. Piasecki (University of Minnesota).

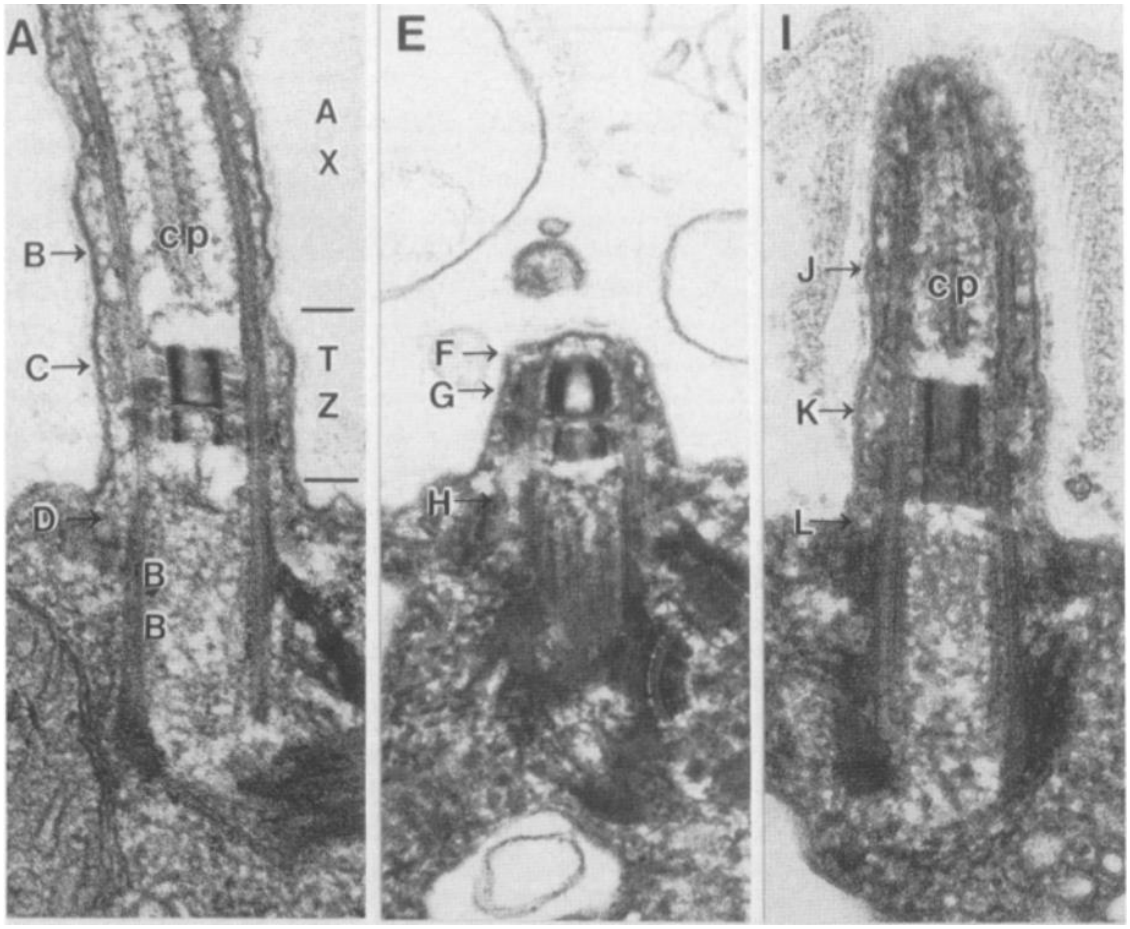

Figure 1.4. ***Chlamydomonas reinhardtii*** **cilium undergoing acid-induced deflagellation**

Note. Left: Before deflagellation. Centre: Immediately after deflagellation. Note intact, present transition zone (Arrow G). Right: Regrowing cilium. Source: Sanders, M. A., & Salisbury, J. L. (1989).

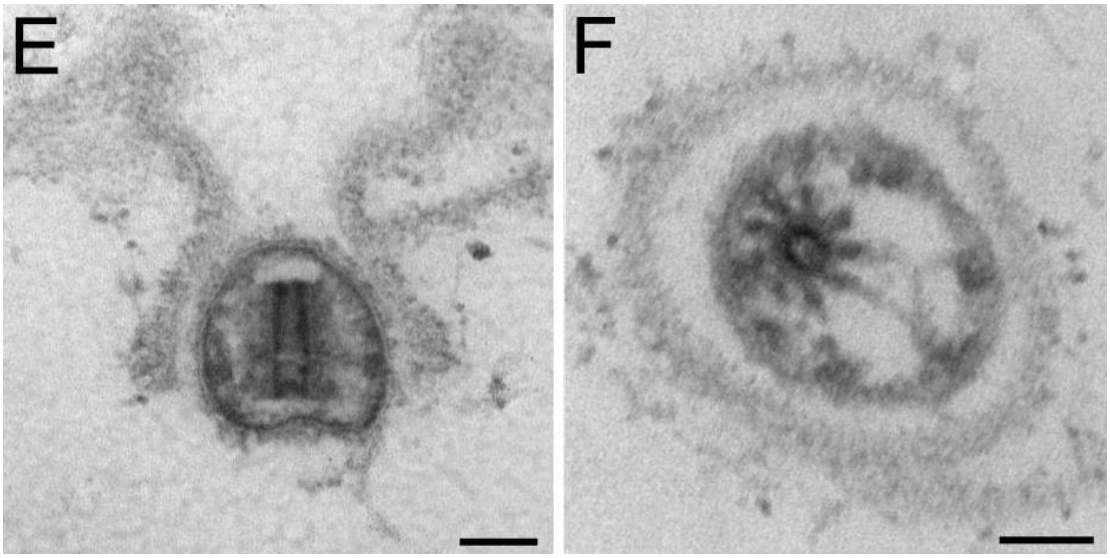

Figure 1.5. Expulsed *Chlamydomonas reinhardtii* transition zones before mitosis

Note. Source: Parker, J. K., Hilton, L. K., Diener, D. R., Rasi, M. Q., Mahjoub, M. R., Rosenbaum, J. L., & Quarmby, L. M. (2010).

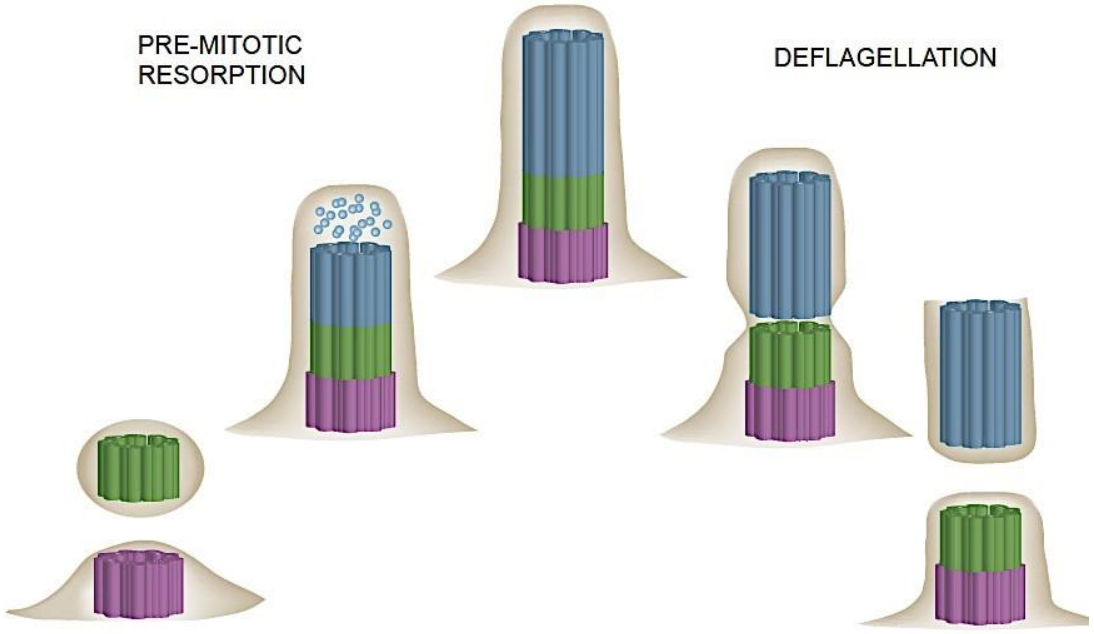

Figure 1.6. Schematic of pre-mitotic resorption vs. deflagellation

Note. Purple indicates the basal body, green the transition zone and blue the flagellar axoneme. Individual blue dots illustrate tubulin-dimer removal from the axoneme during flagellar resorption. Schematic by Laura Hilton, unpublished.

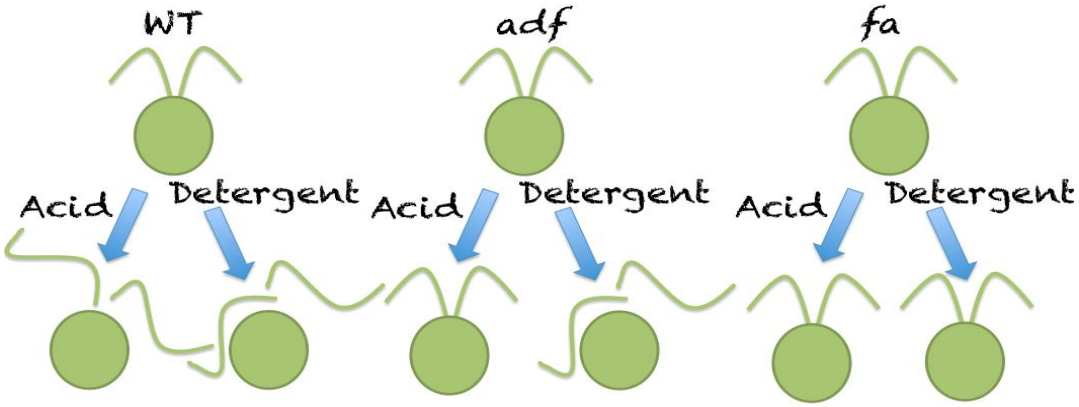

Figure 1.7. Schematic difference between ADF and FA mutants

Note. WT cells shed their flagella in response to acid and detergent. ADF cells only shed their cells in response to detergent, but not acid. FA cells shed their flagella under no known condition. Image by Julie Rodriguez (2013)

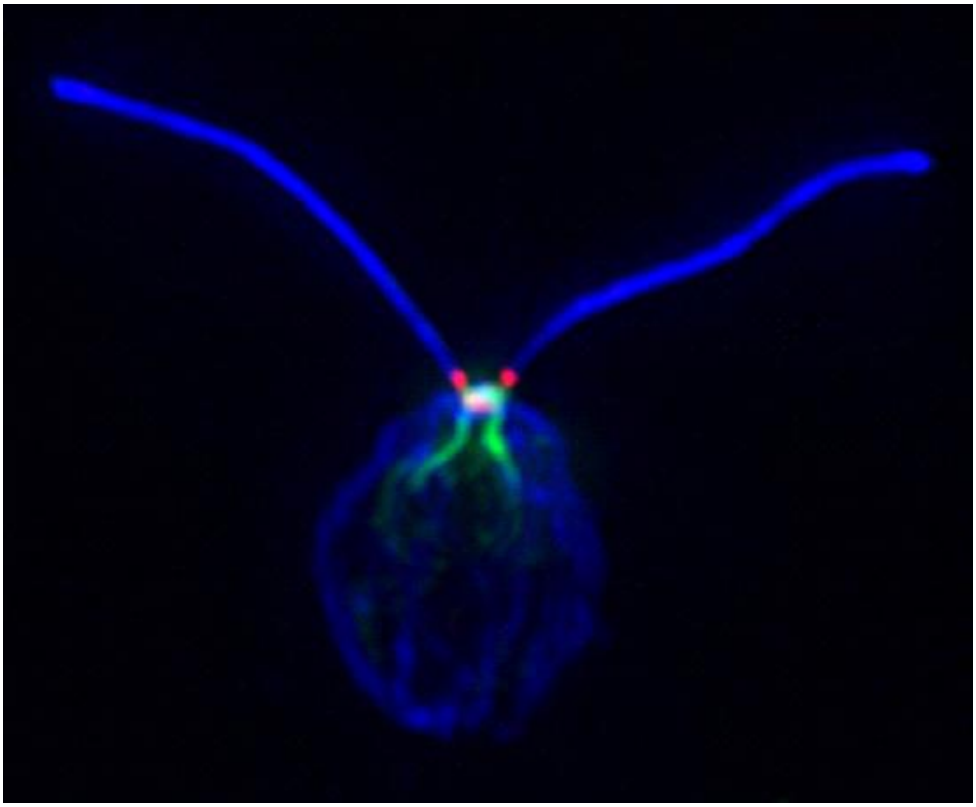

Figure 1.8. Localization of FA2 protein using Immunofluorescence

Note. Blue: anti-α-tubulin, Green: anti-centrin, Red: anti-FA2p-HA. Source: Mahjoub, M. R., Qasim Rasi, M., & Quarmby, L. M. (2004).

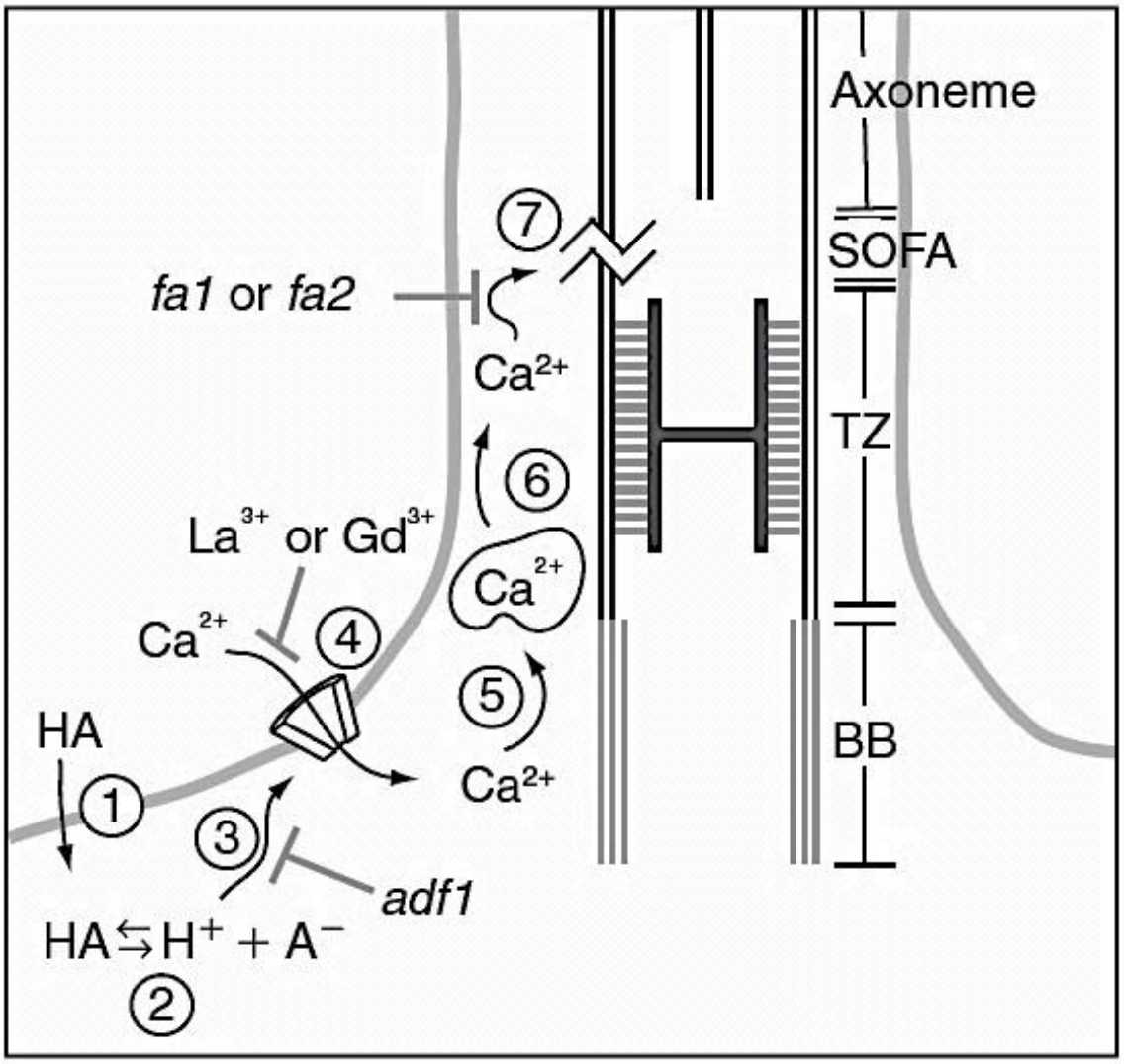

Figure 1.9. Schematic of hypothesized *Chlamydomonas reinhardtii* deflagellation signalling pathway

Note. Source: © Elsevier; *The Chlamydomonas Sourcebook*, Second Edition, 2009. Image by Lynne Quarmby

Chapter 2. A Novel Genetic Screen for New Deflagellation Mutants

I was the lead researcher for the genetic screen, assisted by summer students Paul Buckoll, Fabian Garces and Mihajilo Todorovic. Julie Rodriguez led the mapping and rescue of the adf2-1 mutant isolated in the screen, with assistance from me and Paul Buckoll. Paul also assisted in mapping E4.1P1H3/adf6-1 and our lab technician Irene Qi aided me in the rescue of adf4-1. Previous graduate student Mette Lethan and lab technician Freda Warner led the mapping of the isolated adf5-1 and adf5-2 mutants. A postdoc in the lab, Laura Hilton, aided in library preparation for whole genome sequencing and with the early phase of WGS data analysis.

As only two genes in the pathway had been identified previously (*FA1* and *FA2*), we were excited at the prospect of advances in whole genome sequencing being able to identify causative point mutations introduced by UV mutagenesis more readily, as had been done recently in *Chlamydomonas* (Dutcher, Li et al. 2012; Lin, Miller et al. 2013). Following the lead of Dutcher et. al. and Lin et. al, we were planning to narrow down WGS candidate genes by traditional genome-wide recombination mapping. We hoped to establish whether early hypotheses on signal transduction during deflagellation could be confirmed by identifying novel deflagellation genes responsible for functions that had to be present in this pathway, such as a calcium-sensor, a calcium-channel or a microtubule-severing protein. We reasoned that the previous screen failed to uncover mutations in any deflagellation genes besides *ADF1*, *FA1*, and *FA2* because either such mutations were rare (e.g. due to the small size of a gene or location in a particularly unsuited for the type of mutagenesis performed) and detection of mutants without enriching for them would inevitably not be productive, or that other genes in the pathway might have functions essential for cell survival. As such, unconditional essential mutants die after mutagenesis (Howell and Naliboff 1973). This was then also a key rationale for performing a novel genetic screen. Discovery of a gene essential for cell survival when

studying deflagellation could be because such a gene is also involved in the severing event during pre-mitotic resorption. With the prospects of possibly identifying essential genes, we conducted all enrichment and screening at the restrictive temperature of 33^{o}C. This was done because temperature-sensitive mutations in essential genes is the only way to isolate such mutant strains, as they will survive at the permissive temperature but exhibit a possible deflagellation-defective phenotype at 33C, presumably without dying due to not dividing during the limited time at the restrictive temperature.

We thus set out to conduct a new screen using a protocol to enrich for possible deflagellation mutants. As this would potentially increase the percentage of deflagellation-defective mutant cells in any assayed population, the odds of discovering even cells harbouring rare mutations would be increased. This was especially relevant as UV-mutagenesis introducing a temperature-sensitive mutations compared to a complete loss-of-function mutation was expected to be a rarer event. Furthermore, the number of potentially essential genes involved in deflagellation was likely to be much lower than the number of all genes present in the pathway. This would mean that isolating such mutant strains without enrichment would be even more difficult.

2.1. Background

The important role of calcium in a variety of cellular signaling pathway in eukaryotes and specifically in Chlamydomonas during mating or phototaxis had been known even before the previous screen in 1998 (Schmidt and Eckert 1976; Bessen, Fay et al. 1980; Goodenough, Shames et al. 1993). Because calcium-influx was also necessary to trigger deflagellation, the cell had to be able to distinguish the different kinds of calcium flux in different signaling contexts (Quarmby and Hartzell 1994). This was then the motivation for the previous screen, which tried to analyze how a cell is able to distinguish a calcium-signaling cascade as specific as the signal for deflagellation from other signaling roles of calcium, which it possesses even the context of flagella alone. If novel deflagellation genes were to be uncovered, this would shed light on this signaling cascade and the mechanism of deflagellation. More than 21,000 insertional mutants and 6,000 UV mutants were screened for deflagellation defects, resulting in five

new mutant alleles of *ADF1*, three new alleles of *FA1* and the isolation and discovery of four alleles of the novel deflagellation gene *FA2* (Finst, Kim et al. 1998). While both FA1 and FA2 were identified and localized over the next years, the identity of *ADF1* remained elusive (Finst, Kim et al. 2000; Mahjoub, Montpetit et al. 2002; Mahjoub, Rasi et al. 2004; Kirschner 2009).

2.1.1. Mapping the *ADF1* gene

The Quarmby lab was able to narrow the location of the *ADF1* gene down to a genomic region of ~500kb between 4.5mb and 5mb on Chromosome 9, close to the genetic markers for *PSBO/OEE1*, spanning a total of 42 predicted genes (Figure 2.1) (Kirschner 2009). Complex and poorly described reference DNA sequence in this region however complicated the identification of *ADF1*.

The genetic location of the causative gene was narrowed down using a technique known as PCR-based recombination mapping. A mutant strain is crossed with the highly polymorphic, but phenotypically wild-type reference strain S1D2 (Vysotskaia, Curtis et al. 2001). Multiple progeny are collected and screened for a deflagellation phenotype. If the cell is phenotypically mutant, the ~50% of its genome containing S1D2 DNA cannot contain the causative mutation, as the cell must have inherited it from its mutant parent. Conversely, if a cell is phenotypically wild-type for deflagellation, it cannot contain the causative mutation. Multiple PCR-markers that yield fragments of different sizes for S1D2 DNA and non-polymorphic DNA are known and were tested. If a marker is unlinked to the phenotype and thus the potentially causative gene, the recombination between the phenotype and the DNA approximates 50%, whereas linkage between the phenotype and a specific genomic region is indicated by a recombination percentage approaching 0. Once linkage between large chromosome regions and the deflagellation-defective phenotype is established, custom primers are designed to further narrow down the region.

The ~500kb region described above showed 0% recombination, complicating more precise mapping but establishing that the gene responsible must lie in this region (Kirschner 2009). A number of predicted genes in this region are either very large or very

small, and more than half lack any functional annotation or predicted domains. There is also a gap in sequence coverage that is estimated to be 55 kb in v5.0 of the *Chlamydomonas* genome.

2.1.2. *adf1-3* BAC Rescue Experiments

The Quarmby lab next attempted to rescue the mutant gene with several bacterial artificial chromosomes (BACs), each spanning different parts of the region (Figure 2.1). If a BAC containing just a handful of genes was able to rescue the deflagellation-defective phenotype, this would suggest that one of the genes contained on the BAC was responsible for the rescue and thus the elusive *ADF1* gene. Of the 42 predicted genes in the known *ADF1* region, 35 are covered by at least one BAC clone.

During transformation, Chlamydomonas reinhardtii cuts any foreign insert DNA by unknown endonucleolytic activity and randomly inserts the resulting fragments into various places in the genome (Zhang, Patena et al. 2014; Jinkerson and Jonikas 2015). During this process, DNA may also be lost to digestion, inverted or pieces of insert separated. DNA may also be gained as genomic DNA from cells lysed during transformation is integrated into the genome of another cell (Zhang, Patena et al. 2014).

Furthermore, some of the BAC clones were restriction digested before transformation in order to reduce the size of the plasmid-insert construct, as smaller constructs possess a higher transformation efficiency than larger ones, a behaviour reported in previous studies (Hanahan 1983; Kindle 1990; Shimogawara, Fujiwara et al. 1998). Transformations were performed on the *adf1-3* mutant strain and at least 250 transformants of each of the candidate BACs were then assayed for complementation and gene rescue. From all transformants screened, only one wild-type transformant was obtained from BAC 8981 digested with the restriction enzyme EcoRI, suggesting that *ADF1* might be encoded by one of 8 genes that were intact on this BAC clone (Figure 2.2) (Pike 2013).

We were, however, concerned with only obtaining one rescue strain out of more than 2000 transformants from DNA covering the potentially causative gene. This low rate of rescue left open the possibility that during transformation, a piece of BAC DNA

inserted into a separate gene, causing bypass suppression of the deflagellation-defect in *adf1-3*. This would phenotypically be indistinguishable from a rescue.

In the *adf1-3* rescue, antibiotic resistance did not co-segregate with the rescue of the deflagellation-defect, indicating that pieces of the insert must have landed in different locations in the genome. This also meant that detecting a potential suppressor gene by PCR-amplifying and sequencing the region to the sides of the antibiotic resistance DNA to detect which gene was interrupted would be difficult, as the potential suppressor could have been interrupted by any piece of insert DNA from the BAC. Indeed, novel mutations caused by insert DNA separating into multiple pieces during transformation appear to be common in Chlamydomonas, as in a previous study only ~50% of mutant phenotypes co-segregated with the resistance marker of the insert and the other 50% of mutant phenotypes must thus have been caused by insert pieces that were integrated somewhere else in the genome (Dent, Haglund et al. 2005).

Furthermore, trying to identify whether one of the genes on the BAC was transformed intact was also complicated, as the causative mutation in *adf1-3* was unknown and thus specifically amplifying a fragment containing only the healthy insert copy was not possible. We were thus left unsure whether we had obtained an *adf1-3* rescue or introduced a suppressor mutation. In this thesis, I describe how I address this problem through whole-genome sequencing of both *adf1-3*, to identify the causative mutation, and the *adf1-3* rescue/suppressor strain to test for the presence of a second, wild-type copy of the gene (Lin, Miller et al. 2013; Zhang, Patena et al. 2014).

2.2. Enrichment Screen Protocols

2.2.1. UV Mutagenesis

To mutagenize, $5x10^6$ 137c+ wild-type cells in a 100x15mm petri dish containing 20 ml of TAP were UV-irradiated for 3 minutes at 254nm with the lid off the petri dish from the top while under constant rotation on a shaker to allow equal levels of irradiation of all cells in the liquid. UV-mutagenesis was chosen over alternatives such as EMS or MNNG. This was because not only is ending the process of mutagenesis easier by

simply turning off the UV light source vs washing away the mutagen, it is also less dangerous for the user to deal with. Studies have also shown higher yield of mutants undergoing UV mutagenesis, especially when compared to EMS (Loppes 1970; Harris 2009). Furthermore, MNNG has been shown to introduce multiple mutations close to each other, which would make identifying a specific causative mutation or isolating a temperature-sensitive mutant more unlikely due to a higher potential of causing a null defect by the presence of two mutations in the same gene (Hawks and Lee 1976; Lee and Jones 1976).

The exact conditions of 3 minutes at 254nm were chosen after testing various exposure times for death rates, as too long of an exposure time tended induce cell death and no recoverable colonies, likely due to introduction of too many mutations. Cells were left in the dark for 24h to prevent photoreactivation and allow for the persistence of the mutations introduced (Cox and Small 1985), then transferred to light at 21°C for 18h to and then 33°C for 6 hours. Mutagenized cells were treated with 1.25X volume acid-deflagellation buffer, further referred to as ADB (Finst, Kim et al. 1998) for 45 seconds and the pH was neutralized with 0.1 M $NaHCO_3$. Cells were then pelleted by centrifugation and resuspended in 20 mL fresh TAP medium, after which cells were subjected to one of two enrichment and screening strategies.

2.2.2. Horizontal Enrichment and Manual Screening

For the first of the novel two screens, performed in the Summer of 2012, deflagellation mutants were enriched by using a light source to direct non-deflagellated phototactic cells to swim horizontally away from the pool of deflagellated wild-type cells (Figure 2.3). The hypothesis behind this was that cells that retained their flagella would phototax away from the strong light source, while cells without flagella would remain in place. The level of enrichment was quantified by testing the protocol using wild-type cultures spiked with a set ratio of deflagellation-mutant cells.

Channel plates were prepared by embedding P1000 micropipette tips in molten TAP medium containing 1.5% agar, then removing the tips to leave a channel in the hardened agar. One mL of fresh liquid TAP medium was added to each channel

immediately before use. ADB-treated and neutralized cells were pelleted and resuspended in 700 µl TAP, after which 40 µl was added to the centre of each channel, as adding them to one end resulted in trapping all the cell in the deeper imprint of the pipette-head and no yield. The cells were allowed to phototax away from a light source for 30 minutes, then the liquid at the tip was physically separated from the rest of the channel by inserting a microscope slide cover vertically into the agar. 100 µl of liquid was removed from each channel at the point furthest from the light source and spread onto 1.5% agar TAP plates. We hypothesized that only flagellated cells would be able to swim towards the tip and that this fraction would be enriched for deflagellation-defective mutants compared to the initial sample, a hypothesis that was supported by our proof of concept experiments.

After 4-6 days in continuous light at 21°C, individual colonies were picked and assayed by light microscope for ADF and FA phenotypes (see Materials & Methods). FA-mutants do not deflagellate when treated with either ADB or dibucaine, while ADF-mutants are only defective for acid-induced deflagellation (Quarmby and Hartzell 1994; Finst, Kim et al. 1998). This strategy produced 21 confirmed deflagellation mutants from 18,338 colonies screened (Table 2.1)

2.2.3. Vertical Enrichment and Spectrophotometer Screening

Although our proof of principle tests had indicated that a 10-fold enrichment was possible, the summer 2012 screen yielded an improvement of only 2.3-fold over the 1998 screen – an unsatisfactory result. To improve enrichment we revised our protocol for the continuation of the screen in the summer of 2013. Mutagenized and ADB-treated cells were pelleted, resuspended in 5 ml of a 3% sucrose solution in Sueoka's high salt medium (HSM) and underlayed below 5 ml of sucrose-free HSM (Harris 2009). This was meant to "trap" wild-type cells that deflagellated or bald cells in the sucrose layer, while only cells that retained their flagella would be able to swim vertically towards the top (Figure 2.4). A light source was placed underneath and cells were allowed to negatively phototax for 1 hour, then the top 4 ml of liquid was pipetted out. Early protocol tests using mutant-spiked cultures showed that a second iteration of this deflagellation-phototaxis procedure was necessary for optimal separation of deflagellation-defective

mutant strains. After the second cycle, the top 500ul of liquid was spread on 1.5% agar TAP plates and incubated in constant illumination at room temperature until single colonies were visible. These colonies were then picked, patch-plated and properly labelled.

A second innovation for the summer of 2013 was the addition of an automated assay (see Materials&Methods for detailed procedure) before performing a manual assay as done in the summer of 2012. The biggest advantage of this addition was the time-savings it provided and due to this, allowed for upscaling of our experiment. While four people performed thee first screen in 2012, two people were able to screen 1.5 times as many cells in the summer of 2013 mainly thanks to this automated step. A single well-plate yielded on average 3-5 candidate colonies requiring a manual assay out of 92 tested, while we would have had to assay all 92 without the spectrophotometer.

After colonies were inoculated from TAP patch plates, they were inoculated in 96-well plates containing 100ul of liquid TAP media for two days at 21C, then shifted to the restrictive temperature of 33C for 6 hours. Cells were then treated with the standard acid-shock protocol, neutralized and an initial absorbance reading was taken. After allowing cells to phototax for 30 minutes, the second absorbance reading was taken. Cells that were able to deflagellate when treated with ADB in a 96-well plate would accumulate at the bottom of the round-bottom well, while cells that retained flagella would swim towards the top and form a green ring on the edge of the well, a behaviour described in previous studies (Engel, Ishikawa et al. 2011). This led to measurable differences in absorbance readings between the before- and after-phototaxis readings. A sample spectrophotometer output analysis is shown in table 2.2. Potential mutants were then re-assayed manually by light microscope and out of 28,210 colonies screened by spectrophotometer, 17 deflagellation mutants were recovered (Table 2.1). A schematic of the two different enrichment protocols is shown in figure 2.5.

We evaluated the value of our two screens (horizontal enrichment with manual screen and vertical enrichment with automated and manual screen) by comparing the ratio of confirmed deflagellation mutants recovered to the total number of mutagenized colonies screened between our enrichment-based screen and the un-enriched UV-

mutagenesis screen from Finst et al., 1998. The original screen recovered 3 deflagellation mutants from 6000 colonies screened (a ratio of 1:2000), whereas our horizontal enrichment screen recovered 21 deflagellation mutants from 18,338 colonies assayed (a ratio of 2.3:2000), for a 2.3-fold enrichment. To our surprise and disappointment and in spite of promising proof of principle experiments, the vertical enrichment strategy only produced a 1.2-fold enrichment and 17 deflagellation mutants from 28210 colonies assayed (a ratio of 1.2:2000).

It is possible that the spectrophotometer-based screening method and/or the double-enrichment strategy reduced the efficiency of mutant recovery in this second screen. Our experiments using a spiked culture might have not been truly representative of the ability of all deflagellation-defective strains to swim, but specific to the *adf1-2* strain being a particularly good swimmer. That we might have inadvertently eliminated some deflagellation-defective mutants by using our enrichment protocol might be especially true if strains with mutations in the deflagellation pathway retain their flagella, but possess defects in phototaxis response or motility. This loss of phototactic ability and/or motility has previously been shown to be the case for mutant strains of other flagellar components such as the BBsome, the kinesin subunit FLA10 or the axonemal central pair protein Hydin (Kozminski, Beech et al. 1995; Lechtreck and Witman 2007; Zhang, Nishimura et al. 2013).

Isolated mutants were subjected to preliminary phenotype characterization using pH shock and dibucaine at 21^{o}C and 33^{o}C. Mutants that deflagellate in response to dibucaine but deflagellate poorly in response to pH shock were classified as ADF, while mutants that deflagellate poorly in response to either treatment were classified as FA. Mutants that deflagellated more at 21^{o}C vs 33^{o}C were categorized as temperature sensitive (ts).

2.3. Allele Assignments

2.3.1. Temporary Dikaryon Complementation

Each new ADF mutant isolated from the screen was tested to determine whether it was a potential allele of *ADF1* or potentially a novel ADF gene. To begin, we performed dikaryon complementation assays (see Materials&Methods) If the dikaryons deflagellated (complementation) we categorized the mutants as belonging to a separate complementation group, if the dikaryons failed to deflagellate (non-complementation) we categorized the mutants as belonging to the same complementation group. These dikaryon assays uncovered that at least four of the new mutant isolates belong to complementation group *ADF1*. We also established one mutant strain belonging to each of complementation group *ADF2* and *ADF4*, as well as two strains of complementation group *ADF5*.

We did not perform dikaryon assays for any of the FA mutants we isolated because the Quarmby lab previously showed that the FA defect cannot be complemented in a dikaryon (Finst, Kim et al. 1998). Instead, new FA isolates from the horizontal enrichment screen were crossed with both *fa1-4* and *fa2-2*, and the progeny screened for the presence of wild-type deflagellation. If both *fa1-4*/*fa2-2* and the tested progeny contained mutations in the same gene, then only mutant progeny would be obtained, as between the two strains there was no healthy copy of the gene. If however they contained mutations in different genes, then during meiosis recombination would result in a ratio of 1:2:1 between mutant:wild-type:*fa1-4*/*fa2-2* and thus half the progeny would be phenotypically wild-type. The lack of wild-type progeny after crosses with just one of the two known FA-strains indicates that we have isolated three new alleles of *FA1* and four new alleles of *FA2* (Table 2.3). It is important to note that we did not uncover any novel FA genes.

2.3.2. Mapping

For the mutants that are not alleles of *ADF1*, we next performed recombination mapping using the Chlamydomonas mapping kit to narrow down the location of the

causative mutation in the genome (Vysotskaia, Curtis et al. 2001). This mapping uncovered that *ADF2* is linked to marker CNA34 on chromosome 2 (Figure 2.6) and *ADF4* is linked to marker PPX1 on chromosome 9 (Figure 2.7). More specific linkage to ~150kb from the beginning of chromosome 9 was established using a custom marker (Figure 2.8). The phenotypes of two strains, E3.1 P15 B4 and E21 C7 (of complementation group *ADF5*), are tightly linked to marker TUG on chromosome 6, indicating that they may be allelic (Figures 2.9 and 2.10). We could not establish linkage between E4.1P1H3 (complementation group *ADF6*) and E5.1P8A12 and any of the mapping kit markers (Figures 2.11 and 2.12). The summary of mapping and temporary dikaryon analysis is shown in table 2.4.

Surprisingly, we found that some mutations that were determined by dikaryon analysis not to belong to complementation group *ADF1* are tightly linked to *PSBO*, which is tightly linked with *ADF1*. We performed further dikaryon assays and established three complementation groups linked to *PSBO* with five strains in group I, four strains in group II, and one strain in group III. A detailed breakdown of mapping and temporary dikaryon results is shown in table 2.5. It remained possible that some of this complementation was intergenic. We therefore proceeded with whole-genome sequencing to identify causative mutations and determine the number of distinct ADF genes in this region.

2.4. Whole Genome Sequencing Identifies Candidate Causative Mutations

Previous studies had shown that the use of whole genome sequencing (WGS) was an effective way to determine potential causative mutations in cases when supplemented with PCR-based recombination mapping to narrow the search to a genomic region (Dutcher, Li et al. 2012; Lin, Miller et al. 2013). Our hope was that only one potentially causative mutation would be closely linked to the phenotype and that we would be able to thus identify it. If multiple closely linked candidate mutations were found, custom markers against them analyzed for recombination would then give us final clues, as the recombination between the causative gene and the deflagellation-defect should be 0%.

To identify candidate causative mutations, we first performed WGS on eleven new mutant isolates and the *adf1-3* rescue strain. We first employed two different WGS library prep and sequencing strategies: 1) Illumina MiSeq 150 bp paired-end (PE) sequencing and NEBNext Ultra library prep (PE) and 2) Illumina HiSeq 101 bp PE sequencing using a commercial library prep (see Materials&Methods for details). While overall genome coverage was higher in the HiSeq run, in some difficult-to-sequence regions of the genome, like the *ADF1* region, coverage is higher in the MiSeq results (Figure 2.13). It was possible that the polymerase used in the library preparation kit employed for the MiSeq sequencing was better at amplifying these difficult-to-sequence, high-GC regions than the commercial library preparation used for the first HiSeq run. The importance of library preparation choice on WGS success is known in the literature from studies in other organisms and its impact is considerably larger than the choice of sequencing platform (Solonenko, Ignacio-Espinoza et al. 2013; Head, Komori et al. 2014). Because of this we performed a third run of HiSeq 126 bp PE sequencing using the library preparation previously used in the MiSeq experiment to hopefully achieve more uniform coverage over difficult-to-sequence regions such as *ADF1.* We sequenced additional mutant strains and re-sequenced some strains that had missing coverage in the first HiSeq run. This second run of HiSeq using our own library preparation had coverage more similar to the MiSeq run than the first HiSeq run (Figure 2.13). We thus conclude that to achieve the highest coverage for a difficult-to-sequence region in *Chlamydomonas*, the platform used (MiSeq vs HiSeq) is less important than careful library preparation, a similar finding to studies in other organisms.

A variant analysis pipeline as described in Materials&Methods was applied to process the MiSeq and HiSeq outputs and create a list of variants present in each strain. Since it is already known that the parental strain (CC-125) contains a large number of variants relative to the *Chlamydomonas* reference genome (Lin, Miller et al. 2013), the list of variants for each mutant strain was compared to other mutant strains from the same experiment, and identical variants were removed, producing a greatly reduced number of candidate variants. In the strains sequenced by HiSeq, approximately 15-20% of the variants are unique to each strain, while MiSeq identified a lower number of total variants, but a higher percentage of unique variants (26% and 37%). The summary of the read and variant analyses are shown in tables 2.6 and 2.7.

Since the deflagellation defect is not linked to any of the standard mapping kit markers in E4.1P1H3 and E5.1P8A12, we began by eliminating potential causative mutations from the WGS results if they were close to any mapping kit markers. This strategy left us with only a handful of candidate mutations for E4.1P1H3 and E5.1 P8 A12. We next designed custom PCR mapping markers for each of these candidate mutations and tested each marker for linkage to the deflagellation phenotype. However, we were unable to identify any candidate mutations that were linked to the deflagellation phenotype in either of these strains. A summary of all possible causative mutations identified by whole genome sequencing are shown in table 2.8.

2.5. Materials & Methods

2.5.1. Cells and Deflagellation Assay

The wild-type 137c mt+ (CC-125, wild-type) and S1D2 mt- strains (CC-2290) were obtained from the Chlamydomonas Resource Center at the University of Minnesota. Cells were maintained on solid tris-acetate-phosphate (TAP; Harris 2009) plates containing 1.5% agar at 21°C and under constant illumination. The *adf1-2* and *adf1-3* strains were isolated in the previous genetic screen (Finst, Kim et al. 1998) and are also available from the Chlamydomonas Resource Center.

ADF and FA phenotypes were determined as follows: First, 1.25:1.0 unit ratios of acid-deflagellation buffer (ADB) to cells or 1.0:1.0 unit ratios of dibucaine to cells were mixed for 45 seconds (Harris 2009; Nishikawa, Sakamoto et al. 2010). Initially, the detergent Triton X-100 was used as in previous studies (Finst, Kim et al. 1998), but flagella proved to be more difficult to see under light microscopy, which prompted our switch to use dibucaine. Both however induce the same membrane-permeabilization and deflagellation (Witman 1986). Then, cells were fixed with 1 unit of 3% Glutaraldehyde. 100 cells were assayed by light microscope for flagellation in at least three separate experiments and the percentage of flagellated cells after each treatment was compared to cells simply fixed in a 1.0:1.0 unit ratio with 3% Glutaraldehyde. Deflagellation-percentage was determined by:

(Flagellated before - Flagellated after) / (Flagellated before *100%)

This value was then compared to deflagellation of wt cells and known ADF and FA mutants. ADF-behaviour is characterized by lack of deflagellation using ADB, but deflagellation using dibucaine. FA-behaviour is characterized by lack of deflagellation using both ADB and dibucaine. Wt cells will deflagellate using both ADB and dibucaine (Quarmby and Hartzell 1994; Finst, Kim et al. 1998). In figures, statistical significance/p-values are indicated by the number of *s, where * = $p<0.01$, ** = $p<0.001$, etc.

2.5.2. Temporary Dikaryons

After gametogenesis is induced in Chlamydomonas cells by nitrogen-starvation, cells of opposite mating types (plus and minus) are able to mate. Since we used a plus-type parental strain for mutagenesis, all of our mutant progeny was also plus-type, as they had not undergone sexual reproduction and could not have changed their mating type. When a plus- and minus-type cell mate, they begin fusing after 15-30 minutes and will form a cell with two nuclei and four flagella: a temporary dikaryon (Luck, Piperno et al. 1977). These dikaryons persist for up to two hours, after which flagella are resorbed and cells form a zygote to undergo meiosis. Because temporary dikaryons also share their cytoplasm, soluble proteins interchange between the two cells. If two cells thus have two different defective proteins, the healthy copy from the partnering cell will be added to the shared cytoplasm and the temporary dikaryon ends up with two healthy copies of both mutated proteins.

This rescue of mutant phenotypes with temporary dikaryons is possible for *ADF1*-mutants, but not *FA1* or *FA2* (Quarmby and Hartzell 1994; Finst, Kim et al. 1998). The specific reason for this is unknown, though as both FA1 and FA2 later revealed to be localized to the transition zone, a compartment whose proteins cannot freely exchange with the cytosol, this might explain the inability of a second, healthy copy to rescue the phenotype (Finst, Kim et al. 2000; Mahjoub, Montpetit et al. 2002; Chih, Liu et al. 2012). The healthy protein might simply be unable to leave the transition zone of the first cell to translocate to the transition zone of its partnering cell. Furthermore, the time

for synthesis of new protein to be transported to both transition zones might be too short, given resorption and the initiation of meiosis begins two hours after mating.

2.5.3. PCR-based recombination mapping

The Kit for Molecular Mapping of Chlamydomonas Genes version 1.1 (Chlamydomonas Resource Centre, University of Minnesota) was used for PCR-based recombination mapping, using the standard protocol provided by the kit (Vysotskaia, Curtis et al. 2001). Additionally, custom primers for Cre09.g386731 (Forward: 5'-AAGTACGACTACGGCGAGGA-3', Reverse: 5'-AGCTCTTGTACTCGTCCTCCA-3') were used to link *ADF4* to a more specific genetic locus and to narrow down candidate genes. A mapping kit template with locations of all genetic markers was prepared by BLAST-ing the primer sequences of all mapping kit markers against the *Chlamydomonas* v5.0 genome and setting the marker position appropriately on the genomic map containing the 17 reference Chromosomes of *Chlamydomonas.* The mapping kit marker *YPTC4* did not BLAST to the location on Chromosome 2 indicated by the mapping kit – we did thus not assign it an exact genomic location. 0% recombination between a marker and the deflagellation-defective phenotype (recombination indicated in red on figures) indicates very tight linkage of a marker to the potential causative gene while numbers approaching 50% indicate no linkage. Recombination between adjacent markers was calculated as well. Lower numbers of recombination between markers (indicated in blue on figures) may be due to either tight linkage between markers or a low number of strains used to observe recombination events.

2.5.4. Automated Spectrophotometer Assay

After 4-6 days in continuous light at 21°C, individual colonies were inoculated into 96-well plates containing 100ul TAP. They were grown for 2 days at 21°C, followed by 6 hours at 33°C. To establish the baseline density of motile cells, absorbance at 510nm was measured before treating wells with 1.25X volumes of ADB for 45 seconds and pH neutralization with 0.1 M $NaHCO_3$. Cells were then left to phototax above a bright light

source for 30 minutes, after which another absorbance reading was taken. The relative change in absorbance was calculated as follows:

$$\frac{A_{510}° - A_{510}'}{A_{510}'}$$

Where $A_{510}°$ = absorbance before deflagellation and A_{510}' = absorbance after deflagellation and phototaxis. Reference absorbance readings of 137c mt+ (fully deflagellated) and an established ADF-mutant (E20 G2 from the vertical enrichment screen) were used to establish that any isolate for which the change in absorbance was greater than 0.3 was flagged for confirmation via a manual deflagellation assay.

2.5.5. Whole Genome Sequencing

The Illumina MiSeq library was prepared using the NEBNext Ultra kit and run on the SFU Illumina MiSeq, while we sent samples for the first HiSeq run to Genscript (Piscataway NJ, USA) for commercial library preparation and sequencing. The second HiSeq run was prepared using the NEBNext Ultra kit and sequenced by HiSeq by The Centre for Applied Genomics (The Hospital for Sick Children, Toronto ON, Canada).

Given the 60% GC-content and repetitiveness of the *Chlamydomonas* genome, we decided on using sequencing with fragment sizes of at least 100bp, to hopefully eliminate as much sequencing bias as we could. While this required larger amounts of genomic DNA, this was not an issue given the ease of extracting genomic DNA from *Chlamydomonas* by simple chloroform extraction.

The MiSeq and HiSeq outputs were processed as follows: The reads were aligned to the reference genome (*C. reinhardtii* v5.0 assembly) using Bowtie2 and BWA-MEM and each analyzed for single-nucleotide variants (SNVs) and indels via the Genome Analysis Toolkit (GATK) Haplotypecaller and samtools mpileup (Li, Handsaker et al. 2009; McKenna, Hanna et al. 2010; Langmead and Salzberg 2012; Jo and Koh 2015). All four variant files were then combined into one and analyzed for overlapping variant calls. Variant calls were filtered for homozygous mutations using SnpSift with the exception of the *adf1-3* Rescue strain, which was filtered for heterozygous mutations to

detect a potential second, wild-type copy of the gene that might have rescued the mutation. Variant calls were then annotated SnpEff for predicted impact severity of mutations (stop codons, splice site mutations, amino acid substitutions, synonymous mutations or UTR/Intron mutations) and using the Chlamydomonas v5.0 assembly of the Join Genome Institute's (JGI) phytozome.net for gene names and predicted functional domains using PFAM, KEGG, Panther and GO annotations (Cingolani, Platts et al. 2012; Goodstein, Shu et al. 2012).

2.6. Figures

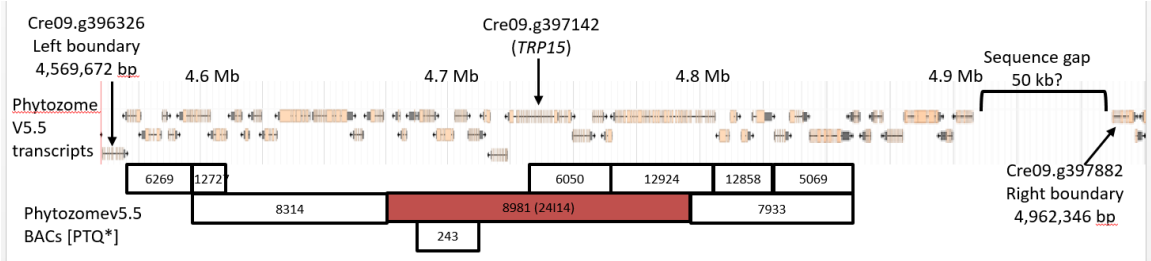

Figure 2.1. Boundaries of *ADF1* region and BACs covering predicted genes

Note. Genomic region illustrated by Joint Genome Institute's JBrowse on www.phytozome.net. Indicated are gene predictions at the top and BACs covering genes in this region and corresponding numbers at the bottom. Highlighted in red is BAC 8981/24I14, which gave rescue to the *adf1-3* rescue. Also indicated is Cre09.g397142/*TRP15*/*ADF1*.

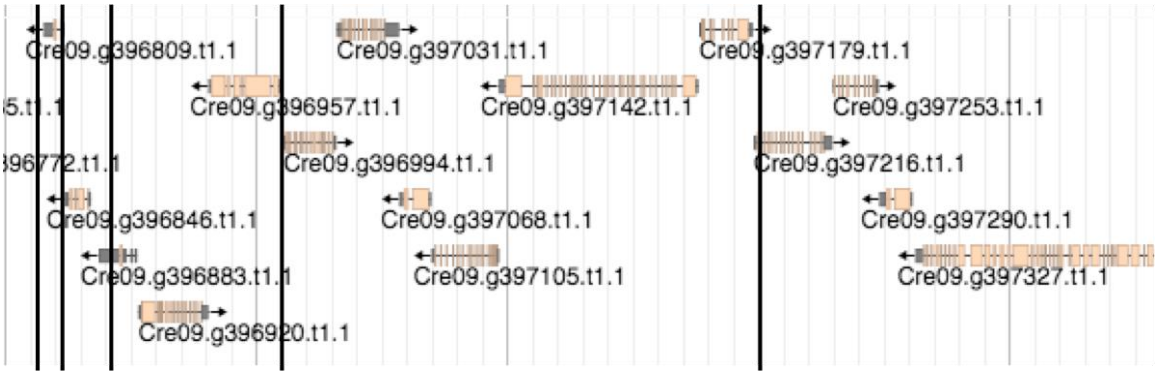

Figure 2.2. Gene predictions on BAC 8981/24I14

Note. Indicated are gene predictions from the *Chlamydomonas* v5.0 assembly present on BAC 8981/24I14. Black lines indicate EcoRI restriction sites, as the BAC that gave rise to the *adf1-3* rescue was digested. Image by Julie Rodriguez (2013)

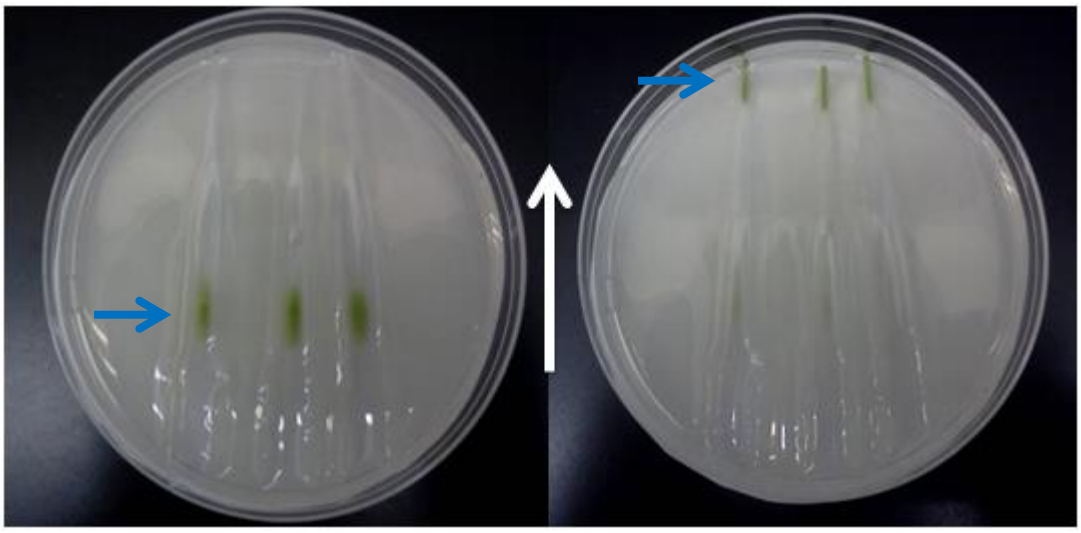

Figure 2.3. Horizontal Phototaxis in Channel plates

Note. White arrow indicates direction of phototaxis, blue arrow points towards location of cells before and after phototaxis. Left plate contains wild-type cells 30mins after acid-shock and neutralization, right plate contains adf1-2 cells 30mins after acid-shock and neutralization.

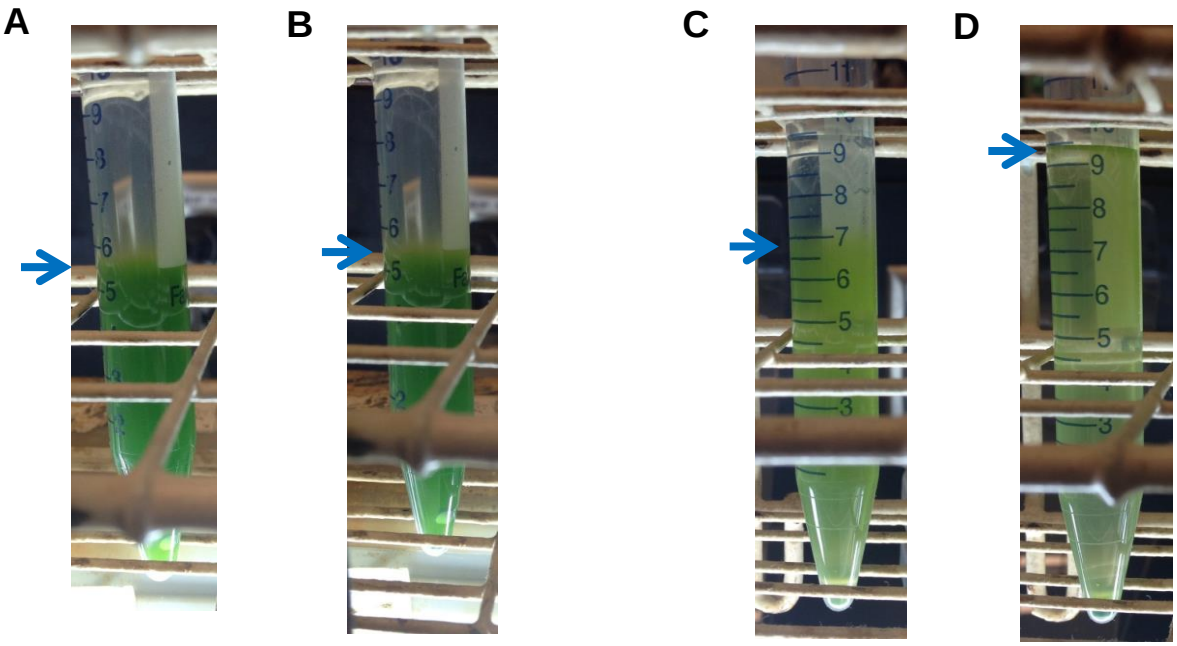

Figure 2.4. Experimental Setup of vertical phototaxis enrichment assay

Note. Blue arrows indicate top detectable cell levels. Wild-type before (A) and after (B) treatment with ADB. E20G2 ADF-mutant cells before (C) and after (D) treatment with ADB. Cells were allowed to phototax, G2 cells can escape sucrose trap whereas wild-type cells cannot. Blue arrows in pictures A&C also are representative of the interface between the HSM- and the sucrose-layer.

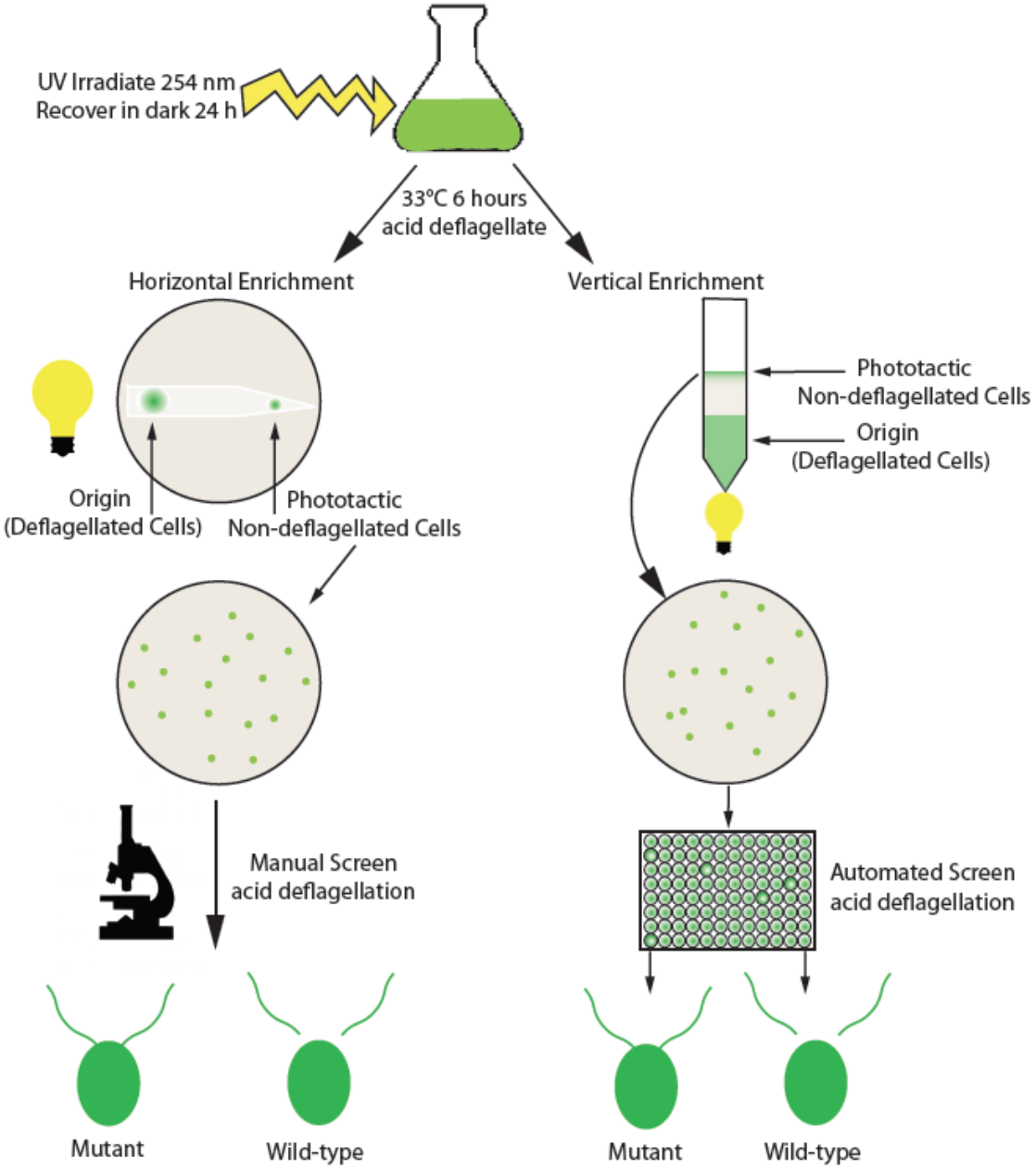

Figure 2.5. Schematic comparing horizontal and vertical enrichment protocols

Note. Horizontal enrichment protocol (left) was followed for the first screen, Vertical enrichment protocol was followed for the second screen. Highlighted in 96-well schematic are presumed deflagellation-wild-type cells (green centre dot) and potential deflagellation mutants (green outer ring) which were selected for manual screen. Diagram by Laura Hilton (unpublished)

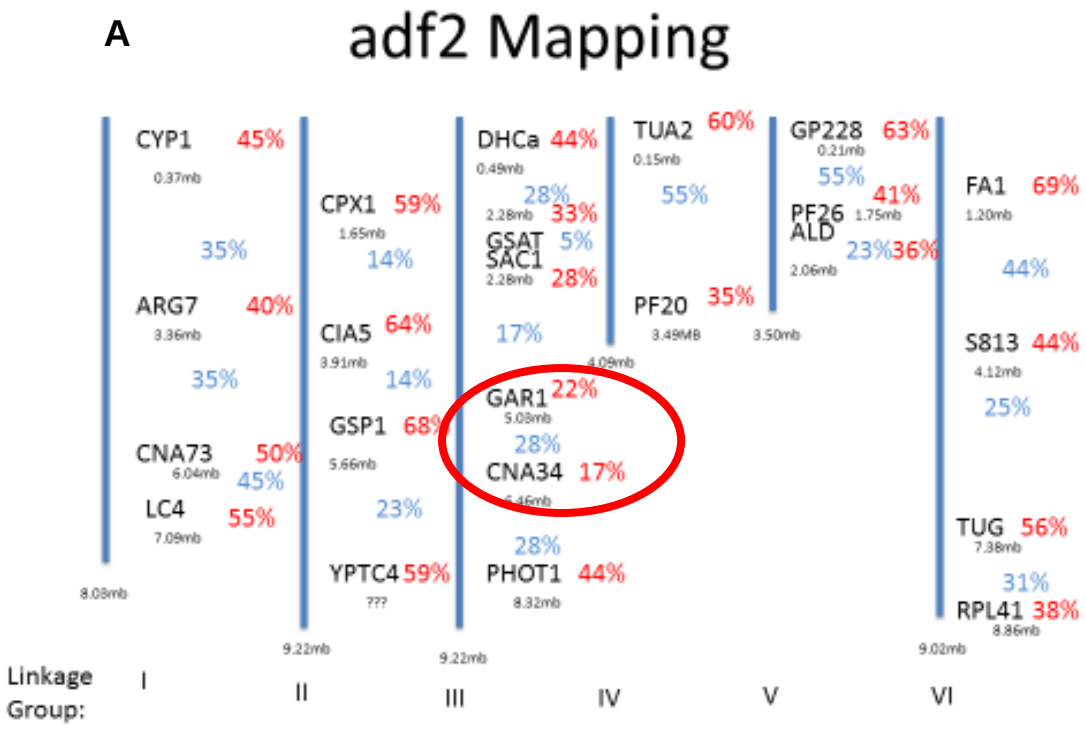
A
adf2 Mapping
CYP1 45%
0.37mb
35%
ARG7 40%
3.36mb
35%
CNA73 50%
6.04mb
45%
LC4 55%
7.09mb
8.08mb
CPX1 59%
1.65mb
14%
CIA5 64%
3.91mb
14%
GSP1 68%
5.66mb
23%
YPTC4 59%
???
9.22mb
DHCa 44%
0.49mb
28%
2.28mb 33%
GSAT 5%
SAC1
2.28mb 28%
17%
GAR1 22%
5.08mb
28%
CNA34 17%
6.46mb
28%
PHOT1 44%
8.32mb
9.22mb
TUA2 60%
0.15mb
55%
PF20 35%
3.49MB
4.09mb
GP228 63%
0.21mb
55%
PF26 41%
1.75mb
ALD
23% 36%
2.06mb
3.50mb
FA1 69%
1.20mb
44%
S813 44%
4.12mb
25%
TUG 56%
7.38mb
31%
RPL41 38%
8.86mb
9.02mb
Linkage Group:
I
II
III
IV
V
VI

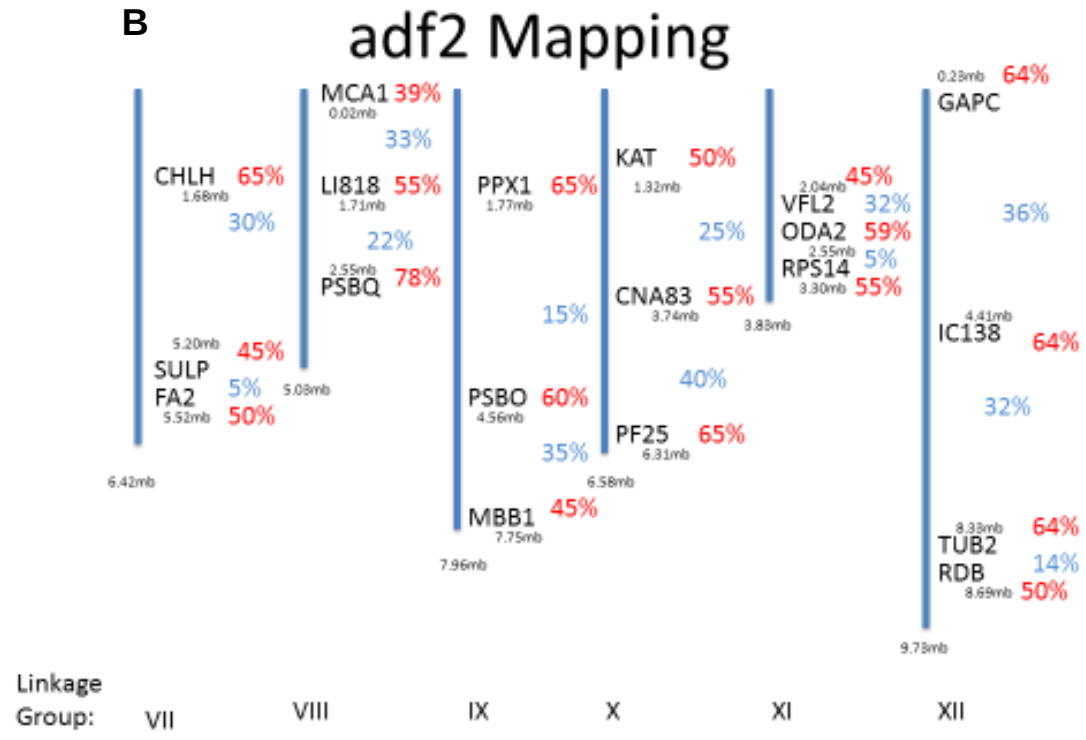
B
adf2 Mapping
CHLH 65%
1.68mb
30%
5.20mb 45%
SULP
FA2 5%
5.52mb 50%
6.42mb
MCA1 39%
0.02mb
33%
LI818 55%
1.71mb
22%
2.55mb
PSBQ 78%
5.08mb
PPX1 65%
1.77mb
15%
PSBO 60%
4.56mb
35%
MBB1 45%
7.75mb
7.96mb
KAT 50%
1.32mb
25%
CNA83 55%
3.74mb
40%
PF25 65%
6.31mb
6.58mb
2.04mb 45%
VFL2 32%
ODA2 59%
2.55mb
RPS14 5%
3.30mb 55%
3.83mb
0.23mb 64%
GAPC
36%
4.41mb
IC138 64%
32%
8.33mb 64%
TUB2
RDB 14%
8.69mb 50%
9.73mb
Linkage Group:
VII
VIII
IX
X
XI
XII

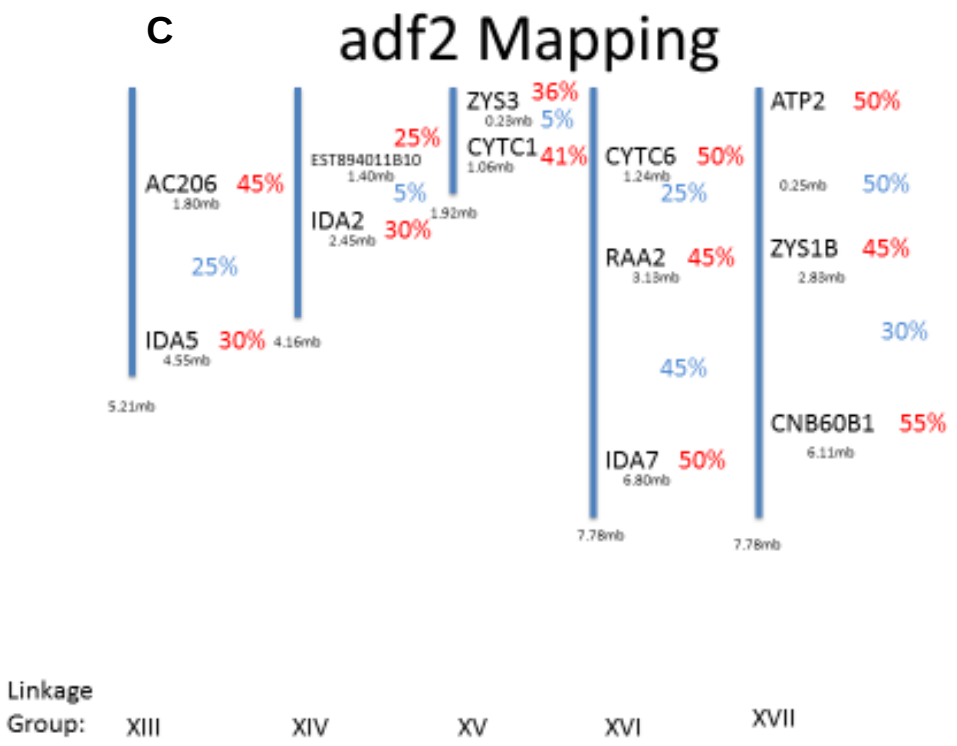

Figure 2.6. ***ADF2*** **PCR-based recombination map**

Note. Panels A-C show *Chlamydomonas* linkage groups I to XVII. PCR-based recombination markers from the *Chlamydomonas* mapping kit and their coordinates are indicated. In red is percent recombination between the deflagellation-defective phenotype and the corresponding marker. In blue is the recombination between two adjacent. Red circle indicates linkage to mapping kit marker found.

A

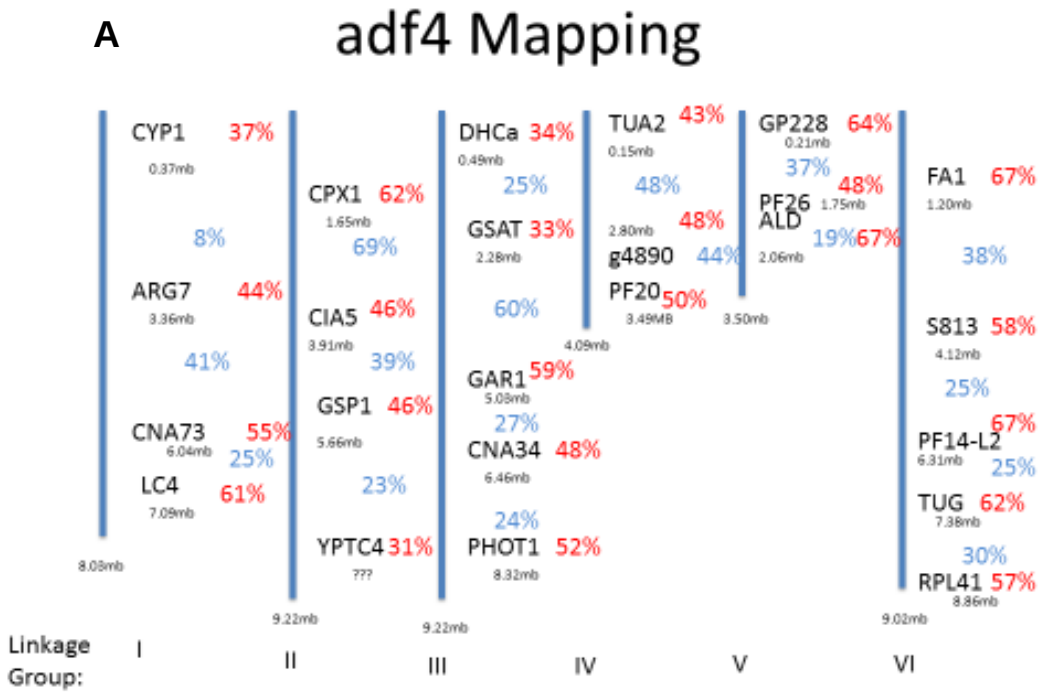
adf4 Mapping
CYP1 37%
0.37mb
8%
ARG7 44%
3.36mb
41%
CNA73 55%
6.04mb
25%
LC4 61%
7.09mb
8.08mb
CPX1 62%
1.65mb
69%
CIA5 46%
3.91mb
39%
GSP1 46%
5.66mb
23%
YPTC4 31%
???
9.22mb
DHCa 34%
0.49mb
25%
GSAT 33%
2.28mb
60%
GAR1 59%
5.08mb
27%
CNA34 48%
6.46mb
24%
PHOT1 52%
8.32mb
9.22mb
TUA2 43%
0.15mb
48%
2.80mb
48%
g4890 44%
PF20 50%
3.49MB
4.09mb
3.50mb
GP228 64%
0.21mb
37%
48%
PF26 1.75mb
ALD
19%67%
2.06mb
FA1 67%
1.20mb
38%
S813 58%
4.12mb
25%
67%
PF14-L2
6.31mb
25%
TUG 62%
7.38mb
30%
RPL41 57%
8.86mb
9.02mb
Linkage Group:
I
II
III
IV
V
VI

B

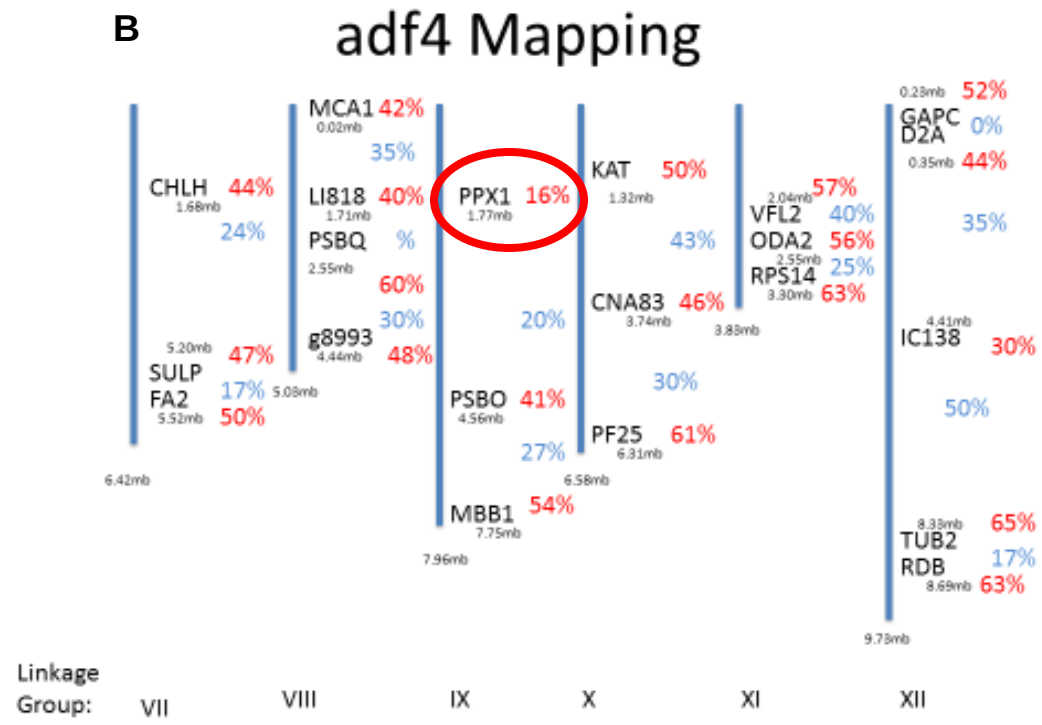
adf4 Mapping
CHLH 44%
1.68mb
24%
5.20mb
SULP 47%
FA2 17%
5.52mb 50%
6.42mb
MCA1 42%
0.02mb
35%
LI818 40%
1.71mb
PSBQ %
2.55mb
60%
g8993 30%
4.44mb 48%
5.08mb
PPX1 16%
1.77mb
20%
PSBO 41%
4.56mb
27%
MBB1 54%
7.75mb
7.96mb
KAT 50%
1.32mb
43%
CNA83 46%
3.74mb
30%
PF25 61%
6.31mb
6.58mb
2.04mb 57%
VFL2 40%
ODA2 56%
2.55mb
RPS14 25%
3.30mb 63%
3.83mb
0.23mb 52%
GAPC
D2A 0%
0.35mb 44%
35%
4.41mb
IC138 30%
50%
8.33mb 65%
TUB2
RDB 17%
8.69mb 63%
9.73mb
Linkage Group:
VII
VIII
IX
X
XI
XII

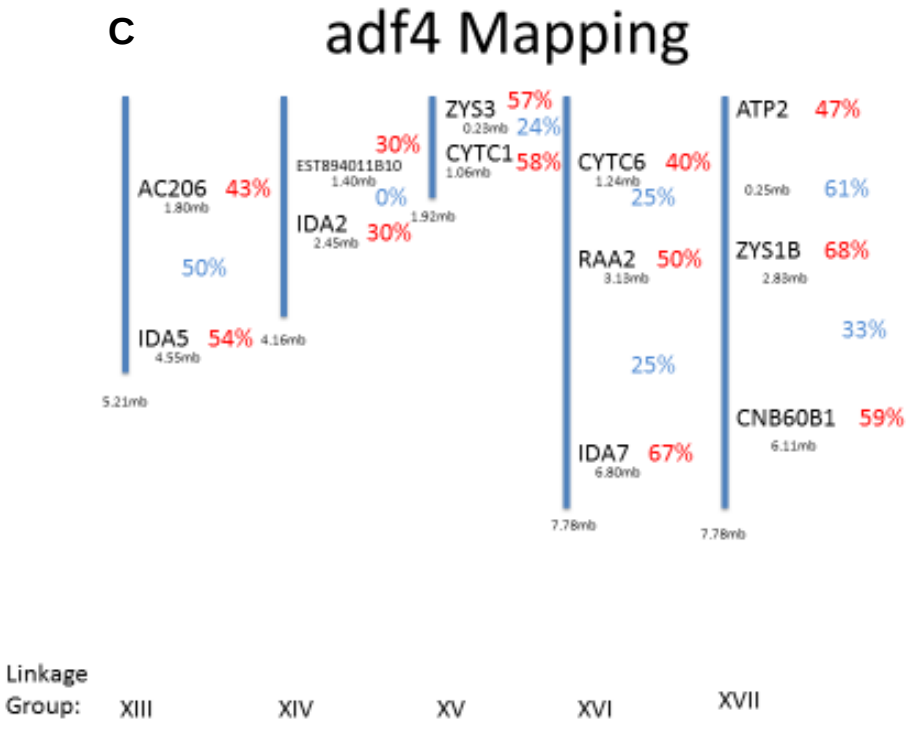

Figure 2.7. ***ADF4*** **PCR-based recombination map**

Note. Panels A-C show *Chlamydomonas* linkage groups I to XVII. PCR-based recombination markers from the *Chlamydomonas* mapping kit and their coordinates are indicated. In red is percent recombination between the deflagellation-defective phenotype and the corresponding marker. In blue is the recombination between two adjacent. Red circle indicates linkage to mapping kit marker found.

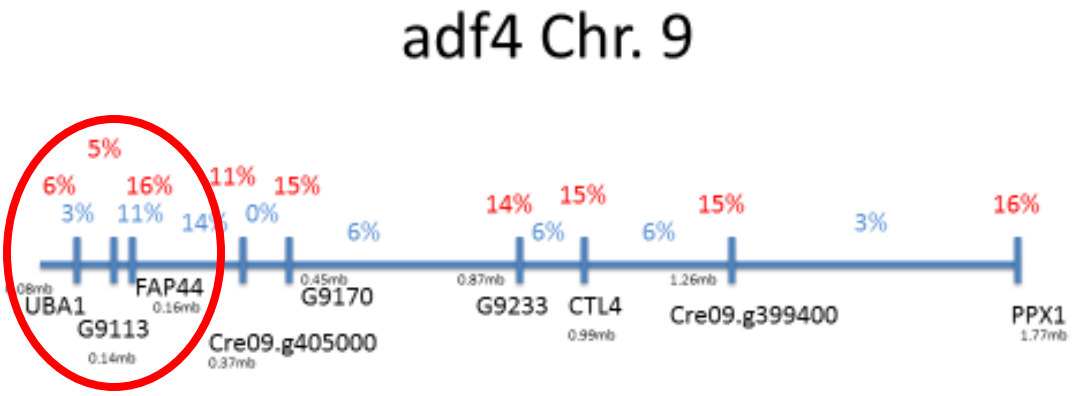

Figure 2.8. Detailed *ADF4* PCR-based recombination map of Chromosome 9

Note. Shown is chromosome 9 between beginning of the chromosome and the mapping kit marker PPX1. Custom primers used for mapping listed in Materials&Methods. In red is percent recombination between the deflagellation-defective phenotype and the corresponding marker. In blue is the recombination between two adjacent markers. Red circle indicates linkage to a marker found.

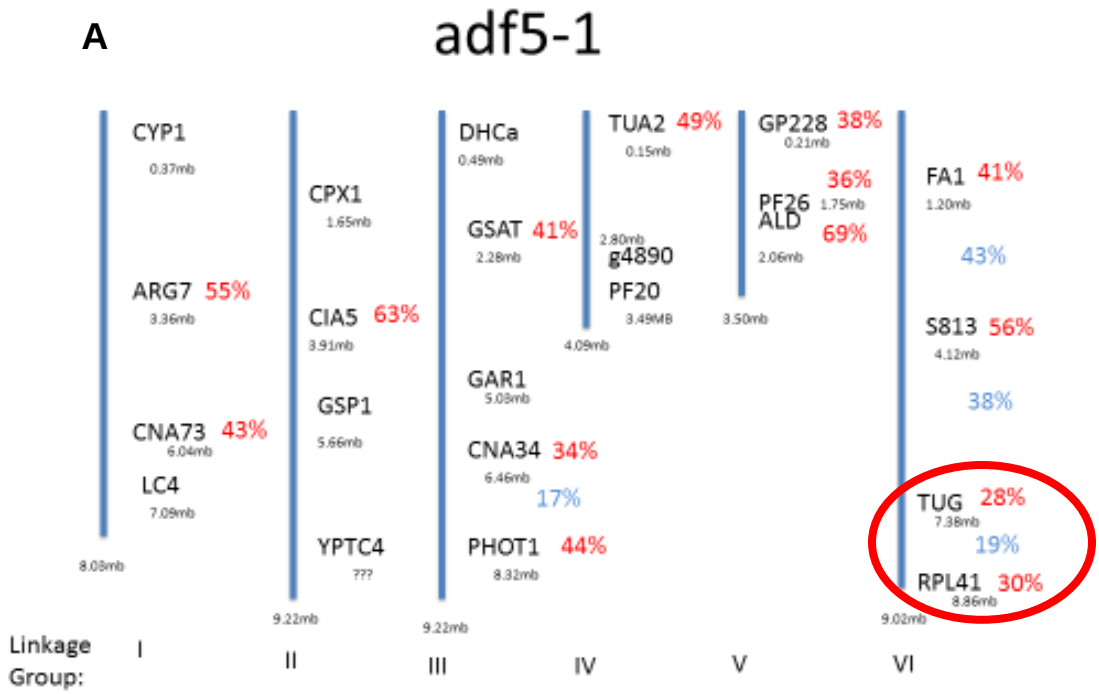
A
adf5-1
CYP1
0.37mb
ARG7 55%
3.36mb
CNA73 43%
6.04mb
LC4
7.09mb
8.08mb
CPX1
1.65mb
CIA5 63%
3.91mb
GSP1
5.66mb
YPTC4
???
9.22mb
DHCa
0.49mb
GSAT 41%
2.28mb
GAR1
5.08mb
CNA34 34%
6.46mb
17%
PHOT1 44%
8.32mb
9.22mb
TUA2 49%
0.15mb
2.80mb
g4890
PF20
3.49MB
4.09mb
GP228 38%
0.21mb
36%
PF26 1.75mb
ALD 69%
2.06mb
3.50mb
FA1 41%
1.20mb
43%
S813 56%
4.12mb
38%
TUG 28%
7.38mb
19%
RPL41 30%
8.86mb
9.02mb
Linkage Group:
I
II
III
IV
V
VI

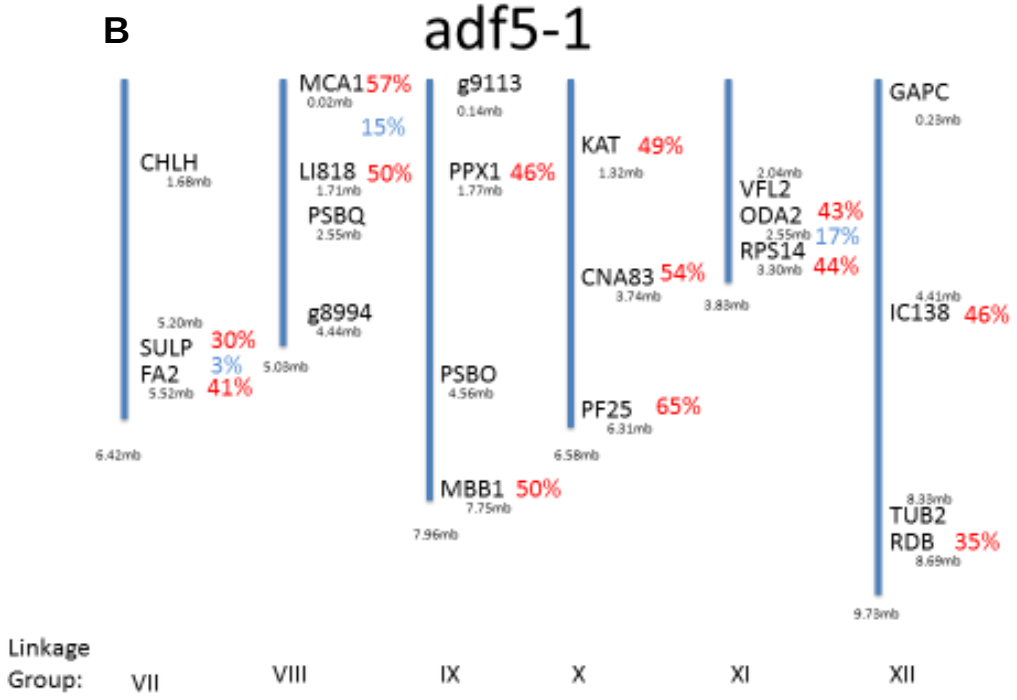
B
adf5-1
CHLH
1.68mb
5.20mb
SULP 30%
FA2 3%
5.52mb 41%
6.42mb
MCA1 57%
0.02mb
15%
LI818 50%
1.71mb
PSBQ
2.55mb
g8994
4.44mb
5.08mb
g9113
0.14mb
PPX1 46%
1.77mb
PSBO
4.56mb
MBB1 50%
7.75mb
7.96mb
KAT 49%
1.32mb
CNA83 54%
3.74mb
PF25 65%
6.31mb
6.58mb
2.04mb
VFL2
ODA2 43%
2.55mb 17%
RPS14 44%
3.30mb
3.83mb
GAPC
0.23mb
4.41mb
IC138 46%
8.33mb
TUB2
RDB 35%
8.69mb
9.73mb
Linkage Group:
VII
VIII
IX
X
XI
XII

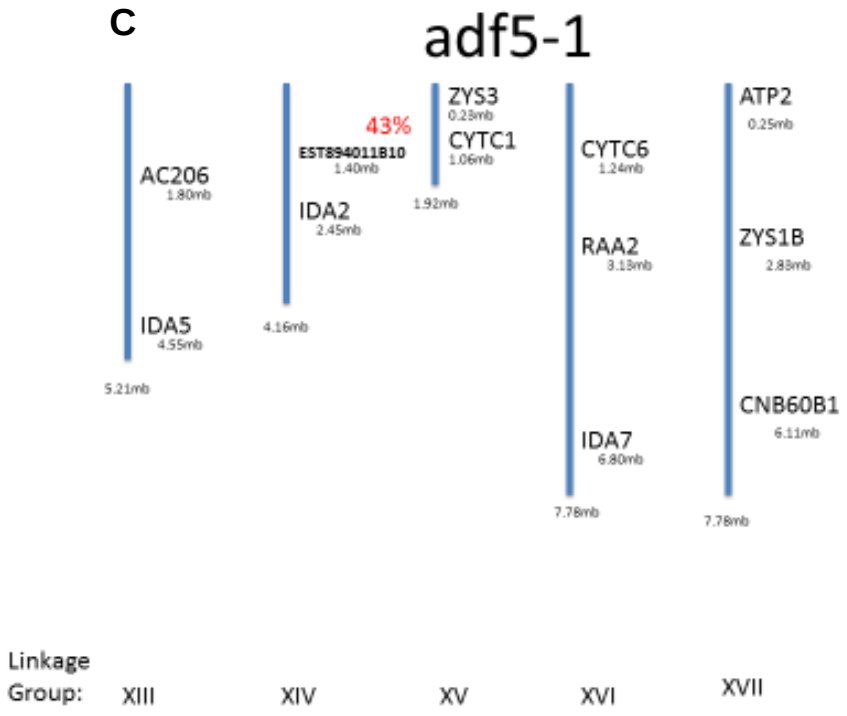

Figure 2.9. ***adf5-1*** **PCR-based recombination map**

Note. Panels A-C show *Chlamydomonas* linkage groups I to XVII. PCR-based recombination markers from the *Chlamydomonas* mapping kit and their coordinates are indicated. In red is percent recombination between the deflagellation-defective phenotype and the corresponding marker. In blue is the recombination between two adjacent. Red circle indicates linkage to mapping kit marker found. Mapping was performed until linkage to TUG/RPL41 markers revealed potential allelism with adf5-2.

A

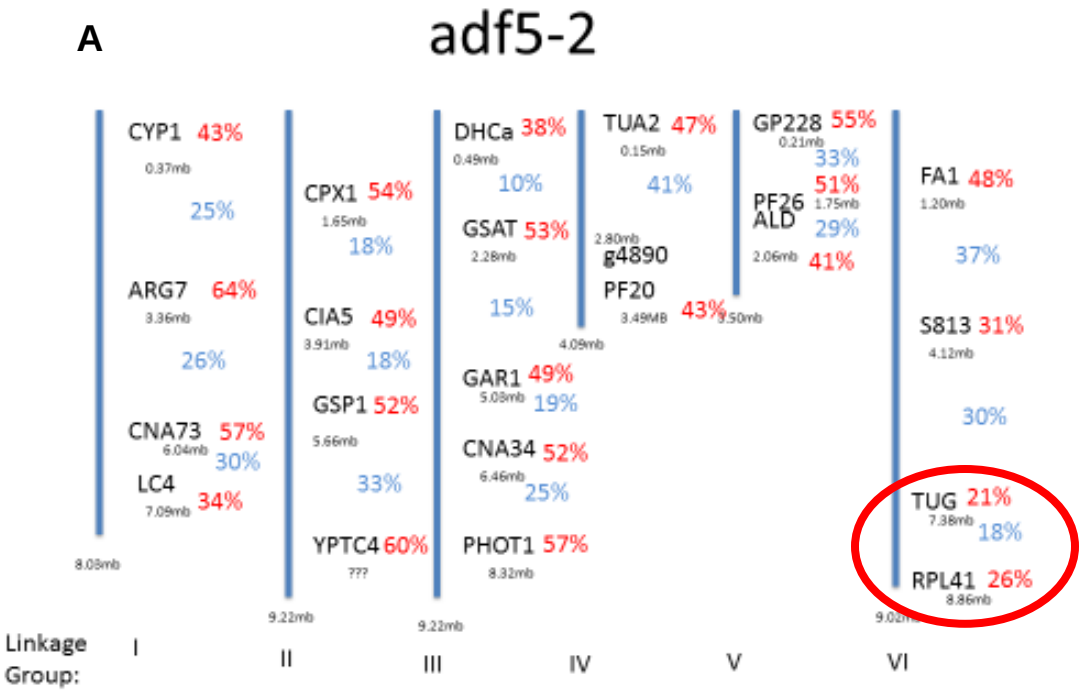
adf5-2
CYP1 43%
0.37mb
25%
ARG7 64%
3.36mb
26%
CNA73 57%
6.04mb
30%
LC4 34%
7.09mb
8.03mb
CPX1 54%
1.65mb
18%
CIA5 49%
3.91mb
18%
GSP1 52%
5.66mb
33%
YPTC4 60%
???
9.22mb
DHCa 38%
0.49mb
10%
GSAT 53%
2.28mb
15%
GAR1 49%
5.08mb 19%
CNA34 52%
6.46mb
25%
PHOT1 57%
8.32mb
9.22mb
TUA2 47%
0.15mb
41%
2.80mb
g4890
PF20
3.49MB 43%
4.09mb
GP228 55%
0.21mb
33%
PF26 51%
1.75mb
ALD 29%
2.06mb 41%
3.50mb
FA1 48%
1.20mb
37%
S813 31%
4.12mb
30%
TUG 21%
7.38mb
18%
RPL41 26%
8.86mb
9.02mb
Linkage Group:
I
II
III
IV
V
VI

B

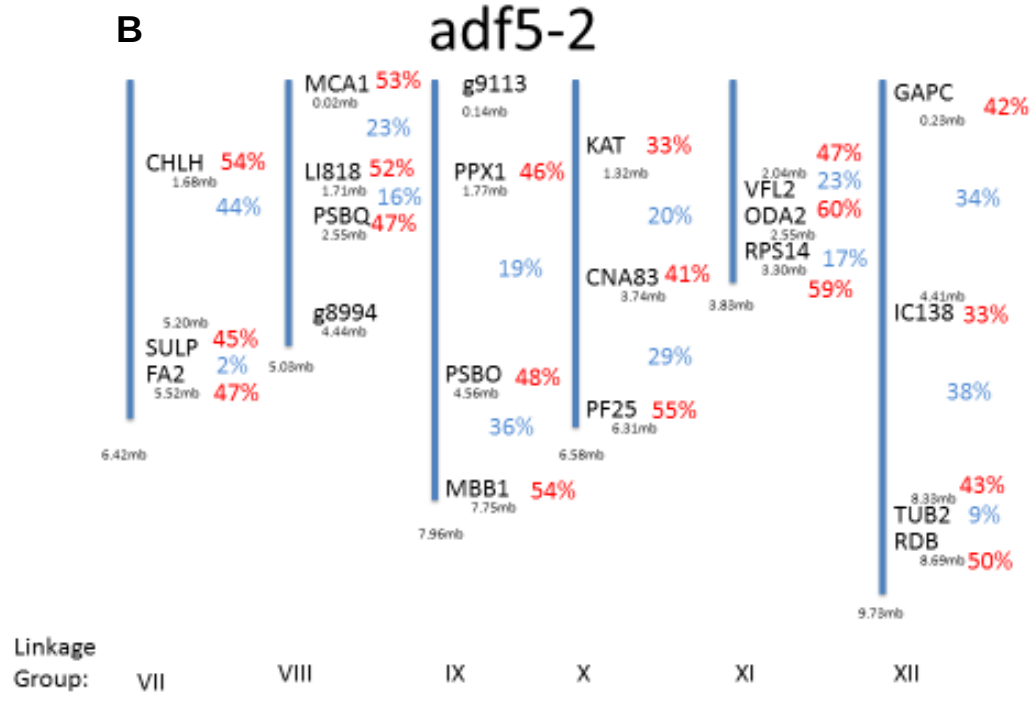
adf5-2
CHLH 54%
1.68mb
44%
5.20mb
SULP 45%
FA2 2%
5.52mb 47%
6.42mb
MCA1 53%
0.02mb
23%
LI818 52%
1.71mb 16%
PSBQ 47%
2.55mb
g8994
4.44mb
5.08mb
g9113
0.14mb
PPX1 46%
1.77mb
19%
PSBO 48%
4.56mb
36%
MBB1 54%
7.75mb
7.96mb
KAT 33%
1.32mb
20%
CNA83 41%
3.74mb
29%
PF25 55%
6.31mb
6.58mb
2.04mb 47%
VFL2 23%
ODA2 60%
2.55mb
RPS14 17%
3.30mb 59%
3.83mb
GAPC 42%
0.23mb
34%
4.41mb
IC138 33%
38%
8.33mb 43%
TUB2 9%
RDB 50%
8.69mb
9.73mb
Linkage Group:
VII
VIII
IX
X
XI
XII

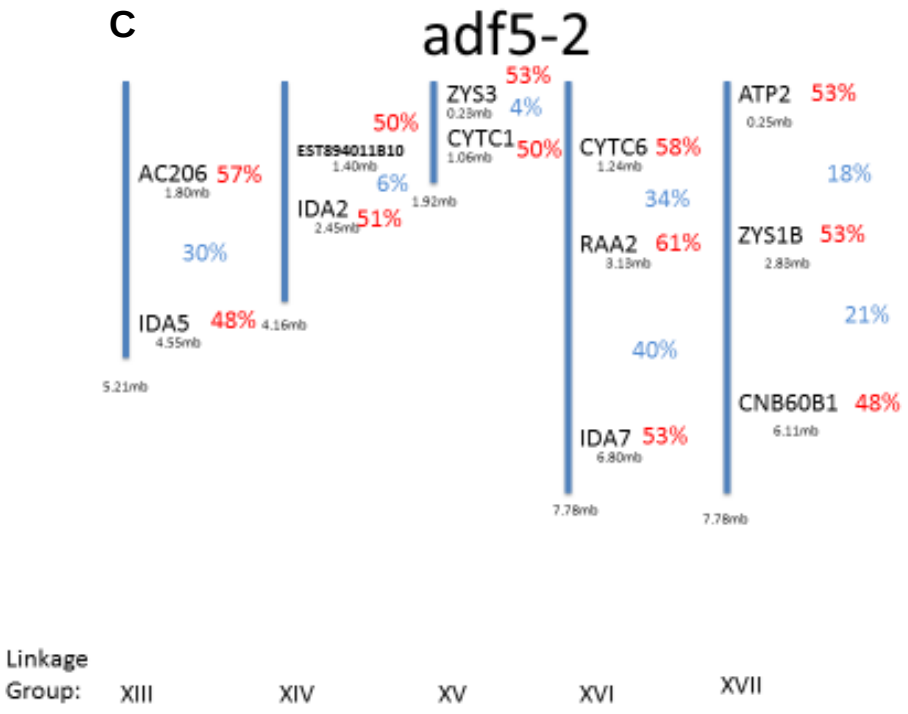

Figure 2.10. ***adf5-2*** **PCR-based recombination map**

Note. Panels A-C show *Chlamydomonas* linkage groups I to XVII. PCR-based recombination markers from the *Chlamydomonas* mapping kit and their coordinates are indicated. In red is percent recombination between the deflagellation-defective phenotype and the corresponding marker. In blue is the recombination between two adjacent. Red circle indicates linkage to mapping kit marker found.

A

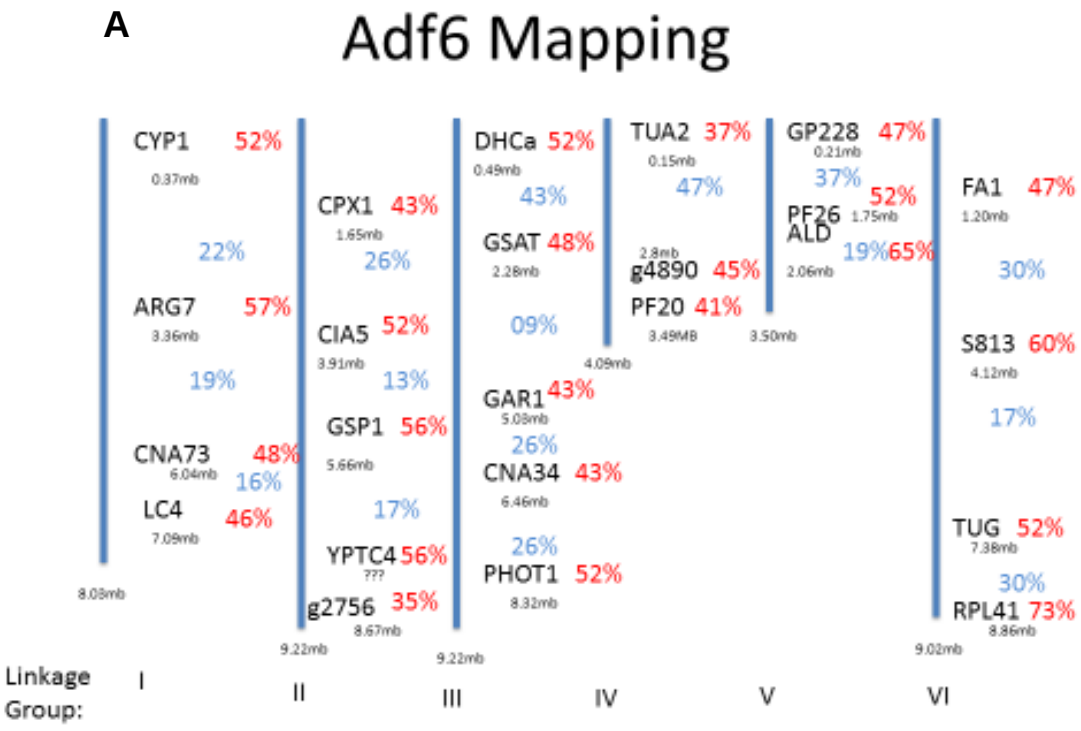
Adf6 Mapping
CYP1 52%
0.37mb
22%
ARG7 57%
3.36mb
19%
CNA73 48%
6.04mb
16%
LC4 46%
7.09mb
8.08mb
CPX1 43%
1.65mb
26%
CIA5 52%
3.91mb
13%
GSP1 56%
5.66mb
17%
YPTC4 56%
???
g2756 35%
8.67mb
9.22mb
DHCa 52%
0.49mb
43%
GSAT 48%
2.28mb
09%
GAR1 43%
5.08mb
26%
CNA34 43%
6.46mb
26%
PHOT1 52%
8.32mb
9.22mb
TUA2 37%
0.15mb
47%
2.8mb
g4890 45%
PF20 41%
3.49MB
4.09mb
GP228 47%
0.21mb
37%
52%
PF26 1.75mb
ALD
19%65%
2.06mb
3.50mb
FA1 47%
1.20mb
30%
S813 60%
4.12mb
17%
TUG 52%
7.38mb
30%
RPL41 73%
8.86mb
9.02mb
Linkage Group:
I
II
III
IV
V
VI

B

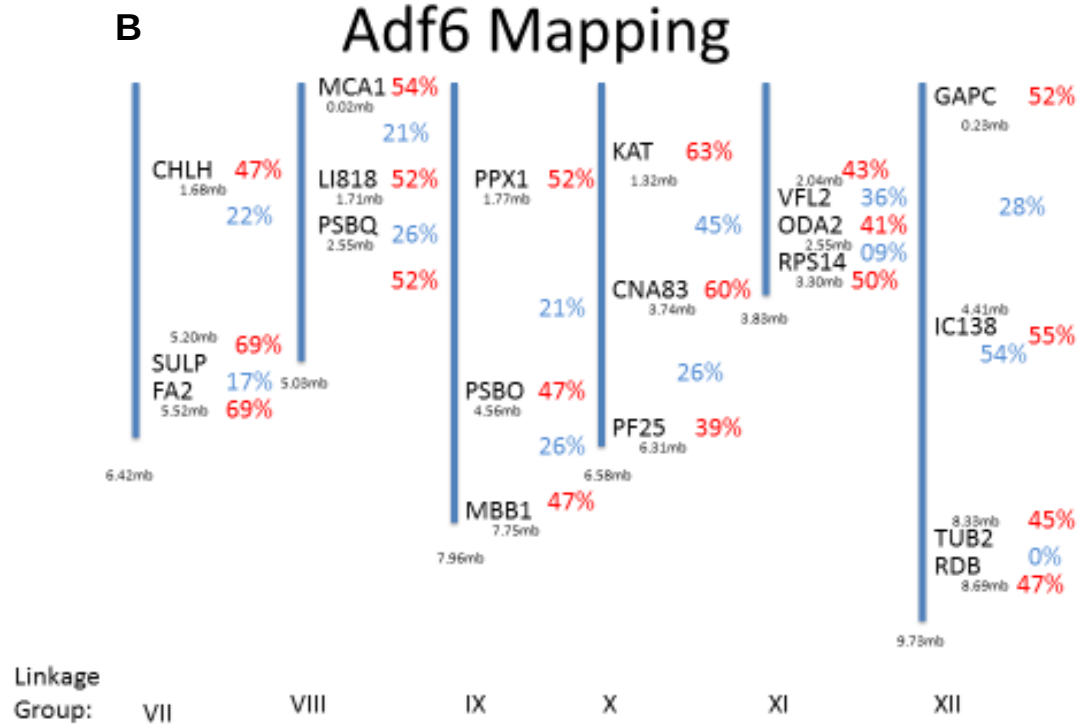
Adf6 Mapping
CHLH 47%
1.68mb
22%
5.20mb 69%
SULP
FA2 17%
5.52mb 69%
6.42mb
MCA1 54%
0.02mb
21%
LI818 52%
1.71mb
PSBQ 26%
2.55mb
52%
5.08mb
PPX1 52%
1.77mb
21%
PSBO 47%
4.56mb
26%
MBB1 47%
7.75mb
7.96mb
KAT 63%
1.32mb
45%
CNA83 60%
3.74mb
26%
PF25 39%
6.31mb
6.58mb
2.04mb 43%
VFL2 36%
ODA2 41%
2.55mb
RPS14 09%
3.30mb 50%
3.88mb
GAPC 52%
0.23mb
28%
4.41mb
IC138 55%
54%
8.33mb 45%
TUB2
RDB 0%
8.69mb 47%
9.73mb
Linkage Group:
VII
VIII
IX
X
XI
XII

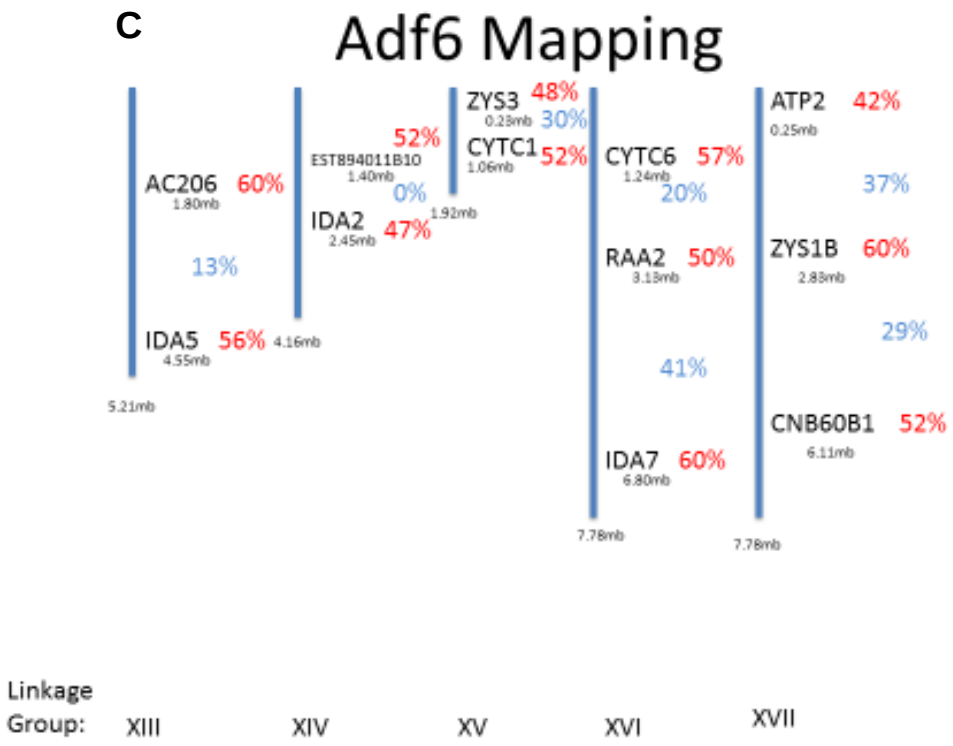

Figure 2.11. *ADF6* PCR-based recombination map

Note. Panels A-C show *Chlamydomonas* linkage groups I to XVII. PCR-based recombination markers from the *Chlamydomonas* mapping kit and their coordinates are indicated. In red is percent recombination between the deflagellation-defective phenotype and the corresponding marker. In blue is the recombination between two adjacent. Red circle indicates linkage to mapping kit marker found.

A Mapping E5.1 P8 A12

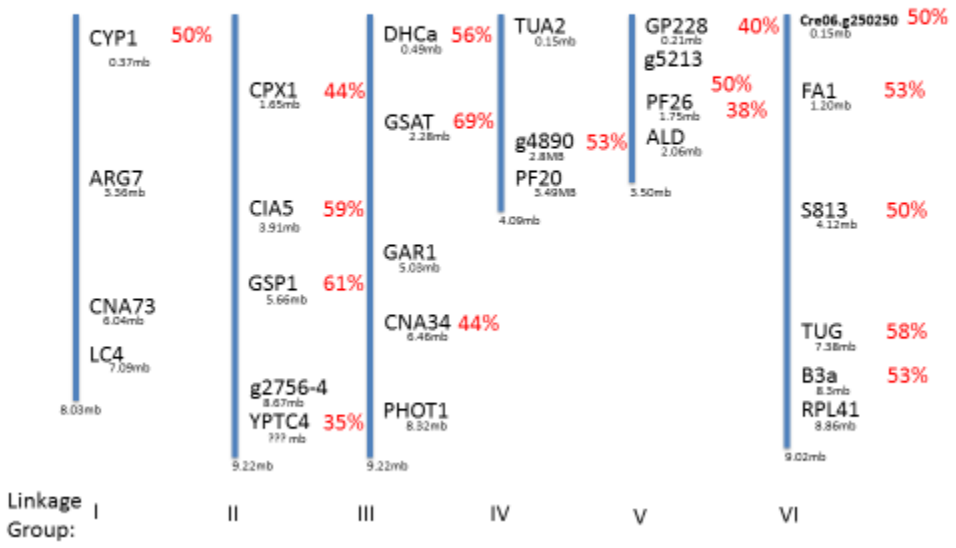

B Mapping E5.1 P8 A12

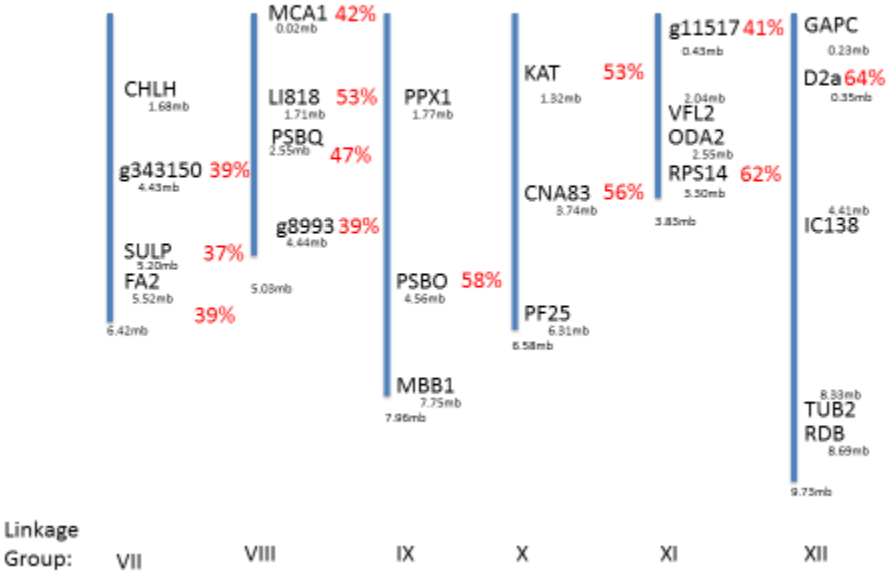

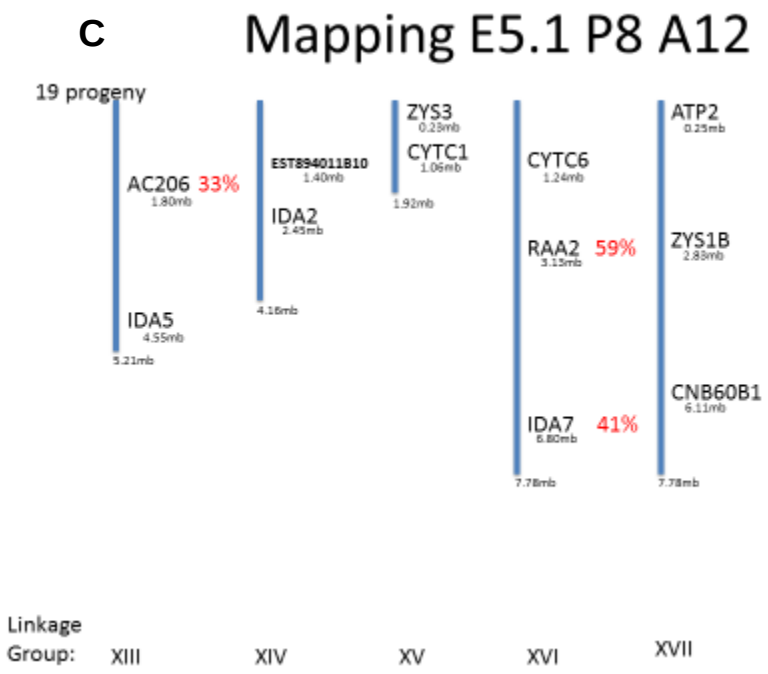

Figure 2.12. E5.1P8A12 PCR-based recombination map

Note. Panels A-C show *Chlamydomonas* linkage groups I to XVII. PCR-based recombination markers from the *Chlamydomonas* mapping kit and their coordinates are indicated. In red is percent recombination between the deflagellation-defective phenotype and the corresponding marker. In blue is the recombination between two adjacent. Red circle indicates linkage to mapping kit marker found. However, only mapping kit markers where WGS revealed a nearby potential causative mutation were analyzed.

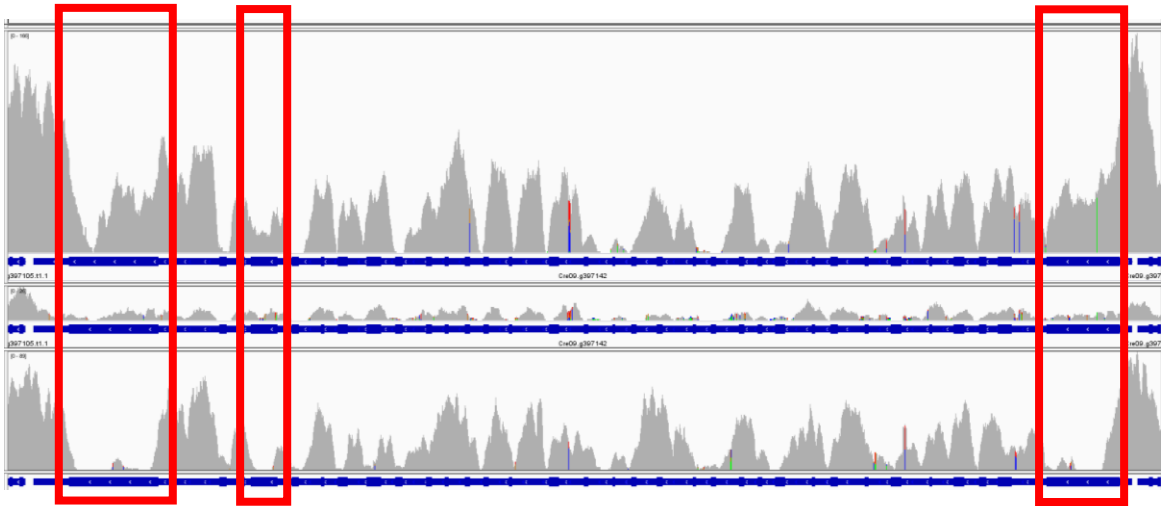

Figure 2.13. Comparison of coverage of adf1-gene region using HiSeq1, MiSeq and HiSeq2

Note. Top: HiSeq2. Middle: MiSeq1. Bottom: HiSeq1. Highlighted in red are exons that noticeably differed in coverage between sequencing runs. Strain sequenced was E20G2

2.7. Tables

Table 2.1. Summary of the two deflagellation mutant screens performed

Screen	Enrichment strategy	Screen strategy	# screened	#ADF (ts)	#FA (ts)	Mutant yield	Relative fold-enrichment over 1998 screen
1	Horizontal phototaxis	Manual	18,338	14 (1)	6 (0)	1.1:1000	2.3
2	Vertical phototaxis	Spectro-photometer + Manual	28,210	16 (0)	1 (0)	0.6:1000	1.2

Table 2.2. Sample Spectrophotometer Analysis Output

	1	2	3	4	5	6	7	8	9	10	11	12
A	0.033927	-0.22618	-0.15598	-0.15068	-0.13465	-0.09717	-0.52508	-0.22953	-0.70468	-0.34702	-0.27907	-0.35931
B	-0.18276	-0.08192	-0.26005	-0.29332	-0.17355	-0.22695	-0.14705	-0.16643	-0.08779	-0.20784	0.176437	-0.29717
C	-0.06495	-0.05382	-0.11663	-0.17321	-0.38202	-0.31958	-0.25141	-0.02682	-0.35467	0.0029	-0.06765	-0.07021
D	0.056795	-0.08141	0.166551	0.043256	-0.22394	0.040093	0.154053	-0.26041	-0.04917	-0.33922	-0.02445	0.658067
E	0.017598	-0.00716	-0.49831	-0.33833	-0.14463	-0.28397	-0.05846	-0.67351	-0.35235	-0.14197	0.144017	-0.21446
F	0.193617	-0.25978	-0.20455	0.067552	-0.04686	0.158961	-0.15927	-0.01405	-0.13469	-0.30709	0.171945	-0.10675
G	-0.22044	-0.03351	0.054551	-0.00258	0.322353	-0.25273	-0.17068	-0.20315	0.09516	0.129514	0.088889	-0.29506
H	0.020547	-0.19632	-0.1247	-0.09987	-0.18449	-0.40141	-0.06105	-0.28439	0.02881	-0.1496	-0.17487	0.44579

Note. The number in each well is the relative absorbance difference between pre-ADB-treatment and post-ADB-treatment. Cells D12 and H12 are E20G2 mutant control wells, cells D11 and H11 are wild-type control cells. Cell G5 is a potential deflagellation mutant highlighted for further analysis because its relative absorbance difference is >0.3, as described in Materials&Methods

Table 2.3. Identification of fa isolates from the horizontal enrichment screen.

Mutant	x *fa1-4*		x *fa2-2*		Allele
	FA progeny	WT progeny	FA progeny	WT progeny	
E12 AA40	12	0	60	46	*fa1-5*
E12 AN8	27	0	63	18	*fa1-6*
E15.2 P12 E6	21	0	ND	ND	*fa1-7*
E12 AA8	19	3	76	0	*fa2-5*
E12 AC10	81	29	92	0	*fa2-6*
E12 AE48	11	3	30	0	*fa2-7*
E22 A12	17	9	57	0	*fa2-8*

Table 2.4. Representative results of recombination mapping and dikaryon complementation groups

Isolate ID	Complementation group	Closest mapping kit marker recombination (recombinant:parental)
E4 N23	adf2	45R:106P Marker CNA34 Chromosome 3
E4.1 P1 H3	adf6	Not linked to any markers in mapping kit
E4.1 P3 H3	adf4	6R:32P Marker PPX1 Chromosome 9
E3.1 P15 B4	adf5	10R:26P Marker TUG Chromosome 6
E21 C7	adf5	19R:69P Marker TUG Chromosome 6
E21 B5	Group I	1R:20P Marker PSBO Chromosome 9
E12 M20	Group II	0R:26P Marker PSBO Chromosome 9
E20 G2	Group III	2R:28P Marker PSBO Chromosome 9
E5.1 P8 A12	Unassigned	Not linked to any markers in mapping kit

Table 2.5. Initial Dikaryon Experiment Results of mutant alleles

Mutants	*ADF1*	*ADF2*	*ADF4*	*ADF5*	Group I	Group II	Group III	Complementation Group
E12 AJ30	Yes	No	No	No				*ADF1*
E12 P1	Yes	No	No	No				*ADF1*
E16 A19	Yes	No	No	No				*ADF1*
E12 AI18	Yes	No	No	No				*ADF1*
E2.2 P2 A12	Maybe	No	No	No	Maybe	Maybe		*ADF1*
E4 N23	No	Yes	No	No	No	No		*ADF2*
E3.1 P15 B4	No	No	No	Yes	No	No		*ADF5*
E21 C7	No	No	No	Yes	No	No		*ADF5*
E4.1 P3 H3	No	No	Yes	Yes	No	No		*ADF4*
E4.1 P1 H3	No	No	No	No	No	No	No	*ADF6*
E21 B5	No	No	No	No	Yes	No		Group I
E1 P19 C5		No	No	No	Yes			Group I
E21 C13	No	No	No	No	Yes	No		Group I
E6.1 P3 A4		No	No	No	Yes			Group I
E6.1 P3 A7	No	No	No	No	Yes			Group I
E11.1 E26	No	No	No	No		Yes		Group II
E12 M20	No	No	No	No	No	Yes		Group II
E21 A11	No	No	No	No		Yes		Group II
E21 B12	No	No	No	No		Yes		Group II
E20 G2	No	No	No	No	No	No	Yes	Group III
E21 B16	No					No		ADF
E4.2 P10 H9	Maybe	No	No	No	Maybe	Maybe		ADF
E4.2 P4 C12	Maybe	No	No	No	Maybe	Maybe		ADF
E4.2 P5 G9	Maybe	No	No	No	Maybe	Maybe		ADF
E5.1 P8 A12	No	No			No	No		ADF
E14.2 P2 G9	No							ADF
E7.1 P1 C12								ADF
E7.1 P1 D1								ADF
E7.1 P1 D2								ADF
E8.2 P12 A12	No	No	No	No	Maybe	Maybe		ADF
E12 P7	No					No		ADF

Note. Yes indicates non-complementation and thus allelism by temporary dikaryon experiments. Maybe indicates inconclusive results. No indicates either complementation (and non-allelism) or non-linkage through PCR-based recombination mapping.

Table 2.6. Summary of sequencing results from NGS.

Sample	Sequencing Type	Read Length	Total Reads	Mapped Reads	%Mapped (BWAMEM)	Coverage
P8 A12	HiSeq 1	101	46212679	41603183	90.03	35.02
adf1-3 R	HiSeq 1	101	50195504	46465997	92.57	39.10
adf2-1	MiSeq	151	17770141	16147064	90.87	20.32
E4.1P1H3	HiSeq 1	101	48667980	40841326	83.92	34.37
adf4-1	HiSeq 1	101	41454437	36880433	88.97	31.04
adf5-1	MiSeq	151	12005878	11714323	97.57	14.74
adf5-2	HiSeq 1	101	51256001	39581709	77.22	33.31
P1H3	HiSeq 1	101	45043411	38643143	85.79	32.52
E26	HiSeq 1	101	45645076	41617564	91.18	35.03
M20	HiSeq 1	101	58458403	54568943	93.35	45.93
G2	HiSeq 1	101	53869707	44591841	82.78	37.53
G2	HiSeq 2	126	72881761	66811758	91.67	70.15
A7	HiSeq 2	126	51712016	46450023	89.82	48.77
B12	HiSeq 2	126	48204171	42159214	87.46	44.27
A11	HiSeq 2	126	48704966	44348170	91.05	46.57
C5	HiSeq 2	126	62216711	54235385	87.17	56.95
adf1-2	HiSeq 2	126	31448228	26570956	84.49	27.90
adf1-3	HiSeq 2	126	74966324	70375932	93.88	73.89
adf1-6	HiSeq 2	126	53405756	49281993	92.28	51.75
adf1-10	HiSeq 2	126	54395349	50515073	92.87	53.04

Table 2.7. Summary of WGS variant analysis

Sample	Total Variants	Unique Variants	%Unique Variants
P8 A12	8725	1833	21.01
adf1-3 Rescue/Suppressor	264015	49431	18.72
adf2-1	7190	1891	26.30
E4.1P1H3	8537	1887	22.10
adf4-1	8449	2035	24.09
adf5-1	7340	2758	37.57
adf5-2	8554	1577	18.44
P1H3	8414	1799	21.38
E26	8682	1673	19.27
M20	8072	1287	15.94
G2	7471	1439	19.26
G2	10762	1836	17.06
A7	9726	2221	22.84
B12	10462	2464	23.55
A11	10257	2123	20.70
C5	10562	2382	22.55
adf1-2	232411	5952	2.56
adf1-3	255376	21892	8.57
adf1-6	257873	32072	12.44
adf1-10	10282	2076	20.19

Table 2.8. Potential causative mutations in ADF mutants, identified by WGS

Strain	Causative Mutation	Gene ID	Gene locus
adf1-10	Q761*	*ADF1 / TRP15*	Cre09.g396142
adf1-2	G692FS	*ADF1 / TRP15*	Cre09.g396142
adf1-3	FH173CR	*ADF1 / TRP15*	Cre09.g396142
adf1-3 R	Unidentified	*ADF1 / TRP15*	Cre09.g396142
adf1-6	A1724D	*ADF1 / TRP15*	Cre09.g396142
adf2-1	W71*	*ADF2 / ITPK1*	Cre03.g182100
E4.1P1H3/*adf6-1*	Unidentified	Unidentified	Not mapped to a locus
adf4-1	D780N	*ADF4* / Glycosyl-transferase	Cre09.g138732
E21B5/ *adf3-1*	Unidentified	Unidentified	Mapped close to *PSBO*
E1P19C5/*adf3-2*	Unidentified	Unidentified	Mapped close to *PSBO*
E6.1P3A7/*adf3-3*	Unidentified	Unidentified	Mapped close to *PSBO*
E12M20	W560L	*ADF1 / TRP15*	Cre09.g396142
E11.1E26	H1720FS	*ADF1 / TRP15*	Cre09.g396142
E21A11	E974*	*ADF1 / TRP15*	Cre09.g396142
E21B12	K1469*	*ADF1 / TRP15*	Cre09.g396142
G2	L139FS	*ADF1 / TRP15*	Cre09.g396142
adf5-1	Splice-site Exon 19	*ADF5 / FAP16*	Cre06.g303400
adf5-2	Y841*	*ADF5 / FAP16*	Cre06.g303400
P8A12	Unidentified	Unidentified	Not mapped to a locus

Chapter 3. The Identity of Several Novel Deflagellation genes and *ADF1*

3.1. *ADF1*

3.1.1. Complementation Groups

Whole-genome sequencing revealed that nine of the sequenced strains have mutations in the same gene, Cre09.g397142 / *TRP15*. To our surprise, this includes all strains of complementation groups II, III and *ADF1*. This means that either intragenic complementation occurred, or a significant number of the mutations are not causal.

Since I expected the *adf1-3* Rescue strains to be the only strain with two copies of the potential causative gene (one mutated copy and one healthy copy inserted by transformation), it was the only strain where I went looking for heterozygous mutations. Indeed, the *adf1-3* rescue strain has multiple weak-coverage heterozygous mutations in *TRP15*, consistent with complementation with wild-type *TRP15* from the EcoRI-digested BAC.

Temporary dikaryon analysis indicated that strains of complementation groups I, II and III might be different tightly-linked genes or rescue was occurring due to intergenic complementation. It was possible that the mutations in common in *TRP15* were purely coincidental, because as a large gene it might be inherently more likely to accumulate mutations during UV-mutagenesis. This however would have likely lead to mutations in *TRP15* randomly amongst all our strains sequenced, which is not the case. With the exception of E4.1P1H3, all strains that had mutations in *TRP15* also had phenotypes linked to the mutation, while all other unlinked strains (such as *adf2-1*, *adf4-1*, *adf5-1* and *adf5-2*) contained no *TRP15* mutations. Mutations in *TRP15* occurring only amongst a select few strains whose phenotypes were all linked to it seemed exceedingly unlikely.

The mutations identified in *TRP15* occur throughout the predicted protein and it is therefore difficult to reconcile with the idea that different complementation groups correspond to complementary functional domains of the same protein. If mutations of each complementation group had only been found to be located at different ends of the predicted protein, the explanation that different wild-type protein domains may stabilize each other, producing intragenic complementation, would have been more obvious.

While no previously known *ADF1* alleles were rescuable by each other, indicating that they all do not form ADF1 protein or form insoluble protein, this does not necessarily hold true for all possible alleles of *ADF1*. If the *adf1-2* mutant strain that the temporary dikaryon experiments were performed with forms an insoluble protein that by itself is non-functional, it might still be able to be rescued by a second ADF1-protein with mutations in a different part of the protein. If the mutations in strains of complementation groups II and III still form soluble protein, it might then be able to rescue *adf1-2* via intragenic complementation. I hypothesize that given the data obtained from mapping, temporary dikaryons and whole genome sequencing, this is the most likely explanation and have therefore assigned all strains of complementation groups II and III as novel alleles of *ADF1*.

WGS of E4.1P1H3 also indicated the possibility of a mutation within *TRP15*. As WGS-analysis only indicated low confidence in the variant, I sought to confirm the mutation with Sanger sequencing. This was done as unlike complementation groups II and III, repeated PCR-based recombination mapping showed no linkage between the *PSBO* marker that is linked with *TRP15* and the phenotype in E4.1P1H3 and this potential variant being causal thus seemed unlikely. I used PCR to amplify a region covering the mutation for Sanger sequencing confirmation but attempts failed despite testing more than 10 pairs of custom primers, none of which were able to amplify a fragment of predicted correct size. I hypothesize that the variant indicated by WGS is either an artifact I was not able to refute or that the variant has no significant impact on the function of the protein. This is because not only is the potential mutation not a confident variant call from WGS analysis, there is also no linkage between the phenotype and the potential mutation. If the mutation is in fact real, then it having no impact on the gene might be explained by it lying outside of any functional domains – of

all mutations discovered within *TRP15*, this mutation is also the one closest to the C-terminus and furthest past the transmembrane domains. A map of all mutations identified within *TRP15* is shown in figure 3.1.

I have assigned all strains that contained mutations in *TRP15* that were linked to *ADF1* allele numbers of *ADF1*. These assignments and the assignments of all other new deflagellation mutant strains for which I was able to assign alleles can be seen in table 3.1. The acid-induced deflagellation phenotypes of the three mutant strains of complementation group *ADF3*, as well as all novel alleles of *ADF1* are shown in figure 3.2.

3.1.2. TRP15 Characterization

After hypothesizing since the original analysis of the deflagellation pathway that a calcium-permeable ion channel had to be part of the pathway, we were excited to find out that ADF1 is a potential calcium-permeable ion channel (Quarmby and Hartzell 1994; Finst, Kim et al. 1998). TRP15, a predicted 2340 amino acid (AA) big protein, is annotated with 9 potential transmembrane-spanning regions. One thing to note is that the reference sequence for *TRP15* contains two anomalies. Firstly, there is a reference sequence gap between Exons 17 and 18 which has no sequencing coverage and no RNAseq data spans the region (Figure 3.3). Secondly, the very large last exon (538AA's or ~23% of the full predicted protein) is not connected by RNAseq to the rest of the sequence (Figure 3.4). Both these data points indicate that the sequence annotation for *TRP15* might be incorrect. Given that mutations identified in WGS span sequences both before and after the reference gap, I hypothesize that this reference gap is insignificant and probably just intronic. No mutations were detected in the last exon, however, and I cannot be sure whether this last exon is part of the protein. TRP15 is thus likely a protein of size ~2100AA-2340AA. Six of the transmembrane-spanning regions are found tightly clustered in the centre of the protein, while the remaining three are found closer towards the N-terminus. All proteins in the various TRP-families are ion channels permeable to a multitude of cations such as calcium or sodium and all contain six transmembrane domains, supporting the hypothesis that TRP15 is in fact a member of the TRP-channel

family (Hardie and Minke 1992; Clapham, Runnels et al. 2001; Nilius and Owsianik 2011).

We next wanted to find out whether TRP15 belongs to one of the defined TRP families. As TRP channels are themselves highly divergent from one another and this is particularly so when comparing Chlamydomonas genes with mammalian genes, we restricted the phylogenetic analysis to only using the channel domains. Figure 3.5 shows the resulting phylogenetic tree. While ADF1/TRP15 did not tightly cluster with other TRP channels, it shows closest homology to a *Chlamydomonas*-exclusive clade of potentially TRPV-related channels. Because of the lack of close homology and the fact that TRP channels in general vary in terms of sequence (Reaves and Wolstenholme 2007), I am not confident in definitely assigning TRP15 to a specific family of TRP channels. *Chlamydomonas* possesses at least 18 other proteins annotated as potential TRP channels, none of which are annotated as belonging to a specific family of mammalian TRPs and as our phylogeny revealed possess significant variance from them as well. A large family of Chlamydomonas-specific TRP-channels shows some homology with the family of TRPV-channels and is also the family that shows closest homology to TRP15. With a branch support value of 0.34 of a maximum of 1, this however is much smaller than the support for homology between the larger *Chlamydomonas* and the TRPV family (0.9).

In conclusion, more than 20 years after its discovery, I identify ADF1 as the potential calcium-channel TRP15.

3.2. *ADF2*

3.2.1. Identification

As described in Chapter 2, I uncovered one allele of the novel deflagellation gene we call *ADF2*. The *adf2-1* strain is the only mutant we recovered with a temperature-sensitive acid deflagellation phenotype. At the permissive temperature (21°C), *adf2-1* mutant cells deflagellate on average by 68%, while wild-type cells deflagellate by 98% in response to pH shock. At the restrictive temperature (33°C), on average only 36% of

adf2-1 cells deflagellate in response to pH shock compared to 99% of WT cells (Figure 3.6). *Adf2-1* deflagellated at wild-type levels in response to dibucaine at both the restrictive and the permissive temperature (data not shown). Based on this, I have determined that *adf2-1* is a temperature-sensitive ADF. PCR-based recombination mapping established that the potential causative gene was linked to the mapping kit marker CNA34 (Pike 2013), and I thus had a good idea of where potentially causative variants discovered by WGS would have to be located.

The combination of mapping and our WGS results indicated that the causative mutation in *adf2-1* may be a W71* mutation in a gene annotated as an Inositol 1,3,4-trisphosphate 5/6-kinase, which corresponds to a gene typically annotated based on its predicted function as *ITPK1* (Majerus, Wilson et al. 2010), a 592AA-protein encoding gene named as Cre03.g182100. To test whether this was the causative mutation, we co-transformed *adf2-1* cells with a BAC spanning the ITPK1 gene (BAC8679) and the selectable marker pSI103. From transformations with this BAC we obtained 3 phenotypically wild-type transformants (Figure 3.7). I carefully re-examined our WGS sequencing results and confirmed that no other homozygous mutations occur in any coding regions covered by this BAC to eliminate the possibility that a different gene on the BAC was responsible for rescuing the ADF phenotype of *adf2-1*. I thus conclude that the W71* mutation in ITPK1 causes the deflagellation-defective phenotype in *adf2-1*.

3.2.2. *ITPK1* Characterization

A search for homologous proteins in other organism by BLAST reveals a high sequence similarity with ITPK5 in maize (zea mays), ITPK6 in rice (oryza sativa), ITPK6 in grass (Sorghum bicolor) and ITPK4 in Arabidopsis (Arabidopsis thaliana) (all with significance of >e^33). Similarly, a phylogenetic analysis based on the predicted kinase domain and representative ITPK-family members as well as an outgroup consisting of AtPI3K, a different member of the inositol-pathway, revealed that five proteins also share the closest homology based on phylogenetic analysis (Figure 3.8). Intriguingly, these four genes have been grouped together in a previous study analyzing the phylogeny of ITPKs (Du, Liu et al. 2011). I am thus confident in identifying *ADF2* as the

Chlamydomonas reinhardtii homologue of *ITPK1*, belonging to a specific subfamily of *ITPK1*-members consisting of *ZmITPK5*, *OsITPK6, SbITPK6* and *AtITPK4*.

3.3. *ADF3*

The B5 strain of complementation group I showed a stop-codon within *TRP15*, suggesting that it was an allele of *ADF1*. WGS coverage was low in this region and I therefore sought to verify this potential variant by Sanger sequencing PCR-fragments spanning the mutation I amplified using two different custom primer pairs. This revealed that the *TRP15* mutation in B5 was an artifact (Figure 3.9), as Sanger sequencing data showed no difference between wild-type and B5. Importantly, no *TRP15* mutations were found in other strains of complementation group I either. I thus hypothesize that the three strains of complementation group I are alleles of a different, novel deflagellation gene I call *ADF3*.

No variants in common between strains of this complementation group were detected by WGS and rescue attempts with three BACs (1K7, 2I23 and 33I9) spanning candidate genes that had mutations in the B5 and C13 strains also failed, despite more than 400 transformants screened per BAC – more than twice as many as were needed to obtain wild-type rescue of *adf2-1*, *adf4-1*, *adf5-1* and *adf5-2*. The identity of *ADF3* thus remains unknown, likely due to the causative gene being located in a difficult-to-sequence region far enough away from mapping kit markers to not reveal linkage to any of them.

3.4. *ADF4*

3.4.1. Identification

Having determined that *adf4-1* is tightly linked to the mapping kit marker *PPX1* on chromosome 9, I designed custom primers for genes in the beginning of this chromosome to further narrow down the location of the potential causative gene. I was able to link the deflagellation-defect most tightly to a custom primer for gene

Cre09.g386731 at ~140kb from the beginning of the chromosome. I then proceeded to examine the WGS data to identify potential causative mutations in that region of the genome. A potential causative mutation was found within Cre09.g386732, a gene annotated as encoding a potential glycosyltransferase just 100bp upstream of the gene for which I had designed the custom primer. With this marker, I identified 2 recombinant progeny and 35 parental progeny. This rate of recombination would usually indicate that the identified mutation is not causal, as the causative mutation should have 0% recombination with the deflagellation-defective phenotype. Two recombination events between adjacent genes is exceedingly unlikely, given the rates of recombination between adjacent markers we had observed when performing recombination mapping. The more likely explanation is that there were errors in the assignment of phenotype to the progeny of mapping crosses. These errors might have arisen because at the time of mapping we did not appreciate nor were we aware that the *adf4-1* mutation is conditional (see below). Other candidate mutations were too far away from this mapping kit marker, and were therefore ruled out. I thus proceeded to try to confirm this gene assignment by rescuing the mutant phenotype with two different BACs that span the candidate gene Cre09.g386732.

Two BACs (3607 and 8268) were independently co-transformed into *adf4-1* along with the selectable marker plasmid pSI103. I screened transformants of both BACs and obtained 1 rescue with BAC 3607 and 2 rescues with BAC 8268 (Figure 3.10). Of the six genes overlapping between both BACs, one (the *UBA1* gene) had missing exon coverage in the WGS performed. To eliminate the possibility that an undiscovered mutation in this exon was causative, I PCR-amplified a fragment spanning the exon with missing coverage from *adf4-1* DNA to send for Sanger sequencing. This revealed that in fact no mutation was present in this exon (Figure 3.11) and I thus identify the *ADF4* gene as Cre09.g386732, a potential glycosyltransferase.

3.4.2. Characterizing the nutrient-sensitive phenotype of ADF4

While working with *adf4-1* cultures, I observed that the deflagellation-defective phenotype was often weak. It was not enhanced at higher temperatures, so *adf4-1* is not temperature-sensitive. However, I did observe that cultures maintained in liquid TAP for

long periods of time (5 days or longer) had stronger deflagellation-defective phenotypes than freshly inoculated cultures. I hypothesized that nutrient starvation was responsible for this effect. As nitrogen-starvation by inoculation in low-N TAP medium also induces gametogenesis after 24h in *C. reinhardtii* (Abe, Kubo et al. 2004), I tested whether *adf4-1* cells becoming gametes upon nitrogen-starvation was linked to this phenotype. To test this I inoculated fresh two-day cultures of *adf4-1*+ and *wt*+ *wt*- and an *adf4-1*+ rescue strain as controls in fresh liquid TAP for 48 and then resuspended the cultures in low-N TAP for 24h to induce gametogenesis. I then mated the *wt*+/*wt*-, *adf4-1*+/*wt*- and *adf4-1*+ *Rescue*/*wt*- strains to measure the rate of mating by counting quadra-flagellate cells (QFC's) as well as measuring their deflagellation in acid (Figure 3.12). To get an estimate of the maximum deflagellation-defective behaviour of a regular ADF mutant and its mating capabilities, I also included *adf1-12* as a control. This revealed that the deflagellation-defective phenotype is not linked to gametogenesis, as even *adf4-1* cells that are able to mate deflagellate effectively.

Next I thus wanted to test whether a longer exposure to nitrogen-starvation would be able to induce a stronger deflagellation-defect. 48 hours after inoculation in low-N TAP cells appeared to stop mating, possibly because transcriptional upregulation of mating-related genes is strongest 6-8 hours after nitrogen-withdrawal and rapidly decreases 10+ hours after that, likely rendering cells unable to mate. (Abe, Kubo et al. 2004; Lin and Goodenough 2007). The deflagellation-defect of *adf4-1*, however, appeared to become stronger over time, which is why I next focused on nitrogen-starvation itself as a potential inducer of the deflagellation-defective phenotype.

An important nutrient *Chlamydomonas reinhardtii* takes up from its environment is nitrogen and upon deprivation of this nutrient, it switches to less photosynthetic energy production (due to the downregulation of chlorophyll biosynthesis) and focuses on protein breakdown to recycle nitrogen (Philipps, Happe et al. 2012; Schmollinger, Muhlhaus et al. 2014). Nitrogen starvation also induces many other transcriptomic changes (Msanne, Xu et al. 2012). To thus test the effects of nitrogen-starvation on *adf4-1*, I inoculated *adf4-1* and *wt* cells that had been grown on solid TAP-plates for a 7 days in liquid TAP medium and let them grow for 48h, then treated them in one of three ways: 1) centrifugation and resuspension in fresh liquid TAP for 48h; 2) centrifugation

and re-suspension in fresh TAP for 24h followed by another round of centrifugation and resuspension in low-N tap for 24h; or 3) centrifugation and resuspension in low-N liquid TAP for 48h. The acid-deflagellation defect was strongest after 48 h low-N TAP, suggesting that longer nutrient starvation indeed was responsible in inducing the phenotype (Figure 3.13). I thus conclude that nitrogen is one nutrient that, when *Chlamydomonas* cells are starved for it, causes a deflagellation-defective phenotype in *adf4-1*.

This starvation-specific phenotype is a completely novel condition in the deflagellation pathway in *C. reinhardtii* and raises interesting questions about the interconnection between the state of nutrient supply and flagella.

3.4.3. ADF4, a Glycosyltransferase-family member

BLAST-homology search only revealed similarity with several similarly poorly described gene, most of them (~88%) bacterial and not eukaryotic (only~3%), a distribution significantly higher than that of the three other deflagellation genes included for comparison shown in table 3.2. Of the 100 top BLAST hits, only 15 are eukaryotic and outside of un-annotated hits in *Chlamydomonas*' closest evolutionary neighbour, *Volvox carteri*, the top 68 hits are all bacterial or archaeal, suggesting closer homology with families of bacterial genes than eukaryotic ones. The highest annotated eukaryotic BLAST hits were against the putative mannosyltransferase F18K10.25 and the glycosyltransferase AT3G10630 in *Arabidopsis thaliana* (both hits with significance e^-39). Both of these proteins, however, are only annotated based on predicted functional domains and no experimental evidence. The closest well-described BLAST hit is the pimA gene of the actinobacterium *Mycobacterium smegmatis* (e^-11). There, pimA is also known as GDP-mannose-dependent alpha-(1-2)-phosphatidylinositol mannosyltransferase and mediates an early, essential step in membrane glycolipid synthesis by incorporation of GDP-D-mannose into phosphatidylinositol (PI) (Kordulakova, Gilleron et al. 2002).

Furthermore, when I analyzed the Cre09.g386732/ADF4 protein for predicted functional domains, I discovered a potential Concanavalin A-like Lectin/Glucanase

domain (Figure 3.14). While being part of diverse families of proteins, they share the ability to bind to specific carbohydrates, a function involved in proteins transferring sugar groups (Mandal and Brewer 1992; Saso, Valentini et al. 1998; Ramstrom, Lohmann et al. 2004; Gomez-Casati, Martin et al. 2013). Binding to carbohydrates is also important for other protein functions, such as cell recognition and adhesion or organizing membrane architecture (Codogno, Doyennette-Moyne et al. 1988; Knibbs, Perini et al. 1989).

I thus identify ADF4 as the potential glycosyltransferase Cre09.g386732. I also characterized the nitrogen-starvation specific deflagellation-defect of *adf4-1*, a completely novel phenotype in this pathway.

3.5. *ADF5*

3.5.1. Identification

Both *adf5-1* and *adf5-2* have a strong acid-, but also a weak dibucaine-induced deflagellation defect. While ADF-mutants are thought to be involved in mediating the initial acid-sensing or calcium-influx and their defect can be bypassed by permeabilizing the membrane and allowing calcium entry, FA-mutants are thought to be flagellar components more closely involved in flagellar severing and do not deflagellate in response to any stimulus. Neither the acid nor dibucaine deflagellation phenotypes are significantly increased at the restrictive temperature (33°C, Figure 3.15). Since we were unable to identify conditions under which axonemal severing was as severely inhibited as it is in the *FA1* and *FA2* strains, we chose to classify this mutant as an ADF. We did so because if *ADF5* was a true FA closely involved in axonemal severing, it would not be able to deflagellate under any known condition. The fact that it is still able to do so, unlike *FA1* and *FA2*-mutants, indicate that the severing machinery is still intact and it is thus likely primarily involved in upstream signaling.

PCR-based recombination mapping early on indicated that these two strains might be allelic, as they both showed a very mild FA-phenotype and both mapped near the mapping kit marker *TUG*. Indeed, WGS then revealed that both strains contained

mutations in the same gene, which also were the only variants in a gene in common in this region. This gene was the flagellar-associated gene *FAP16*/Cre06.303400, encoding a 1749AA-protein annotated with several WD40-domains. Based on this, I assigned them the two allele numbers *adf5-1* and *adf5-2* and identify *ADF5* as *FAP16*. The two mutations identified were a C->G transversion and the loss of the splice site before exon 19 in *adf5-1* and a Y841* SNV in *adf5-2*. The predicted resulting proteins, if expressed, are shown in Figure 3.16.

To definitively confirm this gene assignment, *adf5-1* and *adf5-2* cells were transformed with BAC DNA (BAC9022) and one wild-type isolate of 200 transformants screened was recovered in each strain (Phenotypes of rescues shown in Figure 3.15), confirming that they are both mutant alleles of *FAP16*, as no mutations in other genes covered by the BAC were detected by WGS.

3.5.2. *FAP16* Characterization

The predicted FAP16 protein is annotated with several WD40 domains. This in itself gives very little info about potential function, as WD40-domains are common among a multitude of proteins with varying functions. They serve, in general, to provide binding sites for protein-protein interactions, but are non-specific in terms of what type of interaction they mediate (Stirnimann, Petsalaki et al. 2010). Based on BLAST homology and phylogenetic analysis, FAP16 does however bear close similarity to the family of echinoderm-microtubule binding proteins, or EMLs, specifically EML5 and EML6 (Figure 3.17). While these two are the least thoroughly characterized members of the EML protein family, other members of this family have been discovered to be required for proper microtubule formation (such as human EML4) or can cause ciliopathies when mutated (such as human EML1) (Pollmann, Parwaresch et al. 2006; Lyman and Chetkovich 2015). Furthermore, like all FAPs, they were annotated as such as they were discovered in a study trying to uncover all flagellar-associated proteins in *Chlamydomonas* and are found in its flagellar proteome (Li, Gerdes et al. 2004; Pazour 2004). As a flagellar-associated protein, FAP16 adds another interesting piece to the deflagellation puzzle.

3.6. Materials & Methods

3.6.1. Transformations and BAC Rescue

The Qiagen Plasmid Maxi Kit was used to prepare BAC DNA. Plasmid DNA was prepared for Chlamydomonas transformation using the Qiagen Plasmid Midi Kit. Chlamydomonas cells were transformed by the glass bead method (Kindle 1990). Transformations were performed on B5 and C13, two of the mutant alleles isolated and characterized as part of complementation group I, together with the psI103 plasmid conferring resistance to the antibiotic paramycin (Sizova, Fuhrmann et al. 2001).

3.6.2. Media and Deflagellation Assays

TAP medium was prepared as described in previous literature (Harris 2009). Low-N Tap medium was created using the standard TAP buffer, but only adding a quarter as much NH_4Cl. Acid-deflagellation buffer (ADB) was prepared and experiments for deflagellation assays and PCR-based recombination mapping carried out as described in the previous chapter. Temperature-sensitive experiments (*adf2-1*) were carried out at the restrictive temperature of 33C after incubation for 6 hours. Low-N experiments (*adf4-1*) were carried after 24h-48h in liquid low-N media – exact times given in specific experimental figure notes.

3.6.3. Gene and Protein data

Gene and protein information as well as RNAseq data was obtained from the Joint Genome Institute's (JGI) www.phytozome.net and *Chlamydomonas reinhardtii* assembly v5.0. Sanger sequencing was performed by Genewiz (South Plainfield, NJ). Multiple Sequence Alignment performed using MUSCLE after curation for sequences that aligned without gaps using www.phylogeny.fr's built-in curator. Phylogeny created using PhyML. Tree rendered using TreeDyn (Guindon and Gascuel 2003; Edgar 2004; Chevenet, Brun et al. 2006; Dereeper, Guignon et al. 2008; Dereeper, Audic et al. 2010).

3.6.4. Primers

Custom primer pairs used to verify the *TRP15* mutation in B5 by Sanger sequencing were as follows:

Primer Name	Primer Sequence
B54-Forward	CTTCACCTCCCGCACCTA
B54-Reverse	CCTTTTCCACCCCTTGACCT
B57-Forward	TGGCTCCTCCCAGTTAACTT
B57-Reverse	AAAGTGCGGTTCATCCCAAC

Custom Primers used for Sanger sequencing of Exon 7 of the *UBA1* gene were as follows:

Primer Name	Primer Sequence
UBA1EX7-2-Forward	TGGTCCAGCGGAGTAGACAC
UBA1EX7-2-Reverse	GAACGTGATGGGTAATGCAG

Custom primers used for detailed *ADF4* mapping on chromosome 9 were as follows:

Primer Name	Primer Sequence
g9113-Forward	AAGTACGACTACGGCGAGGA
g9113-Reverse	AGC-TCTTGTACTCGTCCTCCA
Cre09.g399400-Forward	TCGCTTACATATGGGGCAGT
Cre09.g399400-Reverse	CGCTCCAATACCAGTTGCTG
g9233-Forward-Reverse	AAGTTTTCGCGGACAC-TGAC
g9233-Reverse	AACAGCAGCTTCAGGTACCT
g9170-Forward	CTACAGCCGGTG-AAGGTGGT
g9170-Reverse	ACGTGTGCTGCTGTCCTGA
Cre09.g405000-Forward	TAC-AGGTGGGTGCTTGCGA
Cre09.g405000-Reverse	CTCCGTCTCATCCTCTTCCC
FAP44-Forward	CTGGATGCCTTTGACGACG
FAP44-Reverse	GCATTCTCAGTGCCACGATG
UBA1-Forward	GTCTGGACCTGGTTGTGAAC
UBA1-Reverse	CGATGCGGTTGTGGAAGTAG
CTL4-Forward	GCACCTACATCACCTTCAGC
CTL4-Reverse	TGATGGCAAAGAACG-CGTAG

3.7. Figures

3.7.1. *ADF1*

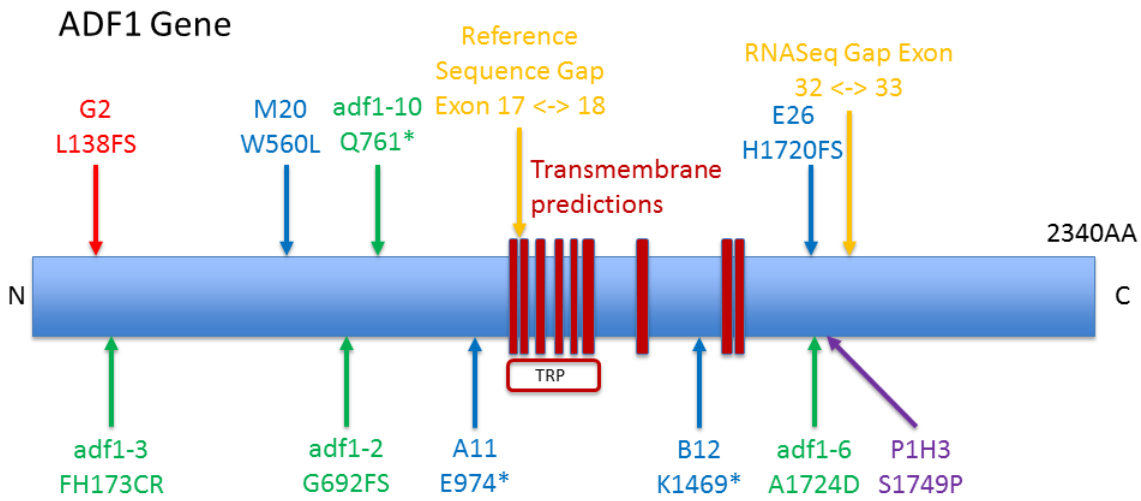

Figure 3.1. Overview of all mutations identified by WGS within ADF1

Note. Different colours indicate different complementation groups as predicted by temporary dikaryons. Green = *ADF1*, Blue = Group II, Red = Group III. Shown in yellow are locations of gaps in reference DNA and RNAseq data, shown in dark red are the predicted transmembrane domains of TRP15.

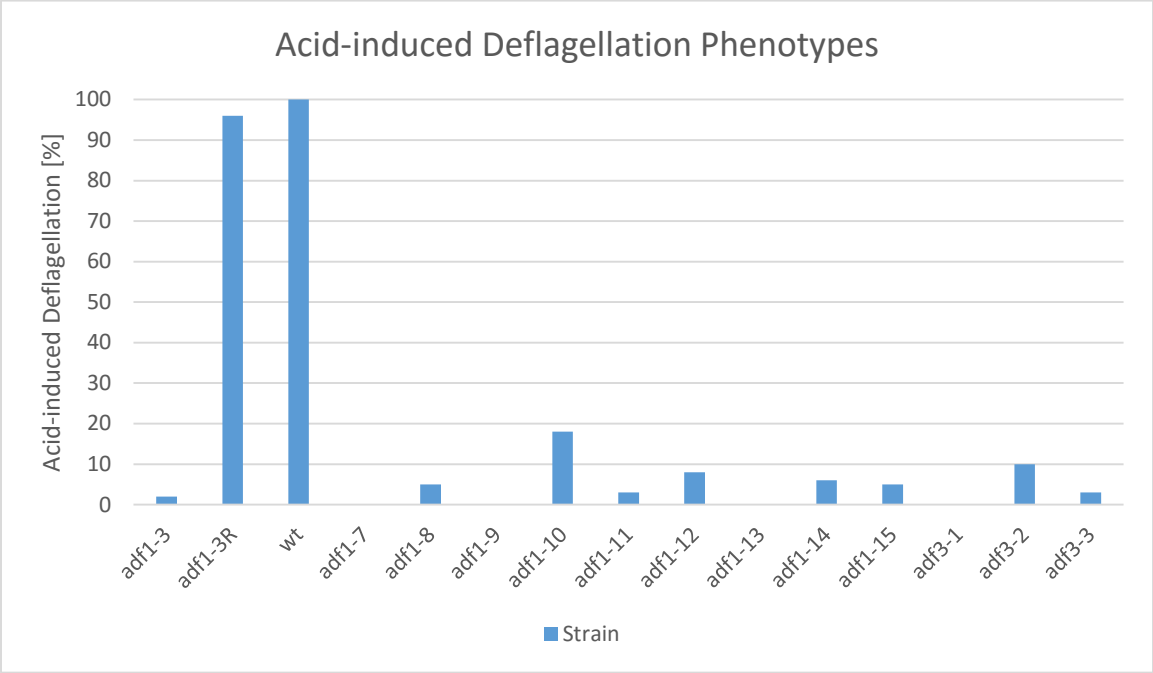

Figure 3.2. Acid-induced Deflagellation Phenotypes

Note. Contains phenotype data for new alleles of *ADF1* and *ADF3*. *adf1-3*, *adf1-3* Rescue and wild-type strains shown as controls. Standard pH-shock protocol followed after inoculation of cells in liquid TAP for 2 days.

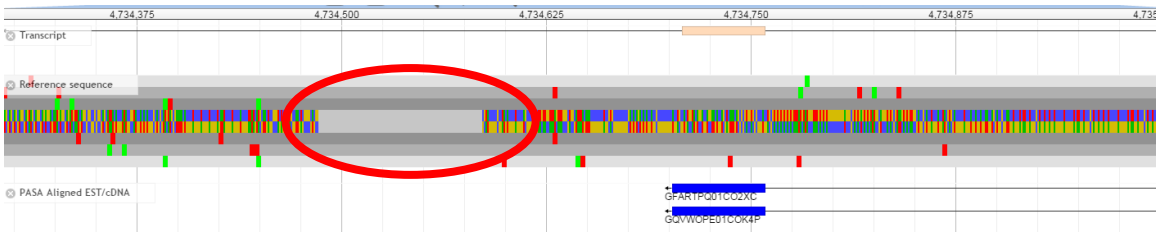

Figure 3.3. Gap in Reference Sequence of *TRP15*

Note. Reference sequence gap highlighted in red. Sequence obtained from *Chlamydomonas reinhardtii* Assembly 5.0, visualized in Broad Institute's Integrated Genomic Viewer (IGV) (Thorvaldsdottir, Robinson et al. 2013).

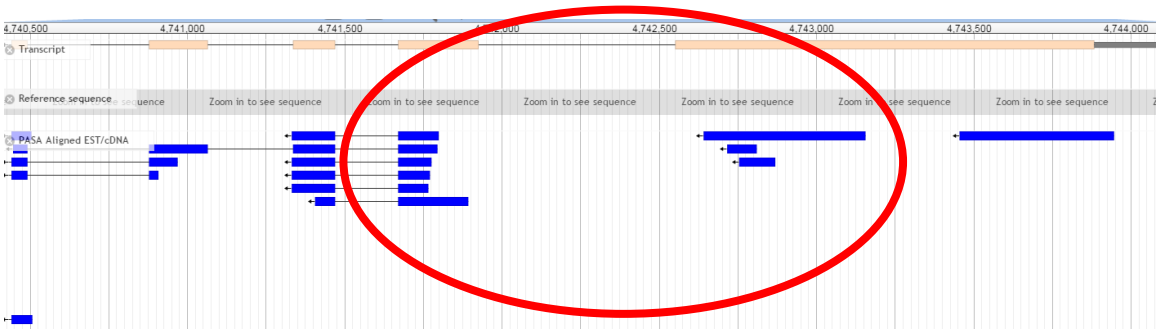

Figure 3.4. Gap in RNAseq coverage between the last and penultimate exon of *TRP15*

Note. RNASeq gap highlighted in red. *Chlamydomonas reinhardtii* assembly 5.0 visualized within Join Genome Institute's (JGI) phytozome genome browser (JBrowse).

.

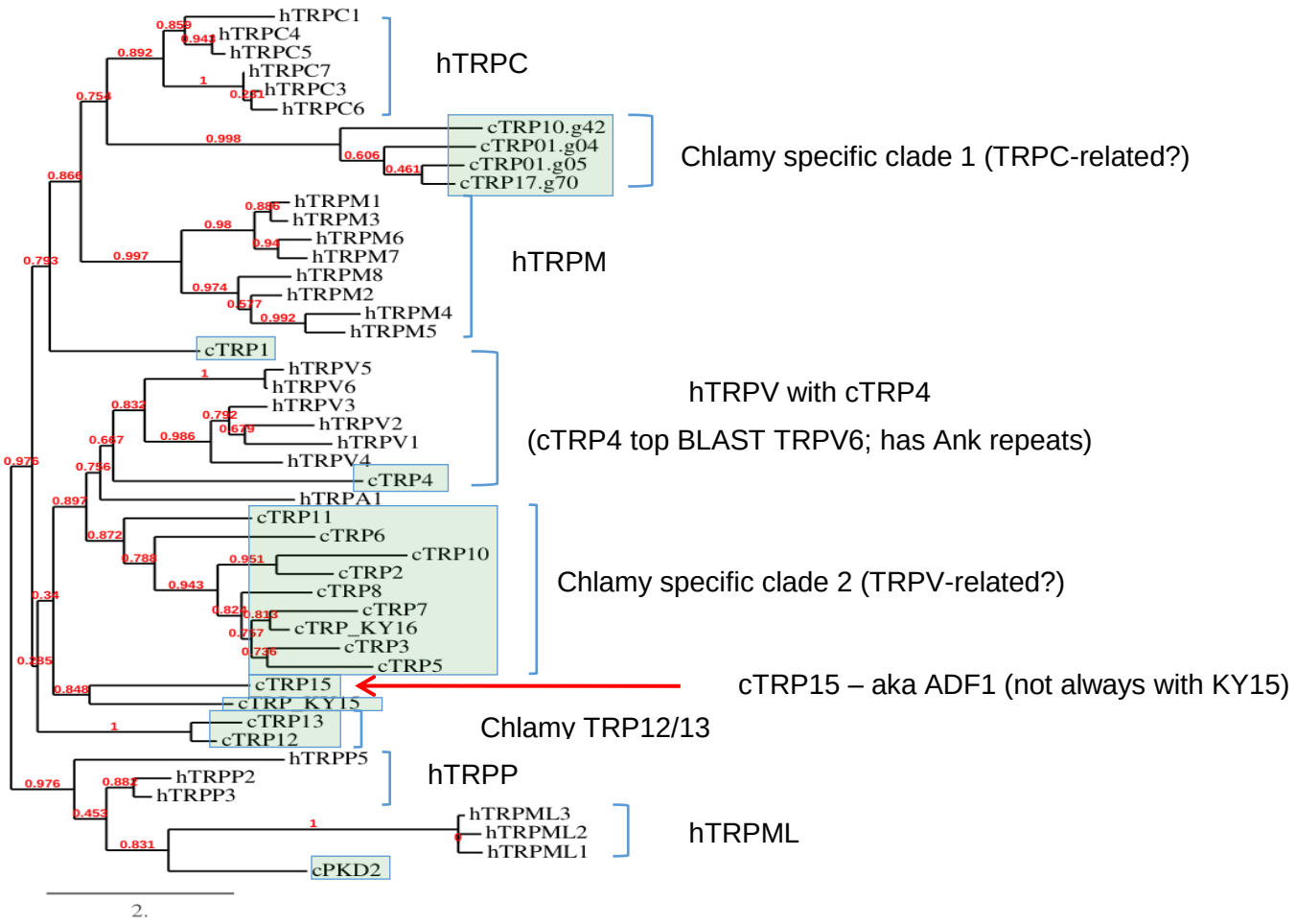

Figure 3.5. Phylogeny of mammalian and Chlamydomonas TRP families

Note. Phylogeny created using only channel domains and XXX MECHANISM. Phylogenetic analysis by Lynne Quarmby. Numbers in red indicate branch support, where 0 is no support and 1 is very strong support

3.7.2. *ADF2*

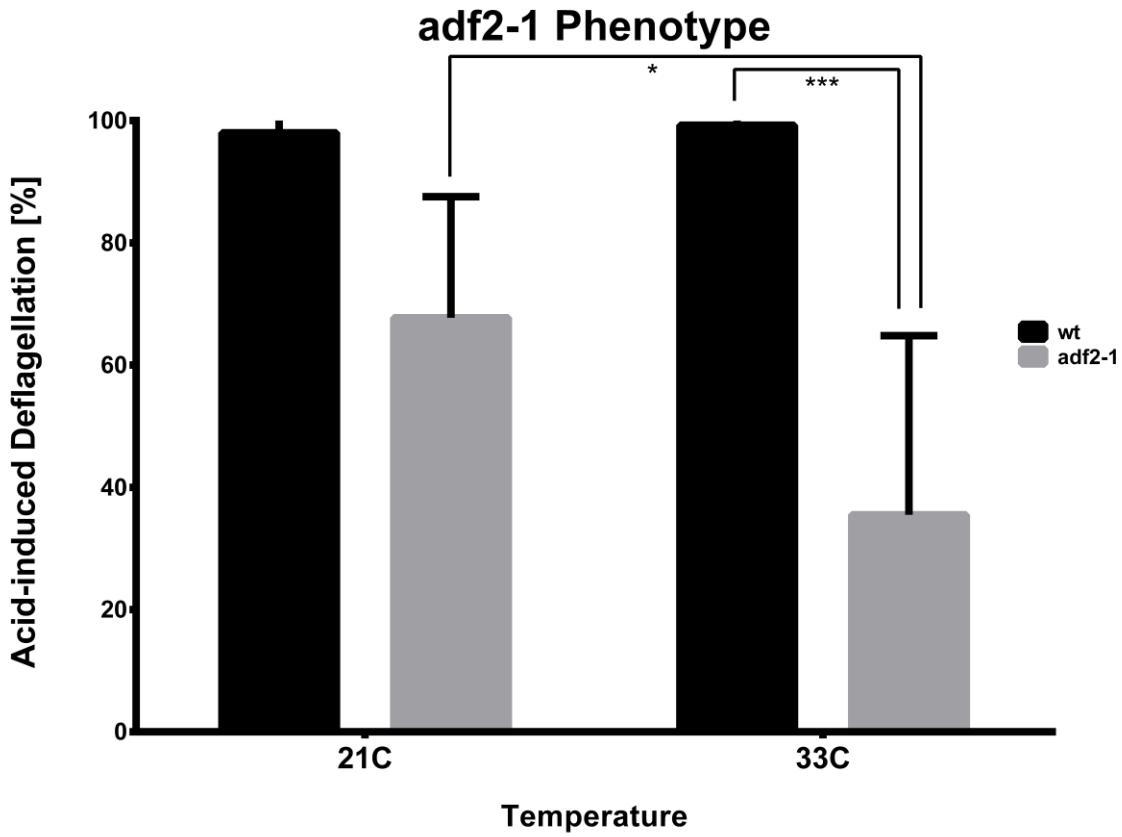

Figure 3.6. Temperature-Sensitive Acid-Induced Deflagellation Phenotype of *adf2-1*

Note. Cells were inoculated for 2 days in liquid TAP at the restrictive temperature (21C), then separated into two cultures and one was shifted to the restrictive temperature (33C) for 6 hours. Standard pH-shock protocol was used to test the deflagellation-phenotype.

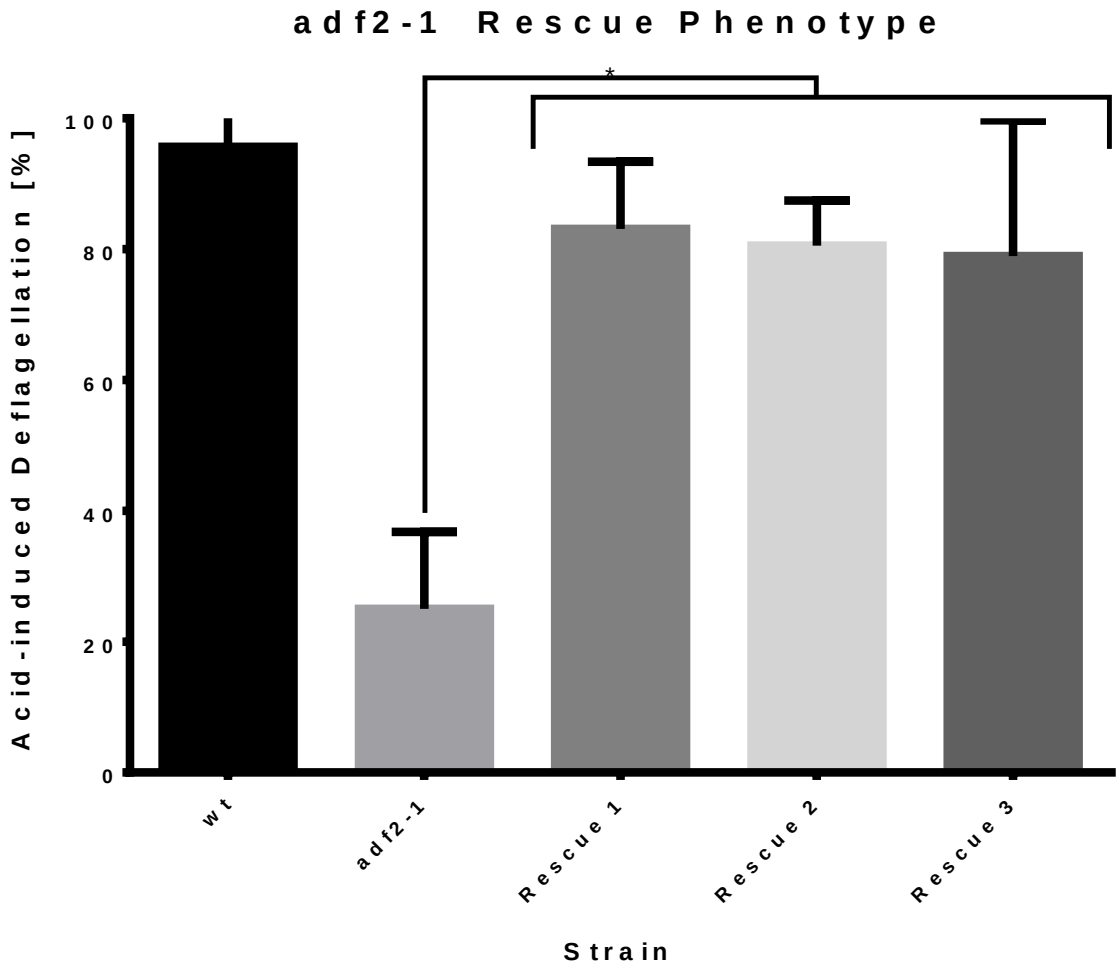

Figure 3.7. Acid-Induced Deflagellation Phenotypes of *adf2-1* Rescue strains

Note. Experiment performed at restrictive temperature of 33C. wt and parental *adf2-1* strains included as controls.

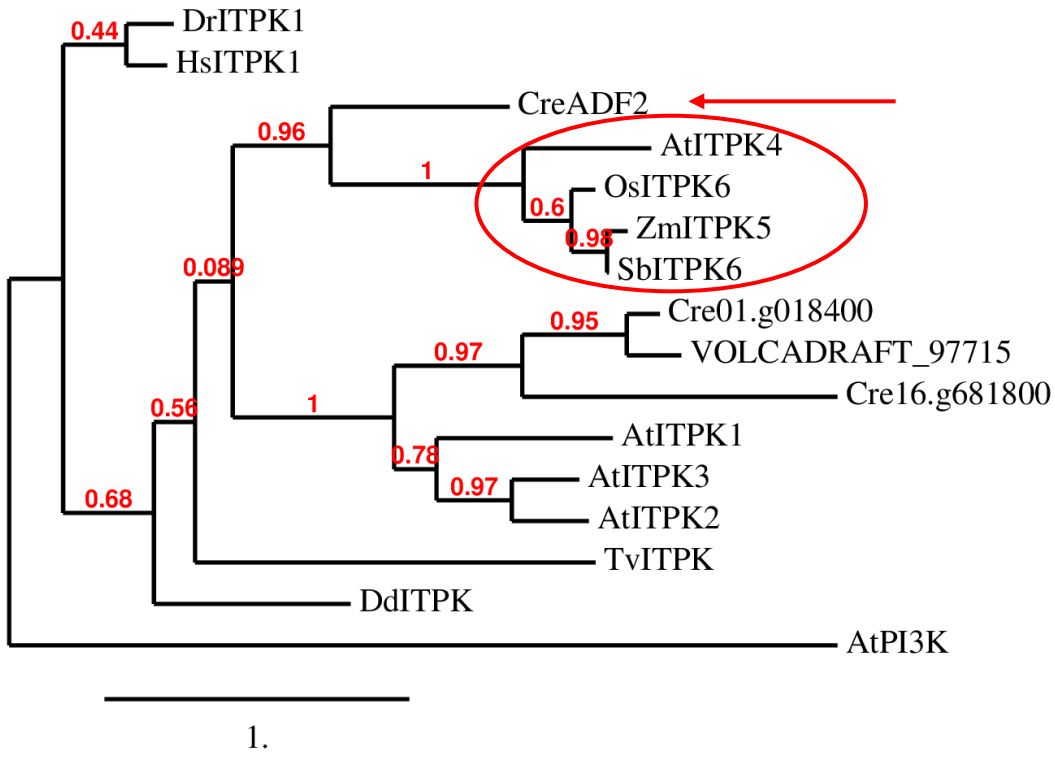

Figure 3.8. Phylogenetic Analysis of ADF2/CreITPK1 and other representative ITPK's.

Note. Red arrow indicates CrITPK1/ADF2. Red circle indicates group of related ITPK members as discussed in Chapter 4.1.2. A different member of inositol metabolism, Arabidopsis thaliana PI3K, was included as the outgroup. For species abbreviations, please consult List of Acronyms, page XI. Members chosen using best BLAST-alignment hits.

3.7.3. *ADF3*

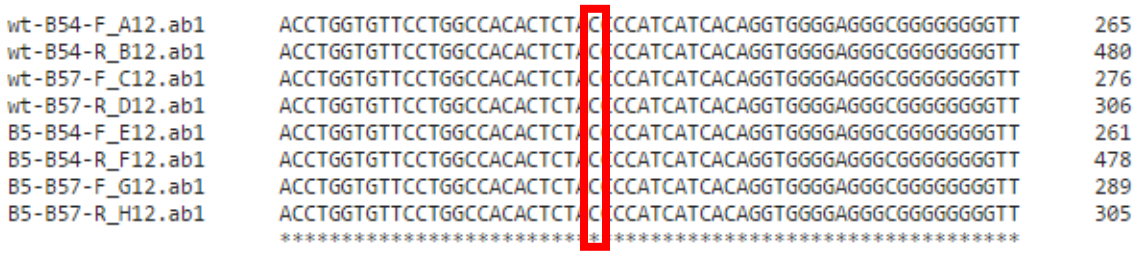

Figure 3.9. Sanger Sequencing Result of B5 and wt Strains

Note. B54 and B57 were custom primers used. F and R indicate forward/reverse respectively. Highlighted with a red bar is the location of the potential mutation suggested by whole genome sequencing. WGS indicated a taC/taA (Y1337*) stop codon introduction which could not be confirmed by sanger sequencing, as all four sequencing runs of B5 contained the original TAC/Y codon, the same as the wild-type copy.

3.7.4. *ADF4*

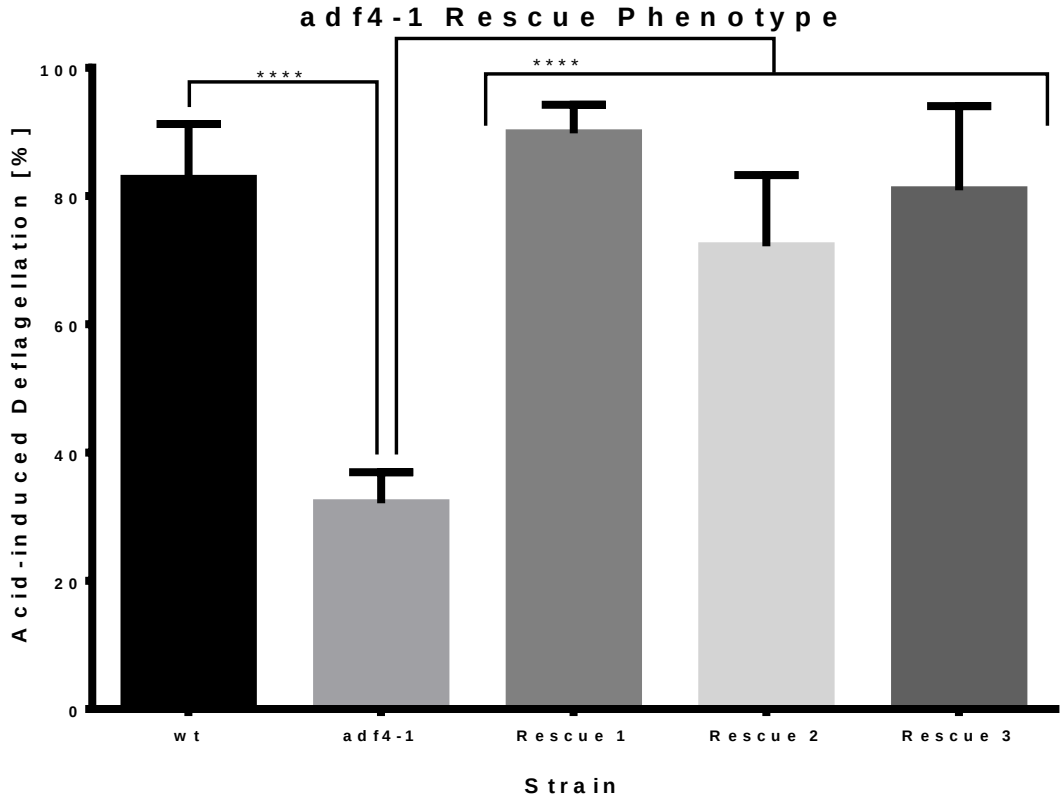

Figure 3.10. Phenotypes of *adf4-1* Rescue Strains

Note. To test whether I had obtained *adf4-1* rescues, we tested their phenotypes under conditions known to induce a deflagellation-defect in the *adf4-1* parental strain, namely 48h in liquid Low-N TAP. Cells were then treated using the standard pH-shock protocol. Wt and *adf4-1* strain shown as controls, as the deflagellation-behaviour of rescues should more closely resemble that of the wild-type strain that that of the *adf4-1* parent.

```
UBA1EX7-2F_adf4      AGGGCCAGGTCTATAGGACATTTTGCCCCCTTGTCGTCCCACCCACTGGCCGCTGCCCTC       80
UBA1EX7-2R_adf4      GGGCCAAGGACTAGAGGACATTTTGCCCCCTTGTCGTCCCACCCACTGGCCGCTGCCCTC      168
UBA1EX7-2F_wt        CGGGCCAGGACTACAGGACATTTTGCCCCCTTGTCGTCCCACCCACTGGCCGCTGCCCTC       79
UBA1EX7-2R_wt        GGGCCAAGGACTAGAGGACATTTTGCCCCCTTGTCGTCCCACCCACTGGCCGCTGCCCTC      300
                      ** * *** *** ******************************************

UBA1EX7-2F_adf4      CCCCCGCCCGCACCTGCATCCCAGCGGCGCGTACTCCTCAGGCCCCGCCGCCGCCAGCTG      140
UBA1EX7-2R_adf4      CCCCCGCCCGCACCTGCATCCCAGCGGCGCGTACTCCTCAGGCCCCGCCGCCGCCAGCTG      228
UBA1EX7-2F_wt        CCCCCGCCCGCACCTGCATCCCAGCGGCGCGTACTCCTCAGGCCCCGCCGCCGCCGCT-G      138
UBA1EX7-2R_wt        CCCCCGCCCGCACCTGCATCCCAGCGGCGCGTACTCCTCAGGCCCCGCCGCCGCCAGCTG      360
                     ***************************************************    *

UBA1EX7-2F_adf4      CTCGGGCTCCGGCAGCGACTCCAGGCTGTCGAAGTAGAGCCACTGGAACACCGGGTGGAA      200
UBA1EX7-2R_adf4      CTCGGGCTCCGGCAGCGACTCCAGGCTGTCGAAGTAGAGCCACTGGAACACCGGGTGGAA      288
UBA1EX7-2F_wt        CTCGGGCTCCGGCAGC-GACTCCGGCTGTCGAAGTAGAGCCACTGGAACACCGGGTGGAA      197
UBA1EX7-2R_wt        CTCGGGCTCCGGCAGCGACTCCAGGCTGTCGAAGTAGAGCCACTGGAACACCGGGTGGAA      420
                     ***************     * ***********************************

UBA1EX7-2F_adf4      CTTGCCGCTGACCGCCTTCACCACCTCCTGGCCCACCACGCCGCCAAACAGGGCCGCCAT      260
UBA1EX7-2R_adf4      CTTGCCGCTGACCGCCTTCACCACCTCCTGGCCCACCACGCCGCCGAACAGGGCCGCCAT      348
UBA1EX7-2F_wt        CTTGCCGCTGACCGCCTTCACCACCTCCTGGCCCACCACGCCCCCAAACAGGGCCGCCAT      257
UBA1EX7-2R_wt        CTTGCCGCTGACCGCCTTCACCACCTCCTGGCCCACCACGCCGCCGAACAGGGCCGCCAT      480
                     ****************************************** ** **************

UBA1EX7-2F_adf4      GGGGCTGACCTCCGCGCCCGCGCAGTGAGCCAGCTTGCCCACCACCGCGCCGTCCACAGC      320
UBA1EX7-2R_adf4      GGGGCTGACCTCCGCGCCCGCGCAGTGAGCCAGCTTGCCCACCACCGCGCCGTCCACAGC      408
UBA1EX7-2F_wt        GGGGCTGACCTCCGCGCCCGCGCAGTGAGCCAGCTTGCCCACCACCGCGCCGTCCACAGC      317
UBA1EX7-2R_wt        GGGGCTGACCTCCGCGCCCGCGCAGTGAGCCAGCTTGCCCACCACCGCGCCGTCCACAGC      540
                     ************************************************************

UBA1EX7-2F_adf4      CTCCAGCCTGGCGGCCGACCCCGCAGCCAGCCCGCCGTTCAGCTGCTCCGCGGCGGCAGT      380
UBA1EX7-2R_adf4      CTCCAGCCTGGCGGCCGACCCCGCAGCCAGCCCGCCGTTCAGCTGCTCCGCGGCGGCAGT      468
UBA1EX7-2F_wt        CTCCAGCCGGGCGGCCGACCCCGCAC-CCGCCCGCCTTTCAGCTGCTCCGCGGCGGCCGT      376
UBA1EX7-2R_wt        CTCCAGCCTGGCGGCCGACCCCGCAGCCAGCCCGCCGTTCAGCTGCTCCGCGGCGGCAGT      600
                     ******** ***************  * ******* ******************** **

UBA1EX7-2F_adf4      CAGCGCGGCGGCGTCGGCGGCGTCGGCGGGGCGCGGCGAGCGGCCGTGCTCGGCCTGCGT      440
UBA1EX7-2R_adf4      CAGCGCGGCGGCGTCGGCGGCGTCGGCGGGGCGCGGCGAGCGGCCGTGCTCGGCCTGCGT      528
UBA1EX7-2F_wt        CAGCGCGGCGGCTTCGGCGGCGTCGGCGGGGCGCGGCGAGCGGCCGTGCTCGGCCTGCGT      436
UBA1EX7-2R_wt        CAGCGCGGCGGCGTCGGCGGCGTCGGCGGGGCGCGGCGAGCGGCCGTGCTCGGCCTGCGT      660
                     ************ ************************************************
```

Figure 3.11. UBA1 Exon 7 Sanger sequencing result

Note. No location where the two sequenced bases of *adf4-1* and the two bases of wt were different were discovered. Locations where bases the two sequences of the same strain were different were attributed to Sanger sequencing errors, possibly due to repetitive and/or high-GC-content sequence.

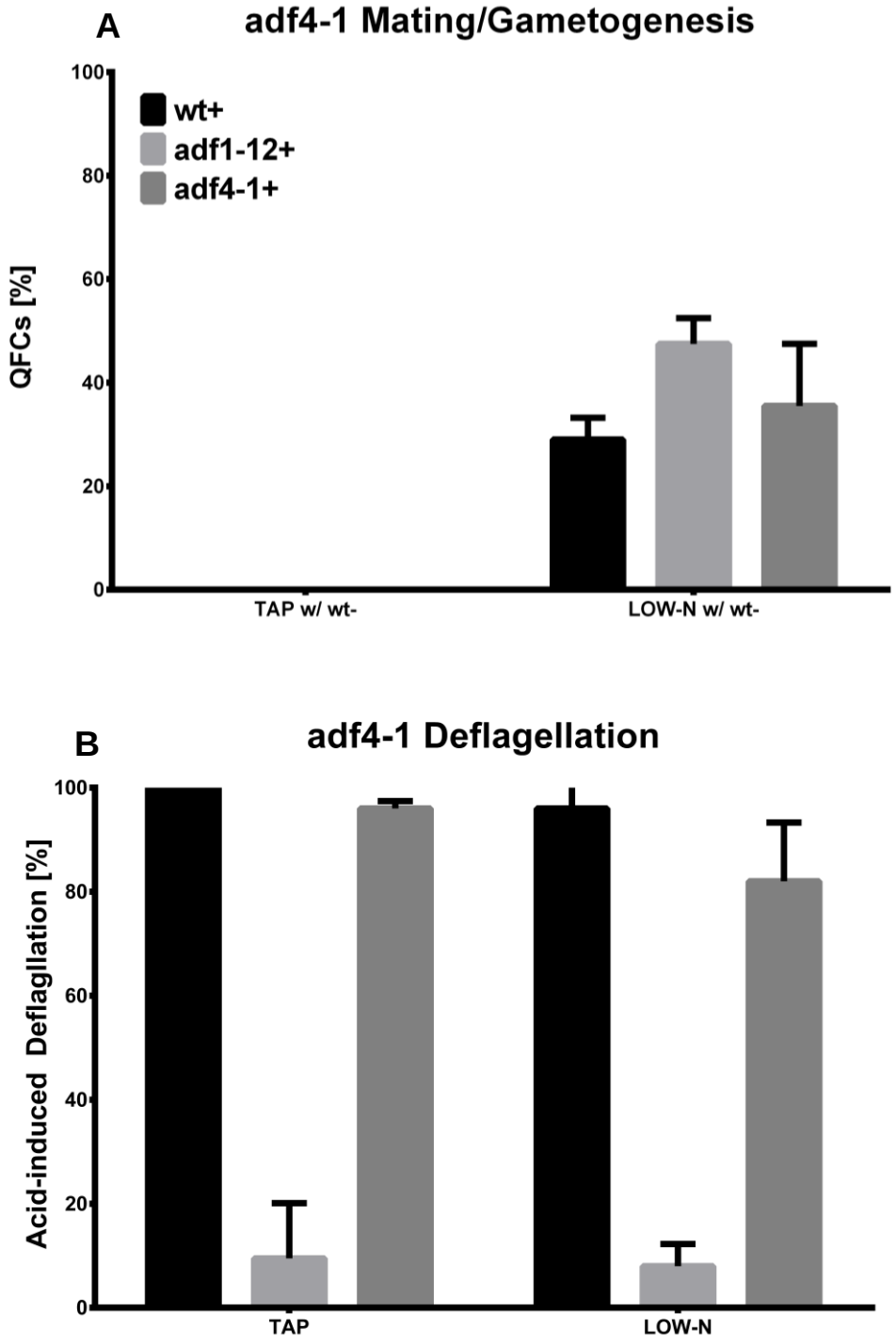

Figure 3.12. ***adf4-1*** **Gametogenesis vs Deflagellation**

Note. To compare gametogenesis with deflagellation, I measured both mating behaviour (A) and deflagellation (B). (A) Axis indicates percentage of quadraflagellate cells as an indication of mating efficiency after cells were inoculated in liquid TAP for 2 days, followed by either 1 day in TAP or low-N TAP. (B) Same conditions as panel A, followed by pH-shock as described in Materials&Methods of Chapter 2.

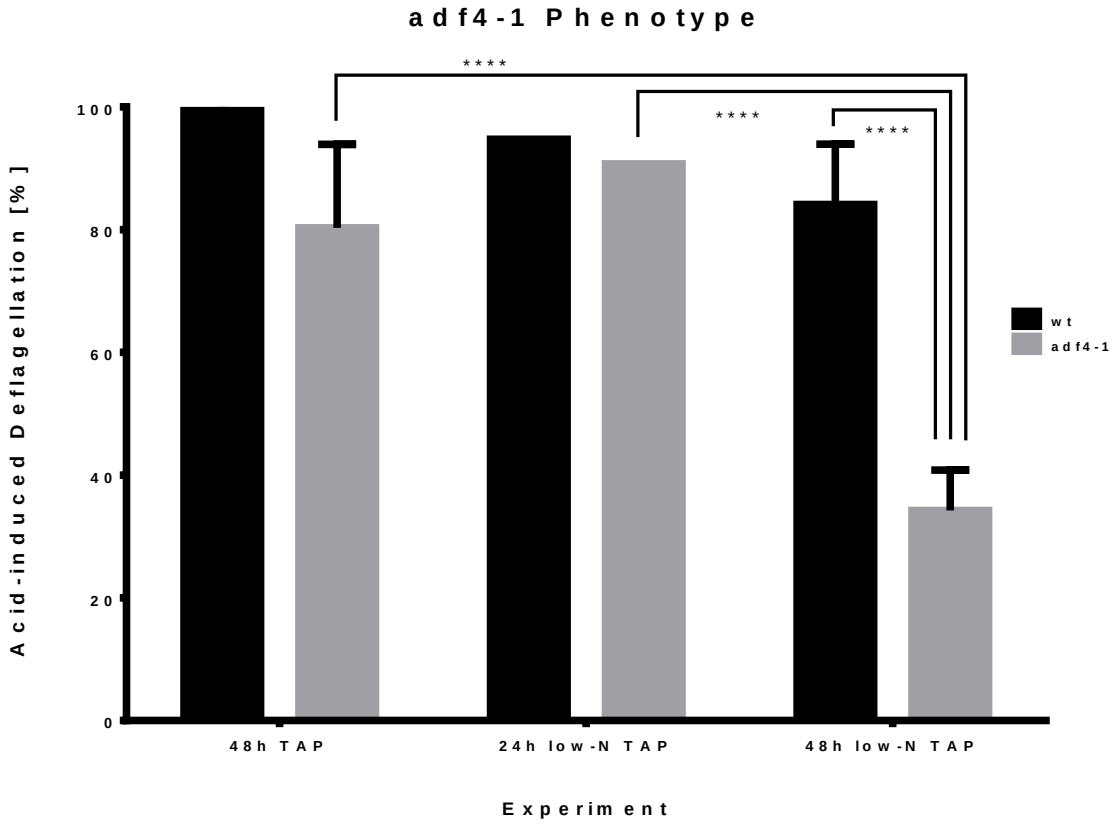

Figure 3.13. The Nitrogen-starvation sensitive ADF-Phenotype of *adf4-1*

Note. Cells were inoculated for 48 hours in liquid TAP medium, then gently centrifuged and resuspended in either low-N TAP (right) or TAP (left and middle). 24 hours later, cells were again gently centrifuged and resuspended in either low-N TAP (middle and right) or TAP (left). Cells were then treated using the standard pH shock protocol. Wt cells included as control.

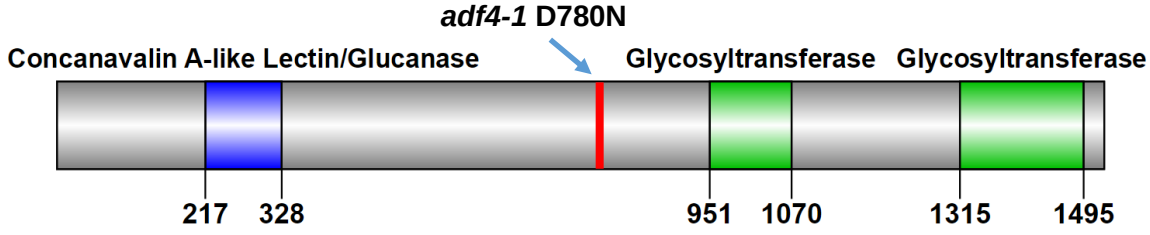

Figure 3.14. Predicted functional domains of ADF4 and causative mutation in *adf4-1*

Note. Predictions based on EMBL-EBI's PFAM (Finn, Bateman et al. 2014). Black numbers indicate start and end of predicted domains. Red line indicates position of predicted D780N mutation in *adf4-1* within the protein.

3.7.5. *ADF5*

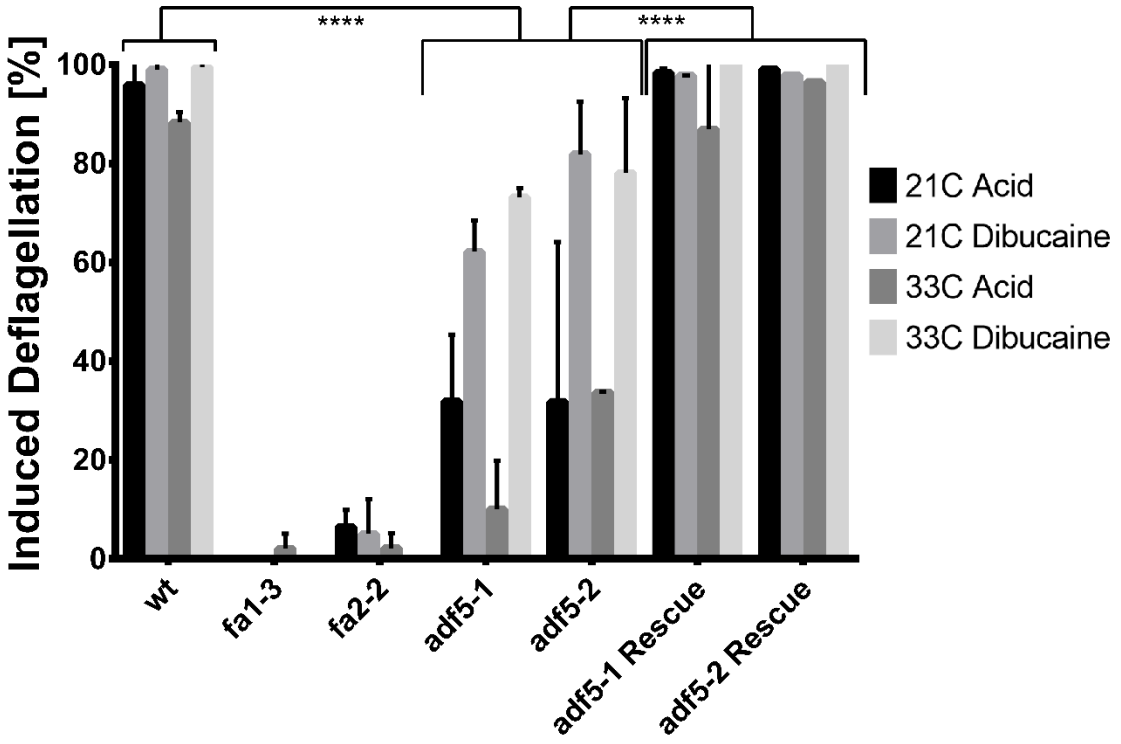

Figure 3.15. Phenotype of *ADF5* and *ADF5*-Rescue strains

Note. Cells were inoculated for 2 days in liquid TAP, then split into two cultures, one of which was moved to 33C for 6 hours. Cells were then treated with standard pH-shock and Dibucaine treatment, respectively. Wild-type, *fa1-3* and *fa2-2* strains were included as controls for potential FA-phenotype.

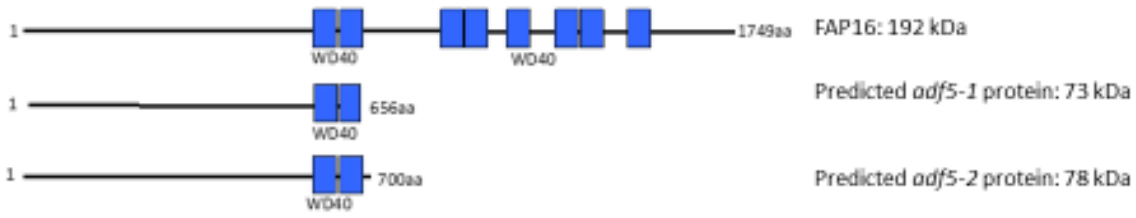

Figure 3.16. Predicted protein and WD40 domains of full-length FAP16 and truncated ADF5-1 and ADF5-2 proteins

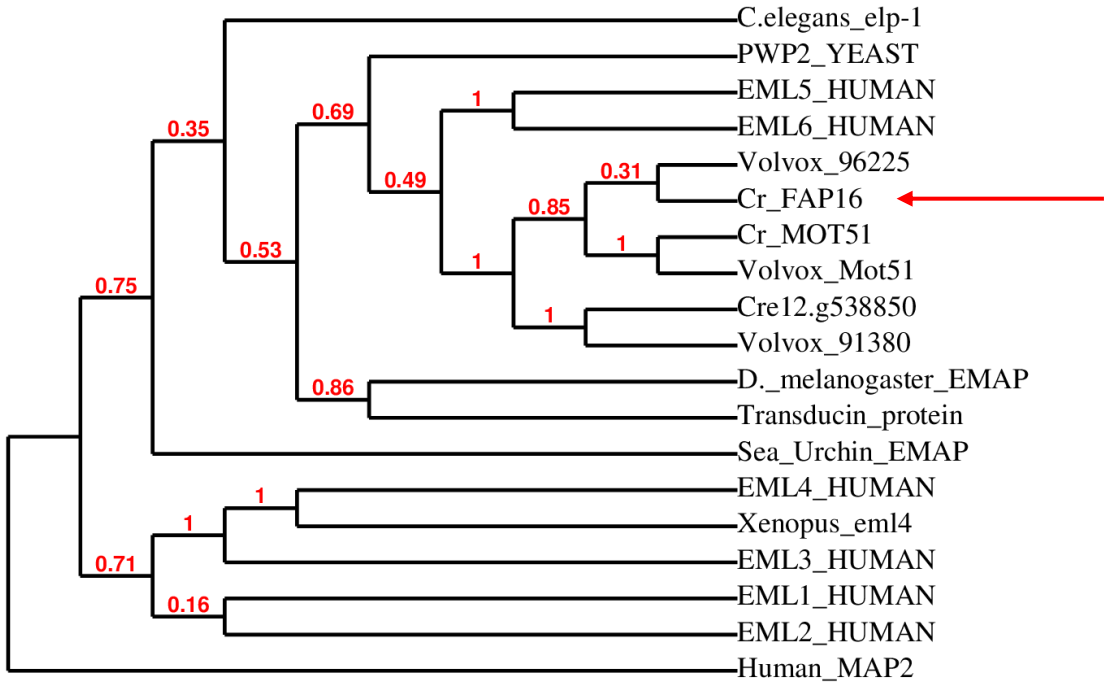

Figure 3.17. Phylogenetic Analysis of FAP16 with EML Proteins

Note. Red arrow indicates FAP16/ADF5. A different microtubule-binding protein, MAP2, was included as an outgroup. Phylogeny created as in Figure 3.8.

3.8. Tables

Table 3.1. Allele Assignments of new deflagellation mutant strains

Strain	Allele Assignment	Supported By
E12 AJ30	*Adf1-7*	Mapping and *adf1-2* non-complementation
E12 P1	*Adf1-8*	Mapping and *adf1-2* non-complementation
E16 A19	*Adf1-9*	Mapping and *adf1-2* non-complementation
E12 AI18	*Adf1-10*	Mapping, *adf1-2* non-complementation and *TRP15* mutation identified by WGS
E12 M20	*Adf1-11*	Mapping and *TRP15* mutation identified by WGS
E11.1 E26	*Adf1-12*	Mapping and *TRP15* mutation identified by WGS
E21 A11	*Adf1-13*	Mapping and *TRP15* mutation identified by WGS
E21 B12	*Adf1-14*	Mapping and *TRP15* mutation identified by WGS
E20 G2	*Adf1-15*	Mapping and *TRP15* mutation identified by WGS
N24	*Adf2-1*	Mapping, *ADF2* mutation identified by WGS and Rescue
E21 B5	*Adf3-1*	Mapping, complementation of *adf1-2* and no *TRP15* mutation identified by WGS
E1P19C5	*Adf3-2*	Mapping, complementation of *adf1-2* and no *TRP15* mutation identified by WGS
E6.1P3A7	*Adf3-3*	Mapping, complementation of adf1-2 and no T*RP15* mutation identified by WGS
E4.1P3H3	*Adf4-1*	Mapping, *ADF4* mutation identified by WGS and Rescue
E3.1 P15 B4	*Adf5-1*	Mapping, *ADF5* mutation identified by WGS and Rescue
E21 C7	*Adf5-2*	Mapping, *ADF5* mutation identified by WGS and Rescue
E4.1P1H3	*Adf6-1*	Not mapped to any other known gene/location

Table 3.2. Kingdom distribution of most significant adf4 BLAST hits

Kingdom	# BLAST-hits ADF4	[%] of total	# BLAST-hits ADF1/ADF2/ADF5	[%] of total
Bacteria	749	88	9/8/0	2/4/0
Eukaryota	25	3	409/184/194	98/96/100
Archaea	73	9	0/0/0	0/0/0
Unclassified	5	0	0/0/0	0/0/0

Note. BLAST performed using http://www.ebi.ac.uk/Tools/hmmer/'s hidden-markov-model BLAST against reference proteomes (Finn, Clements et al. 2011). BLAST-hits with significance of >0.0183 are included. BLAST-hit distribution of ADF1/ADF2/ADF5 included for comparison

Chapter 4. Discussion

4.1. Enrichment

The genetic screen for deflagellation mutants performed by Finst et al. (1998) recovered multiple alleles of all three genes isolated in the screen, most of them using insertional mutagenesis. This indicated that despite the low number of genes found, the insertional mutagenesis screen was saturated, meaning that repeating it with the same conditions was unlikely to yield novel deflagellation mutants, yet based on what was known about deflagellation, it was clear that more than these three genes had to be involved (Quarmby 2009). In the genetic screen presented in this thesis, I have isolated mutant alleles of all three known deflagellation genes as well as mutant alleles of at least four novel deflagellation genes.

Furthermore, as I was able to only isolate one to two alleles of *ADF2*, *ADF4* and *ADF5* and identified no obvious candidate calcium-sensing or microtubule-severing gene, there are likely more players in this pathway still to be found. A possible explanation for not isolating any of these players is that our screen involved an enrichment step that required pH-shocked cells to be able to exhibit phototaxis. If a mutation leads to a cell being unable to shed its flagella, but also renders it unable to swim, we likely would have not identified it in this screen. This explanation is supported by us not identifying any additional FA-mutants. These proteins specifically might be important structural components of the cilium, disrupting which might lead to a swimming defect. This is supported by defects other integral flagellar components such as kinesin, hydin and radial spokes also exhibiting a defect in phototaxis or general motility (Kozminski, Beech et al. 1995; Yang, Yang et al. 2004; Lechtreck and Witman 2007).

I also did not achieve much higher rate of enrichment for mutants than in the previous screen (2.3:2000 in this screen vs. 1:2000 in the previous, for UV mutagenesis only), again indicating that an optimization of the enrichment protocol to retain non-

swimming, but flagellated cells should be considered in further screens. Had the enrichment produced a higher-fold mutant yield, I might have been able to uncover further deflagellation genes, given that this novel screen was likely not saturated yet. One of the reasons for using the restrictive temperature of 33C for our screen was that we hypothesized that essential genes might be part of the pathway, as the Quarmby lab has long hypothesized that deflagellation might share components with the severing event that occurs during pre-mitotic resorption. A higher enrichment yield might thus have also led to the discovery of essential genes, as introducing conditional, temperature-sensitive mutations (the only way to isolate such genes) is much rarer than unconditional variants.

4.2. Whole Genome Sequencing

One of our initial motivations to perform a novel screen was our hope that advances in next-generation sequencing would allow us to more easily identify causative point-mutations when combined with PCR-based recombination mapping. This was because UV-mutagenesis in *Chlamydomonas*, as opposed to insertional mutagenesis, was much more likely to introduce point mutations in genes, which are more readily detected using WGS. Large insertions are more difficult to detect using WGS, which relies on proper assembly of sequenced DNA to the reference genome. While for some strains, assignment of a potential causative gene was readily possible due to the hypothesized presence of multiple alleles (*adf5-1* and *adf5-2*), obvious single candidates from WGS in the mapped region and successes with obtaining rescues (*adf2-1*, *adf4-1*, *adf5-1* and *adf5-2*), I had less success with other strains.

The complementation groups *ADF1*, I, II and III caused problems as some mutations were found in the same gene (*TRP15*), despite QFC-experiments indicating that they were potentially separate genes. WGS sequence was also of highly varying coverage and quality and I was uncertain which mutations were real and which were artifacts. I was only able to successfully PCR-amplify and Sanger sequence a fragment covering one putative *TRP15* mutation in E21 B5 of complementation group I and our sequencing results indicate that the mutation detected by WGS is, in fact, a WGS artifact and not real. Difficulties to create fragments suitable for Sanger sequencing might stem

from the *ADF1*-region being highly repetitive and GC-rich, increasing the potential that primers designed either do not bind or bind to multiple locations and leading to the amplification of multiple similarly-sized fragments.

I was also unable to rescue Group I, Group II or further *ADF1* mutants with either whole BAC DNA or restriction fragments that included the *TRP15* gene. As previous studies' attempts to rescue the *ADF1* gene also led to only the obtaining of a single rescue from over 2000 transformants screened, this might be inherent to *TRP15* and its ~20kb size, given the particular nature of *Chlamydomonas* to digest foreign DNA it is transformed with, as described in Chapter 2.1.2. The gene might also require further upstream or downstream sequences that are more likely to be interrupted by digestion the larger the distance to *TRP15* becomes.

To resolve the issue of poor sequencing coverage, I decided to follow two avenues. Firstly, I re-analyzed the existing sequencing data based on the newly-released v5.0 *Chlamydomonas* reference genome to see if candidate gene predictions changed. Secondly, I decided to re-sequence strains with poor coverage and more un-sequenced strains using our own, PCR-free library preparation, as the choice of library prep as previously described has a large impact on the success of WGS. After re-sequencing I was able to resolve some of the aforementioned issues. The coverage of the *TRP15* gene proved to be much better using our own library preparation when compared to the commercial library preparation (shown using the comparative strain G2, which was sequenced multiple times using different methods), allowing us to identify mutations in *TRP15* in 9 strains sequenced.

Additionally, 3 strains belonging to the complementation group B5 are lacking mutations in *TRP15* and are thus likely alleles of a separate gene I call *ADF3*. I was, however, unable to identify variants in a gene which all three strains had in common and its identity remains unknown. It is possible that NGS did not detect the causative mutations in these strains due to a lack of coverage in difficult-to-sequence regions or mutations that are far enough up- or downstream of coding sequence of a gene that they were not detected as having an impact on the potential causative gene. One way to potentially resolve this would be to narrow down the candidate gene by designing a large

variety of custom primers near the linked *PSBO* region. Then, after hopefully narrowing it down to a reasonable size, one could try and rescue the defects with multiple BACs, similar to how the *adf1-3* Rescue was obtained. Given the low rate of recombination in the *ADF1* region and the large to-be covered genomic region it left for BAC rescues, this might however prove to be similarly difficult.

4.3. Newly Identified Deflagellation Genes

4.3.1. *ADF1*

After 20 years of trying, we have successfully identified *ADF1* as the *TRP15* gene. TRPs are ion channels permeable to a variety of cations such as Calcium or Sodium. They are expressed in a variety of tissues and serve many different functions, such as stress reception (through TRPA and its Ankyrin repeats) and are associated with different diseases. Amongst these diseases is polycystic kidney disease (PKD), which can be caused by mutations in a variety of ciliary genes, further raising our interest in having identified a potential TRP channel as part of the deflagellation pathway (Pazour, Dickert et al. 2000; Gudermann 2005). It is important to note that the Quarmby lab has shown that the NIMA-related kinase FA2, a different previously described protein in the deflagellation pathway, localizes to proximal cilia in mouse kidney cells and mutations in two related proteins, the NIMA-related kinases Nek1 and Nek8 cause polycystic kidney disease in mice models (Mahjoub, Rasi et al. 2004; Mahjoub, Trapp et al. 2005). Nek8 also localizes to the same ciliary region as FA2. This supports the hypothesis that an orthologous pathway might underlie disease progression in the kidney and deflagellation in *Chlamydomonas*.

It was furthermore previously shown that an increase in IP3 occurs together with deflagellation and neomycin, a PLC-inhibitor, blocks both IP3-increase and deflagellation (Quarmby, Yueh et al. 1992; Yueh and Crain 1993). Some TRP-channels are known to be activated by both IP3 and DAG (both breakdown products of PLC-activation) as well (Numata, Kiyonaka et al. 2011; Delgado, Munoz et al. 2014). They may also be activated by N-linked glycosylation (Wirkner, Hognestad et al. 2005). Most interestingly, recent studies have shown that some TRP-channels such as polycystic kidney disease

1-like 3 (PKD1L3) and TRPC5 can be directly activated by sensing changes in pH similar to the acid-shock that is used to trigger deflagellation (Inada, Kawabata et al. 2008; Kim, Jeon et al. 2008). These links provide multiple way in which TRP15-mediated influx of extracellular calcium may be activated to cause deflagellation and supports the identity of TRP15 as a TRP-family member. Because we have long hypothesized that a calcium-channel needed to be part of the deflagellation pathway, we are happy to see multiple experimental results provide evidence that TRP15 is such a channel. I thus hypothesize that ADF1/TRP15 is the ion-channel responsible for the initial calcium-influx during acid-induced deflagellation and may be activated by pH-shock directly, or by mechanisms involving other proteins in the deflagellation pathway. One way to test this potential function of ADF1 would be to perform experiments similar to during early analysis of the deflagellation pathway, where calcium-influx was measured using radiolabelled calcium (Quarmby 1996).

4.3.2. *ADF2*

I have identified ADF2 as the Chlamydomonas homologue of ITPK1 with close similarity to a smaller subgroup of ITPK1's that have been previously clustered together and also cluster together in our own phylogenetic analysis. This subgroup consists of AtITPK4, OsITPK6, SbITPK6 and ZmITPK5, all plant proteins. The two proteins of these that have been studied (AtITPK4 and OsITPK6) both mediate the phosphorylation of inositol-1,3,4-trisphosphate to either inositol-1,3,4,5-tetrakisphosphate or inositol-1,3,4,6-tetrakisphosphate (Sweetman, Stavridou et al. 2007; Du, Liu et al. 2011). The former is a substrate in recycling the secondary messenger inositol-1,4,5-trisphosphate (IP3), while the latter is an important intermediary product in the anabolism of inositol-1,2,3,4,5,6-Hexaphosphate (IP6, also known as phytic acid) (Chamberlain, Qian et al. 2007; Shears 2009; Singh, Mohammad et al. 2011). Mutations in *AtITPK4* or *AtITPK1* lead to 50% decreased levels of IP6, supporting the role of ITPK1 in IP6-metabolism (Kim and Tai 2011).

Some ITPK1's also possess the ability to interconvert inositol-1,3,4,5,6-pentakisphosphate and inositol-3,4,5,6-tetrakisphosphate, another second messenger, as an isomerase (Ho, Yang et al. 2002). AtITPK4 is a notable exception to this

isomerase activity, which is instead capable of isomerizing inositol-1,3,4,5-tetrakisphosphate and inositol-1,4,5,6-tetrakisphosphate, a metabolite of a minor, secondary pathway to generate IP5 and ultimately IP6 from IP3 (Saiardi, Erdjument-Bromage et al. 1999; Sweetman, Stavridou et al. 2007). This minor pathway may also be what causes the remaining synthesis of IP6 in *AtITPK1* knockouts. An overview of the Inositol-pathway with the potential effects of a loss of CrITPK1/ADF2 is shown in figure 4.1.

Because the mutation in *adf2-1* is an early stop codon which lies before any functional domain, I was originally surprised to see that the deflagellation-defective phenotype of *adf2-1* is temperature-sensitive. As a minor-pathway in IP6-synthesis exists and IP3 can be synthesized without recycling as well, this might explain the phenotype. I hypothesize that at the restrictive temperature there is increased need for one or more of the products metabolised redundantly by functional ADF2 and the deflagellation-defective phenotype is caused by the lack ADF2 activity in *adf2-1* cells. This hypothesis is supported by multiple inositol members protecting cells from osmotic pressures at higher temperatures and IP6 content increases in rice as temperature increases (Santos and Da Costa 2002; Su, Lei et al. 2014). ITPK1 in rice is also essential for proper salt stress and drought responses (Du, Liu et al. 2011).

As previously mentioned, IP3 may also be in itself a trigger for deflagellation and can activate TRP-channels by itself (Quarmby, Yueh et al. 1992; Yueh and Crain 1993). It is also an important activator of calcium-release by intracellular calcium-stores (Chu, Sun et al. 2006). Furthermore, inositol 1,4,5,6-tetrakisphosphate and inositol-3,4,5,6-tetrakisphosphate can act as molecular activators or deactivators in response to changes in pH, providing another potential link to acid-shock induced deflagellation (Blum-Held, Bernard et al. 2001). IP6 has anti-tumour capabilities and it has previously been shown that a hallmark of cancer is often the complete absence of cilia to allow for increased cell-division (Pan, Seeger-Nukpezah et al. 2013). Furthermore, gene-wide association studies have shown that a 3.5-fold increase in platelet count is linked with mutations in human *ITPK1*, indicating cell-cycle dysregulation and lending support to the correlation between cell cycle defects and inositol metabolism through ITPK1 (Gieger, Radhakrishnan et al. 2011). It is thus possible that IP6 acts as an anti-tumour factor

through healthy cilia by allowing them to inhibit cell division. Defects in IP6 metabolism would then lead to increased cell division through an impact on proper ciliary function. Indeed, in zebrafish, reduced levels of IPK1, the enzyme that produces IP6 from IP5, lead to inhibited ciliary beating and reduced ciliary length and IPK1 localization is enriched in centrosomes and basal bodies (Sarmah, Winfrey et al. 2007).

Studies have also shown a link between IP6 and calcium-signaling, as IP6 is capable of binding Ca^{2+} and IPK1 knockdown reduces calcium-flux and leads to left-right asymmetry defects during development (Simpson and Wise 1990; Sarmah, Latimer et al. 2005; Sarmah, Winfrey et al. 2007). Interestingly, this process during development relies on proper ciliary beating and calcium oscillations, providing another link between cilia, inositol-metabolism and *ADF2/ITPK1* (Yuan, Zhao et al. 2015). Injection of inositol-1,3,4,6-tetrakisphosphate or IP3 into zebrafish oocytes and inositol-3,4,5,6-tetrakisphosphate in fibroblasts all evoke Ca2+-flux through the release of intracellular calcium stores and the influx of extracellular calcium as well (Ivorra, Gigg et al. 1991; Hashii, Hirata et al. 1994).

As I have identified ADF2 as the Chlamydomonas homologue of ITPK1, it is likely involved in both IP6 and IP3 metabolism. The established relationships between ITPK1, IP6/IP3, ciliopathies, calcium-signaling and the links between IP3, calcium and deflagellation make *ADF2* an extremely interesting gene in the deflagellation pathway. I hypothesize that it might have an effect on the pathway through the IP3-mediated activation of calcium-influx by ADF1 or in calcium homeostasis and –flux modulated by IP6.

4.3.3. *ADF4*

With the exception of its close evolutionary neighbour *Volvox carteri*, the top BLAST-hits for ADF4 (E values between e^-48 and e^-70) were prokaryotic.

Interestingly, a proteomic study revealed that ADF4 localizes to the chloroplast under aerobic conditions, but not under anaerobic conditions (Terashima, Specht et al. 2010). Chloroplasts are the organelle the least divergent from bacteria in eukaryotic cells, a fact supported by plants requiring proteins highly homologous to bacterial

proteins for chloroplast division, as well as ribosomes of both chloroplasts and bacteria sharing higher homology with each other than with ribosomes associated with nuclear DNA (Harris, Boynton et al. 1994; Osteryoung, Stokes et al. 1998). In *Chlamydomonas*, anaerobic metabolism is most commonly induced by either shifting cells into the dark or sulfur-starvation, upon which many transcriptional changes occur that change energy production from photosynthesis to pyruvate/acetate-breakdown. Glycosyltransferases that interact with the Chloroplast are mainly responsible for chloroplast membrane synthesis and all belong to the GT4 family (Ulvskov, Paiva et al. 2013). Intriguingly, members of this family are also responsible for GPI-anchor synthesis (PIG-A) and N-linked glycosylation (ALG2/ALG11).

The closest BLAST-homology hit to the predicted glycosyltransferase (GT) ADF4 with experimental evidence is the phylogenetically distant PimA PROTEIN in *Mycobacterium smegmatis* (e^-11), which shares 53% sequence similarity and 33% sequence identity with ADF4 for the second predicted 214 amino acid glycosyltransferase type 1 domain of ADF4. In this domain, notable sequence conservation between both PimA and ADF4 occurs at a site essential for PimA substrate-binding (PGKG in ADF4 vs. PRKG in PimA), as well as a sequence conserved amongst all type 1 domains (AMAAG sequence completely aligns between both ADF4 and PimA).

The bacterial protein is involved in incorporating GDP-D-mannose into phosphatidylinositol (PI), the essential first step in synthesis of the extracellular-protein anchor PIM (Kordulakova, Gilleron et al. 2002). The primary eukaryotic orthologue of PIM-anchors are Glycophosphatidylinositol (GPI-anchors), and PimA is functionally orthologous to the protein responsible for the first step in GPI-anchor synthesis, PIG-A (Guerin, Kordulakova et al. 2007). GPI-anchors are well-described in the literature as membrane-anchors for extracellular proteins that do not possess transmembrane-domains themselves (Varki 2009). In *Chlamydomonas reinhardtii*, PIG-A is encoded by *GPI1*/Cre01.g006800 which, like ADF4, possesses a glycosyltransferase type 1 transfer domain. However, as ADF4 lacks a predicted PIG-A domain, the functional domain responsible for GPI-anchor synthesis, and it is thus unlikely that ADF4 is directly

involved in GPI-anchor synthesis. Furthermore, as PIM-anchors are present only in bacteria, the relevance of this to predicting ADF4 function is limited.

This hypothesis that ADF4 might be involved in a bacterial-type mechanism adopted by *Chlamydomonas* is supported by some *Chlamydomonas* and *Arabidopsis thaliana* pathways such as urea catabolism being adopted bacterial-like processes instead of eukaryotic ones, establishing precedent of such usage (Sussenbach and Strijkert 1969; Ludwig 1993; Harris 2009). This is especially relevant as urea catabolism is upregulated and required to recycle nitrogen in the absence of an extracellular nitrogen source and the deflagellation-defect in *adf4-1* is strongly enhanced by nitrogen-starvation (Park, Wang et al. 2015). Furthermore, with the many previously discussed ties between ciliopathies and kidney disease, one important thing to note is that the second largest location of urea catabolism in humans is the kidney (Weiner, Mitch et al. 2015). There, polycystic kidney disease (PKD), which the family of the deflagellation gene *FA2* has also been implicated with, among else leads to an increase in serum urea levels, indicating that urea cycle abnormalities correlate with PKD (Mahjoub, Rasi et al. 2004; Ma, Tian et al. 2013). If ADF4 plays a part in the bacterial-type urea catabolism under nitrogen-starvation, this would explain both its defect being nitrogen-starvation specific (as it would primarily be used under those conditions) and its most significant BLAST hits being prokaryotic (as the pathway is adopted from bacteria). I thus hypothesize that *adf4-1*, a nitrogen-starvation-sensitive deflagellation mutant, might be defective in a bacterial-type pathway, possibly related to urea catabolism.

In *Chlamydomonas*, the function and use of GDP-D-mannose is poorly studied, although there is evidence that it is used to produce intermediates in transglycosylation, which is the transfer of glycosylated groups from one protein or lipid to another (Lang 1984). Mannose is also the most common carbohydrate to be added to proteins during N-glycosylation (Mathieu-Rivet, Scholz et al. 2013).

The role of PI, on the other hand, has been much more thoroughly described and it is part of multiple signaling pathways. Firstly, as a breakdown product of glycerophospholipids, PI is a major substrate for inositol phosphate metabolism which may ultimately result in synthesis of secondary messengers such as IP3 or IP6/phytic

acid (Irvine, Letcher et al. 1992; Molendijk and Irvine 1998). The metabolism of both IP3 and IP6 may be also be affected by ADF2/ITPK1, as discussed in the previous section and this provides a potential indirect interaction between ADF2 and ADF4 as components of both the deflagellation pathway and inositol metabolism. Secondly, phosphatidylinositol is itself a phospholipid and membrane component in *Chlamydomonas reinhardtii* and when phosphorylated at one or multiple positions, PI's serve as major docking sites for proteins and mediate intracellular signal propagation (Rochaix, Goldschmidt-Clermont et al. 1998). ADF4 also possesses a predicted Concanavalin A/Lectin-like domain, which aids proteins in recognizing and binding to carbohydrates (Mandal and Brewer 1992; Ramstrom, Lohmann et al. 2004). In a systems-level network analysis of nitrogen-starvation responses in *Chlamydomonas*, myo-inositol, a metabolite of phosphatidylinositol, has been shown to be at the centre of the interaction between nitrogen metabolism and lipid biosynthesis, linking the nitrogen-sensitive phenotype of *adf4-1* to its potential function in the inositol pathway (Valledor, Furuhashi et al. 2014; Park, Wang et al. 2015). I thus hypothesize that ADF4 might bind to glycerophospholipids to catalyze their breakdown and to provide the inositol phosphate pathway with phosphatidylinositol.

It is also possible that ADF4 is itself involved in the bioavailability of nitrogen upon nitrogen-starvation. Intracellular levels of asparagine, whose nitrogen atom is the target of N-linked glycosylation in proteins, are heavily increased upon nitrogen-starvation and proteins that contain asparagine and are subject to N-linked glycosylation are often metabolized to recycle and provide free nitrogen (Tillmann, Gunther et al. 1987; Hanks, Hearnes et al. 2003; Mathieu-Rivet, Scholz et al. 2013). N-linked glycosylation is furthermore one mechanism in which TRP- and other channels can affected in a variety of ways (Cohen 2006). De-glycosylation of TRPV5, for example, traps the channel in the apical membrane and allows for calcium-influx, while glycosylation of the voltage-gated potassium channel Shaker increases its stability and thereby function (Khanna, Myers et al. 2001; Chang, Hoefs et al. 2005). Glycosylation of HERG, a TRP-like channel allows its translocation to the plasma membrane and in a hallmark study it was shown that the same is true for GLUT1, the main glucose transporter (Asano, Katagiri et al. 1991; Petrecca, Atanasiu et al. 1999). Additionally, N-linked glycosylation protects proteins from proteolysis – a process that is increased

during nitrogen starvation (Wormald and Dwek 1999; Strosser, Ludke et al. 2004). As such, ADF4 might protect others members of the deflagellation pathway, specifically ADF1/TRP15, from degradation and the defects in *adf4-1* leading to a decrease in levels of ADF1 might cause its deflagellation-defect upon nitrogen starvation.

In light of all this data, I thus hypothesize that ADF4 might act in one of several ways. Firstly, it might be part of the breakdown of N-glycosylated substrates to provide free nitrogen. A failure to do so in response to nitrogen-starvation might explain the nitrogen-starvation-sensitive deflagellation phenotype of *adf4-1*. It might also play a role in a bacterial-type breakdown of glycosylated phosphatidylinositol to provide the inositol phosphate pathway with a substrate for eventual IP3/IP6 synthesis, both important second messengers potentially linked to deflagellation, providing a possible link to another new member of the deflagellation pathway, ADF2/ITPK1. Lastly, it might also regulate localization or activation of the predicted calcium-channel ADF1/TRP15 itself.

4.3.4. *ADF5*

We have identified ADF5 as the flagellar-associated protein FAP16, which possesses homology to the EML-family of proteins. The single *C.elegans* EML protein, ELP-1, associates with microtubules and is required for touch sensation through its cilia and its loss leads to paralysis and death (Hueston, Herren et al. 2008; Hueston and Suprenant 2009). Human EML1 is required for proper neuron migration and mutations in EML1 can cause Usher's syndrome, a genetic form of deafness-blindness due to ciliary degeneration (Eudy, Ma-Edmonds et al. 1997; Lyman and Chetkovich 2015). EML3 is required for proper chromosomal arrangement during cell division, while EML4 is essential for microtubule formation (Pollmann, Parwaresch et al. 2006; Tegha-Dunghu, Neumann et al. 2008). Gene-wide association studies have also shown a link between schizophrenia and EML5, which is highly expressed in the rat hippocampus and cerebellum (O'Connor, Houtman et al. 2004) (Chen, Lee et al. 2011). Only recently has schizophrenia been discovered as being linked to ciliary defects through proteins such as the basal body protein AHL1 (Amann-Zalcenstein, Avidan et al. 2006). In sea urchin embryos, the sole EML-homologue EMAP is the most abundant microtubule-binding protein in the mitotic apparatus (Suprenant, Tuxhorn et al. 2000). Given the manifold

flagellar interactions and defects caused by the loss of these closely related proteins, this makes FAP16 a particularly interesting protein with regards to deflagellation.

FAP16 shows high co-expression (with a Pearson's coefficient of 0.95, where +1 is total positive correlation) with the flagellar outer row dynein assembly protein ODA7, as the name suggests a protein important in providing a structural link between outer and inner dyneins and the loss of the human orthologue of ODA7 leads to immotile cilia (Freshour, Yokoyama et al. 2007; Duquesnoy, Escudier et al. 2009). Furthermore, of the 23 annotated *Chlamydomonas* genes with the highest co-expression values, more than half (12) are flagellar genes and five encode microtubule-binding proteins, including the two dynein heavy chain-encoding genes DHC2 and DHC13/ODA11.

I hypothesize that FAP16 plays an important role in signal transmission between intracellular and flagellar components of the deflagellation pathway and dynein-mediated IFT/binding to microtubules is required for signals to be transmitted between those two cellular compartments. FAP16 might associate with ODA7 or other microtubule-binding proteins to form a complex to carry out this function. WD-40 proteins such as FAP16 known to associate with dynein exist, such as dynein intermediate chain (DIC) and Lissencephaly 1 (LIS1), a protein essential for dynein function (Ligon, Tokito et al. 2004; Kardon and Vale 2009). Expression data also revealed a 19-fold increase in levels of FAP16 10 minutes after the initiation of ciliogenesis, further lending support that FAP16 plays an integral role not just in flagella in general, but also during flagellar assembly (Albee, Kwan et al. 2013). While the role of WD40-domains in proteins such as FAP16 are hard to predict due to their variety of function, they have some functions specific to cilia. The *Chlamydomonas* WD40-protein POC1, for example, is required for centriole duplication and length control (Keller, Geimer et al. 2009).

The discovery of an additional flagellar protein in the deflagellation pathway with potential microtubule-binding capabilities, human homologues of which play important roles in microtubule dynamics and are involved in ciliopathies is intriguing. Both FA1 and FA2 have been localized to the flagellar transition zone and an additional protein bearing protein-protein interaction domains that is localized to the flagellum might be capable of associating with the axoneme, transition zone or FA1 and FA2 themselves (Finst, Kim et

al. 2000; Mahjoub, Rasi et al. 2004). As the phenotype of *adf5-1* and *adf5-2* is not a FA and cells are still capable of severing the axoneme in response to membrane permeabilization and calcium influx, I do not believe that it is directly involved in the severing process. It might however function upstream in relaying incoming signals. Given the manifold and severe disease phenotypes of FAP16-related proteins, it will be worthwhile to further study the potential effects of defects in *ADF5* and how they potentially relate to acid-induced deflagellation. Several possible binding partners, such as with FA1, FA2 or one of the *Chlamydomonas* dyneins would make interesting candidates for co-localization studies.

4.4. The Updated Deflagellation Pathway

With the discovery of three novel deflagellation genes and the identification of *ADF1*, it is now time to revisit the deflagellation pathway initially described in Chapter 1.4. Combining the identities and potential functions of the genes and proteins uncovered, I propose the following hypothesis for the deflagellation pathway, which is also shown in an updated schematic in figure 4.2.

First, a weak organic acid permeates the cell membrane (1) and is deprotonated intracellularly to induce a decrease in intracellular pH (2). In response, IP3 levels increase (3), mediated at least in part by ADF2/ITPK1 – specifically at higher temperatures, where inositol-members may form one way in which *Chlamydomonas* protects itself from heat-induced cellular stress. This increase in IP3 activates the calcium-channel ADF1/TRP15 (4), leading to an influx of extracellular calcium localized to the base of the flagellum (5). This process can be blocked by the calcium-channel blocker La^{3+} or Gd^{3+}. The glycosyltransferase ADF4 may be involved in either feeding the necessary phosphatidylinositol into the pathway or protecting ADF1 from proteolysis upon nitrogen-starvation. At the base of the flagellum, this influx causes a further release of Calcium from intracellular stores (6). This secondary calcium release triggers a severing-signal that is relayed by FAP16 from the base of the flagellum to the severing complex (7). Once the signal reaches the SOFA, FA1 and FA2 participate in the severing complex to cause axonemal severing and deflagellation occurs (8).

4.5. Conclusion

In summary, I have identified the three novel deflagellation genes *ADF2, ADF4* and *ADF5* as *ITPK1*, a glycosyltransferase and the flagellar-associated gene *FAP16*, respectively. Twenty years after being isolated, I have also identified ADF1 as the predicted calcium-channel TRP15. ADF1 possibly plays a role in the initial localized calcium-influx required to trigger deflagellation and might be the first transition-zone calcium channel. It seems plausible that both ADF2/ITPK1 and ADF4 play roles in regulating messengers required to induce deflagellation, either through inositol-family members such as IP3 or IP6 or changes in membrane dynamics and ADF1 activation and/or localization. While the involvement of IP3 in deflagellation is supported by previous studies, the discovery of proteins so integral to inositol phosphate metabolism is unexpected and poses interesting questions about the link between deflagellation and other, more general cellular processes such as calcium homeostasis.

Further study will be needed to shed insight on whether deflagellation is more central to intracellular signaling than initially predicted, similar to the often underestimated role of flagella in general. Finally, ADF5/FAP16 might link cytoplasmic and ciliary signaling pathways as a microtubule-binding protein with protein-protein interaction domains, whose exact role during both flagellar assembly and health is yet to be revealed. The fact that its close homologues, the EML-family, are involved in a multitude of ciliopathies, further makes it an interesting target of more intense study. I have yet to resolve the identities of more strains, such as the B5-complementation group *ADF3* which maps near *PSBO*, the identity of which might yield more information on other players and roles in the deflagellation-pathway, which with this thesis has grown from two identified genes to six.

4.6. Figures

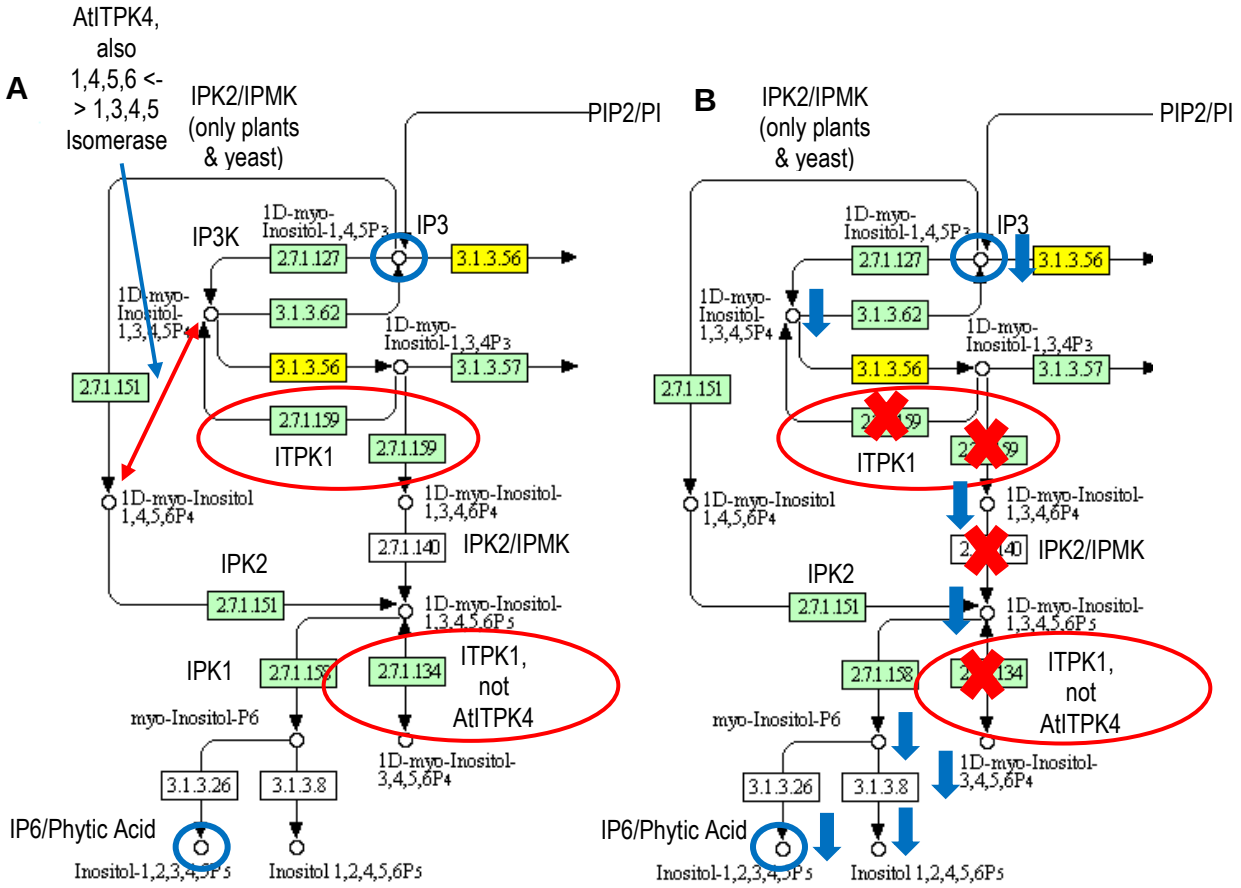

Figure 4.1. Schematic of Inositol Metabolism and Potential Impact of *adf2-1*

Note. A) Blue indicates important metabolites IP3 and IP6. Red circles and arrows indicates reactions catalyzed by ITPK1 and AtITPK4, the close homologue of CrITPK1/ADF2. Also added are other important enzymes mentioned in the discussion that participate in the pathway. B) Potential Impact of loss of ITPK1. Red crosses mark potential loss of catalysis, blue arrows mark potential inhibition/lower levels of a metabolite. Source of schematic: KEGG pathways, Kanehisa Laboratories (Kanehisa and Goto 2000; Kanehisa, Goto et al. 2014).

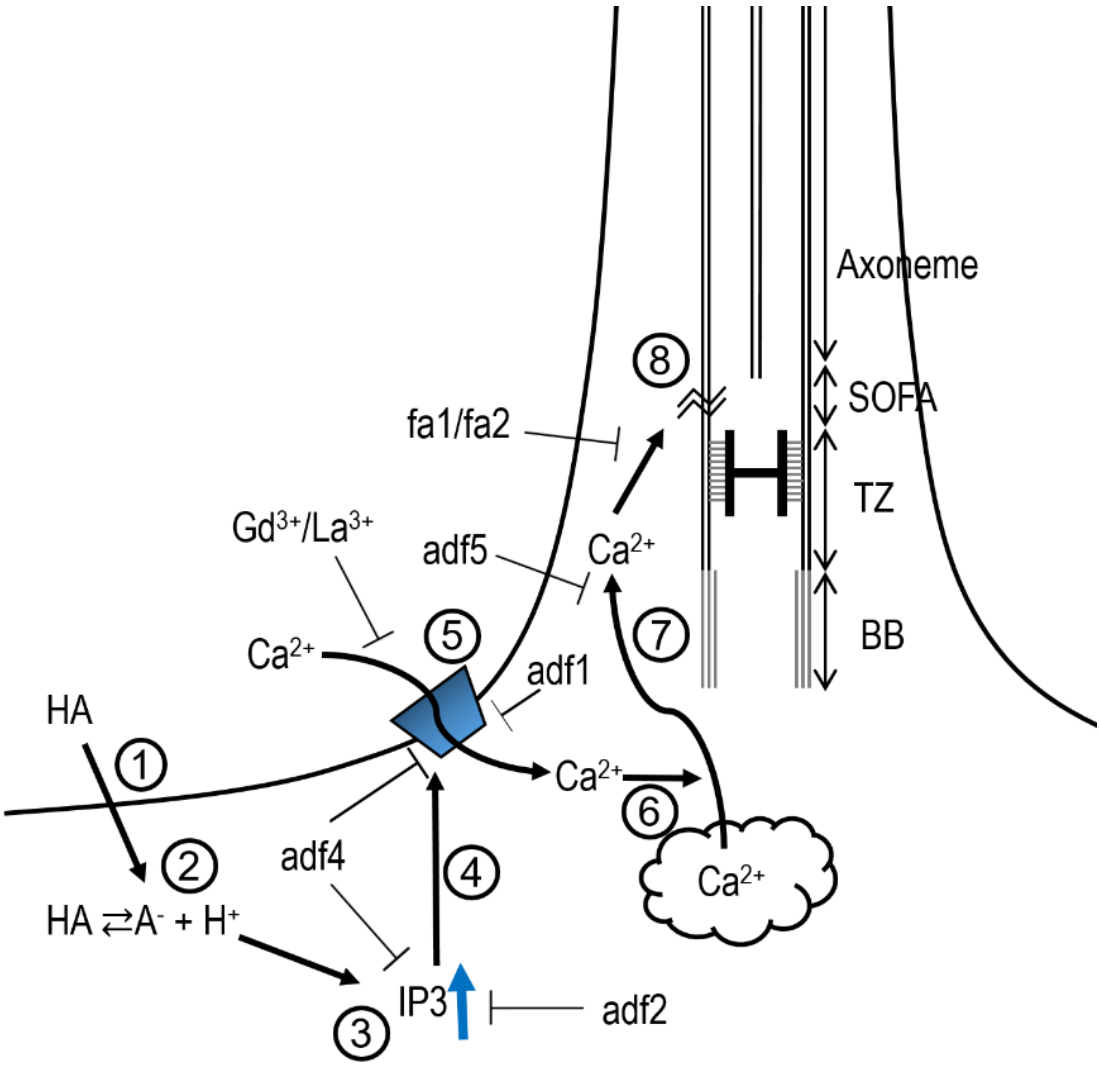

Figure 4.2. Updated Deflagellation Pathway Schematic

Note. Steps and components as described in Discussion. BB = Basal Body, TZ = Transition Zone, SOFA = Site Of Flagellar Autonomy

4.7. References

Abe, J., et al. (2004). "The transcriptional program of synchronous gametogenesis in Chlamydomonas reinhardtii." Curr Genet **46**(5): 304-315.

Albee, A. J., et al. (2013). "Identification of Cilia Genes That Affect Cell-Cycle Progression Using Whole-Genome Transcriptome Analysis in Chlamydomonas reinhardtti." G3 (Bethesda) **3**(6): 979-991.

Amann-Zalcenstein, D., et al. (2006). "AHI1, a pivotal neurodevelopmental gene, and C6orf217 are associated with susceptibility to schizophrenia." Eur J Hum Genet **14**(10): 1111-1119.

Asano, T., et al. (1991). "The role of N-glycosylation of GLUT1 for glucose transport activity." J Biol Chem **266**(36): 24632-24636.

Bessen, M., et al. (1980). "Calcium control of waveform in isolated flagellar axonemes of Chlamydomonas." J Cell Biol **86**(2): 446-455.

Blum-Held, C., et al. (2001). "myo-Inositol 1,4,5,6-tetrakisphosphate and myo-inositol 3,4,5,6-tetrakisphosphate, two second messengers that may act as pH-dependent molecular switches." J Am Chem Soc **123**(14): 3399-3400.

Butterworth, J. F. t. and G. R. Strichartz (1990). "Molecular mechanisms of local anesthesia: a review." Anesthesiology **72**(4): 711-734.

Casano, C., et al. (2003). "Sea urchin deciliation induces thermoresistance and activates the p38 mitogen-activated protein kinase pathway." Cell Stress Chaperones **8**(1): 70-75.

Chamberlain, P. P., et al. (2007). "Integration of inositol phosphate signaling pathways via human ITPK1." J Biol Chem **282**(38): 28117-28125.

Chang, Q., et al. (2005). "The beta-glucuronidase klotho hydrolyzes and activates the TRPV5 channel." Science **310**(5747): 490-493.

Chen, J., et al. (2011). "Two non-synonymous markers in PTPN21, identified by genome-wide association study data-mining and replication, are associated with schizophrenia." Schizophr Res **131**(1-3): 43-51.

Cheshire, J. L. and L. R. Keller (1991). "Uncoupling of Chlamydomonas flagellar gene expression and outgrowth from flagellar excision by manipulation of Ca2+." J Cell Biol **115**(6): 1651-1659.

Chevenet, F., et al. (2006). "TreeDyn: towards dynamic graphics and annotations for analyses of trees." BMC Bioinformatics **7**: 439.

Chih, B., et al. (2012). "A ciliopathy complex at the transition zone protects the cilia as a privileged membrane domain." Nat Cell Biol **14**(1): 61-72.

Chu, W. F., et al. (2006). "Increasing Intracellular calcium of guinea pig ventricular myocytes induced by platelet activating factor through IP3 pathway." Basic Clin Pharmacol Toxicol **98**(1): 104-109.

Cingolani, P., et al. (2012). "A program for annotating and predicting the effects of single nucleotide polymorphisms, SnpEff: SNPs in the genome of Drosophila melanogaster strain w1118; iso-2; iso-3." Fly (Austin) **6**(2): 80-92.

Clapham, D. E., et al. (2001). "The TRP ion channel family." Nat Rev Neurosci **2**(6): 387-396.

Codogno, P., et al. (1988). "Concanavalin A-induced impairment of fibroblast spreading on laminin but not on fibronectin." J Cell Physiol **136**(3): 463-470.

Cohen, D. M. (2006). "Regulation of TRP channels by N-linked glycosylation." Semin Cell Dev Biol **17**(6): 630-637.

Cox, J. L. and G. D. Small (1985). "Isolation of a photoreactivation-deficient mutant of Chlamydomonas." Mutat Res **146**(3): 249-255.

Coyne, B. and J. L. Rosenbaum (1970). "Flagellar elongation and shortening in chlamydomonas. II. Re-utilization of flagellar proteins." J Cell Biol **47**(3): 777-781.

Craige, B., et al. (2010). "CEP290 tethers flagellar transition zone microtubules to the membrane and regulates flagellar protein content." J Cell Biol **190**(5): 927-940.

Davies, J. P. and A. R. Grossman (1994). "Sequences controlling transcription of the Chlamydomonas reinhardtii beta 2-tubulin gene after deflagellation and during the cell cycle." Mol Cell Biol **14**(8): 5165-5174.

Delaval, B., et al. (2011). "The cilia protein IFT88 is required for spindle orientation in mitosis." Nat Cell Biol **13**(4): 461-468.

Delgado, R., et al. (2014). "Diacylglycerol activates the light-dependent channel TRP in the photosensitive microvilli of Drosophila melanogaster photoreceptors." J Neurosci **34**(19): 6679-6686.

Dent, R. M., et al. (2005). "Functional genomics of eukaryotic photosynthesis using insertional mutagenesis of Chlamydomonas reinhardtii." Plant Physiol **137**(2): 545-556.

Dentler, W. (2013). "A role for the membrane in regulating Chlamydomonas flagellar length." PLOS One **8**(1): e53366.

Dentler, W. L. (1980). "Structures linking the tips of ciliary and flagellar microtubules to the membrane." J Cell Sci **42**: 207-220.

Dentler, W. L. and J. L. Rosenbaum (1977). "Flagellar elongation and shortening in Chlamydomonas. III. structures attached to the tips of flagellar microtubules and their relationship to the directionality of flagellar microtubule assembly." J Cell Biol **74**(3): 747-759.

Dereeper, A., et al. (2010). "BLAST-EXPLORER helps you building datasets for phylogenetic analysis." BMC Evol Biol **10**: 8.

Dereeper, A., et al. (2008). "Phylogeny.fr: robust phylogenetic analysis for the non-specialist." Nucleic Acids Res **36**(Web Server issue): W465-469.

Dismukes, G. C., et al. (2008). "Aquatic phototrophs: efficient alternatives to land-based crops for biofuels." Curr Opin Biotechnol **19**(3): 235-240.

Doroudchi, M. M., et al. (2011). "Virally delivered channelrhodopsin-2 safely and effectively restores visual function in multiple mouse models of blindness." Mol Ther **19**(7): 1220-1229.

Du, H., et al. (2011). "Characterization of an inositol 1,3,4-trisphosphate 5/6-kinase gene that is essential for drought and salt stress responses in rice." Plant Mol Biol **77**(6): 547-563.

Duquesnoy, P., et al. (2009). "Loss-of-function mutations in the human ortholog of Chlamydomonas reinhardtii ODA7 disrupt dynein arm assembly and cause primary ciliary dyskinesia." Am J Hum Genet **85**(6): 890-896.

Dutcher, S. K., et al. (2012). "Whole-Genome Sequencing to Identify Mutants and Polymorphisms in Chlamydomonas reinhardtii." G3 (Bethesda) **2**(1): 15-22.

Dutcher, S. K. and E. C. Trabuco (1998). "The UNI3 gene is required for assembly of basal bodies of Chlamydomonas and encodes delta-tubulin, a new member of the tubulin superfamily." Mol Biol Cell **9**(6): 1293-1308.

Edgar, R. C. (2004). "MUSCLE: multiple sequence alignment with high accuracy and high throughput." Nucleic Acids Res **32**(5): 1792-1797.

Engel, B. D., et al. (2011). "A cell-based screen for inhibitors of flagella-driven motility in Chlamydomonas reveals a novel modulator of ciliary length and retrograde actin flow." Cytoskeleton (Hoboken) **68**(3): 188-203.

Eudy, J. D., et al. (1997). "Isolation of a novel human homologue of the gene coding for echinoderm microtubule-associated protein (EMAP) from the Usher syndrome type 1a locus at 14q32." Genomics **43**(1): 104-106.

Evans, J. H. and L. R. Keller (1997) Receptor-Mediated Calcium Influx in Chlamydomonas reinhardtii Journal of Eukaryotic Microbiology Volume 44, Issue 3. Journal of Eukaryotic Microbiology **44**, 237-245

Ferris, P. J., et al. (2005). "Plus and minus sexual agglutinins from Chlamydomonas reinhardtii." Plant Cell **17**(2): 597-615.

Finn, R. D., et al. (2014). "Pfam: the protein families database." Nucleic Acids Res **42**(Database issue): D222-230.

Finn, R. D., et al. (2011). "HMMER web server: interactive sequence similarity searching." Nucleic Acids Res **39**(Web Server issue): W29-37.

Finst, R. J., et al. (2000). "Fa1p is a 171 kDa protein essential for axonemal microtubule severing in Chlamydomonas." J Cell Sci **113 (Pt 11)**: 1963-1971.

Finst, R. J., et al. (1998). "Genetics of the deflagellation pathway in Chlamydomonas." Genetics **149**(2): 927-936.

Freshour, J., et al. (2007). "Chlamydomonas flagellar outer row dynein assembly protein ODA7 interacts with both outer row and I1 inner row dyneins." J Biol Chem **282**(8): 5404-5412.

Garcia-Gonzalo, F. R., et al. (2011). "A transition zone complex regulates mammalian ciliogenesis and ciliary membrane composition." Nat Genet **43**(8): 776-784.

Ghossoub, R., et al. (2011). "The ciliary pocket: a once-forgotten membrane domain at the base of cilia." Biol Cell **103**(3): 131-144.

Gieger, C., et al. (2011). "New gene functions in megakaryopoiesis and platelet formation." Nature **480**(7376): 201-208.

Gomez-Casati, D. F., et al. (2013). "Polysaccharide-synthesizing glycosyltransferases and carbohydrate binding modules: the case of starch synthase III." Protein Pept Lett **20**(8): 856-863.

Goodenough, U. W., et al. (1993). "The role of calcium in the Chlamydomonas reinhardtii mating reaction." J Cell Biol **121**(2): 365-374.

Goodstein, D. M., et al. (2012). "Phytozome: a comparative platform for green plant genomics." Nucleic Acids Res **40**(Database issue): D1178-1186.

Gudermann, T. (2005). "A new TRP to kidney disease." Nat Genet **37**(7): 663-664.

Guerin, M. E., et al. (2007). "Molecular recognition and interfacial catalysis by the essential phosphatidylinositol mannosyltransferase PimA from mycobacteria." J Biol Chem **282**(28): 20705-20714.

Guindon, S. and O. Gascuel (2003). "A simple, fast, and accurate algorithm to estimate large phylogenies by maximum likelihood." Syst Biol **52**(5): 696-704.

Hader, D. P. and M. Lebert (2009). "Photoorientation in photosynthetic flagellates." Methods Mol Biol **571**: 51-65.

Hanahan, D. (1983). "Studies on transformation of Escherichia coli with plasmids." J Mol Biol **166**(4): 557-580.

Hanks, J. N., et al. (2003). "Nitrogen starvation-induced changes in amino acid and free ammonium pools in Schizophyllum commune colonies." Curr Microbiol **47**(5): 444-449.

Hardie, R. C. and B. Minke (1992). "The trp gene is essential for a light-activated Ca2+ channel in Drosophila photoreceptors." Neuron **8**(4): 643-651.

Harris, E. H. (2009). The Chlamydomonas Sourcebook Oxford, U.K., Academic Press.

Harris, E. H., et al. (1994). "Chloroplast ribosomes and protein synthesis." Microbiol Rev **58**(4): 700-754.

Hartzell, L. B., et al. (1993). "Mechanisms of flagellar excision. I. The role of intracellular acidification." Exp Cell Res **208**(1): 148-153.

Hashii, M., et al. (1994). "Ca2+ influx evoked by inositol-3,4,5,6-tetrakisphosphate in ras-transformed NIH/3T3 fibroblasts." FEBS Lett **340**(3): 276-280.

Hawks, B. G. and R. W. Lee (1976). "Methyl methanesulfonate mutagenesis of synchronized Chlamydomonas." Mutat Res **37**(2-3): 221-228.

Head, S. R., et al. (2014). "Library construction for next-generation sequencing: overviews and challenges." Biotechniques **56**(2): 61-64, 66, 68, passim.

Hilton, L. K., et al. (2013). "The kinases LF4 and CNK2 control ciliary length by feedback regulation of assembly and disassembly rates." Curr Biol **23**(22): 2208-2214.

Hilton, L. K. and L. M. Quarmby (2011). Cilia. Cellular Domains. I. R. Nabi. Hoboken, Wiley**:** 245-266.

Hinchcliffe, E. H. and G. Sluder (2001). ""It takes two to tango": understanding how centrosome duplication is regulated throughout the cell cycle." Genes Dev **15**(10): 1167-1181.

Ho, M. W., et al. (2002). "Regulation of Ins(3,4,5,6)P(4) signaling by a reversible kinase/phosphatase." Curr Biol **12**(6): 477-482.

Hoog, J. L., et al. (2014). "Modes of flagellar assembly in Chlamydomonas reinhardtii and Trypanosoma brucei." Elife **3**: e01479.

Hook, P., et al. (2009). "The dynein stalk contains an antiparallel coiled coil with region-specific stability." Biochemistry **48**(12): 2710-2713.

Howell, S. H. and J. A. Naliboff (1973). "Conditional mutants in Chlamydomonas reinhardtii blocked in the vegetative cell cycle. I. An analysis of cell cycle block points." J Cell Biol **57**(3): 760-772.

Hueston, J. L., et al. (2008). "The C. elegans EMAP-like protein, ELP-1 is required for touch sensation and associates with microtubules and adhesion complexes." BMC Dev Biol **8**: 110.

Hueston, J. L. and K. A. Suprenant (2009). "Loss of dystrophin and the microtubule-binding protein ELP-1 causes progressive paralysis and death of adult C. elegans." Dev Dyn **238**(8): 1878-1886.

Hunnicutt, G. R., et al. (1990). "Cell body and flagellar agglutinins in Chlamydomonas reinhardtii: the cell body plasma membrane is a reservoir for agglutinins whose migration to the flagella is regulated by a functional barrier." J Cell Biol **111**(4): 1605-1616.

Imai, H., et al. (2007). "Molecular properties of rhodopsin and rod function." J Biol Chem **282**(9): 6677-6684.

Inada, H., et al. (2008). "Off-response property of an acid-activated cation channel complex PKD1L3-PKD2L1." EMBO Rep **9**(7): 690-697.

Irvine, R. F., et al. (1992). "Inositol polyphosphate metabolism and inositol lipids in a green alga, Chlamydomonas eugametos." Biochem J **281 (Pt 1)**: 261-266.

Ivorra, I., et al. (1991). "Inositol 1,3,4,6-tetrakisphosphate mobilizes calcium in Xenopus oocytes with high potency." Biochem J **273(Pt 2)**: 317-321.

Jain, R., et al. (2012). "Sensory functions of motile cilia and implication for bronchiectasis." Front Biosci (Schol Ed) **4**: 1088-1098.

Jin, H., et al. (2010). "The conserved Bardet-Biedl syndrome proteins assemble a coat that traffics membrane proteins to cilia." Cell **141**(7): 1208-1219.

Jinkerson, R. E. and M. C. Jonikas (2015). "Molecular techniques to interrogate and edit the Chlamydomonas nuclear genome." Plant J **82**(3): 393-412.

Jo, H. and G. Koh (2015). "Faster single-end alignment generation utilizing multi-thread for BWA." Biomed Mater Eng **26 Suppl 1**: S1791-1796.

Johnson, J. L. and M. R. Leroux (2010). "cAMP and cGMP signaling: sensory systems with prokaryotic roots adopted by eukaryotic cilia." Trends Cell Biol **20**(8): 435-444.

Johnson, U. G. and K. R. Porter (1968). "Fine structure of cell division in Chlamydomonas reinhardi. Basal bodies and microtubules." J Cell Biol **38**(2): 403-425.

Jonassen, J. A., et al. (2008). "Deletion of IFT20 in the mouse kidney causes misorientation of the mitotic spindle and cystic kidney disease." J Cell Biol **183**(3): 377-384.

Kanehisa, M. and S. Goto (2000). "KEGG: kyoto encyclopedia of genes and genomes." Nucleic Acids Res **28**(1): 27-30.

Kanehisa, M., et al. (2014). "Data, information, knowledge and principle: back to metabolism in KEGG." Nucleic Acids Res **42**(Database issue): D199-205.

Kardon, J. R. and R. D. Vale (2009). "Regulators of the cytoplasmic dynein motor." Nat Rev Mol Cell Biol **10**(12): 854-865.

Keller, L. C., et al. (2009). "Molecular architecture of the centriole proteome: the conserved WD40 domain protein POC1 is required for centriole duplication and length control." Mol Biol Cell **20**(4): 1150-1166.

Khanna, R., et al. (2001). "Glycosylation increases potassium channel stability and surface expression in mammalian cells." J Biol Chem **276**(36): 34028-34034.

Kim, J., et al. (2009). "Gli2 trafficking links Hedgehog-dependent activation of Smoothened in the primary cilium to transcriptional activation in the nucleus." Proc Natl Acad Sci U S A **106**(51): 21666-21671.

Kim, M. J., et al. (2008). "Molecular determinant of sensing extracellular pH in classical transient receptor potential channel 5." Biochem Biophys Res Commun **365**(2): 239-245.

Kim, S. I. and T. H. Tai (2011). "Identification of genes necessary for wild-type levels of seed phytic acid in Arabidopsis thaliana using a reverse genetics approach." Mol Genet Genomics **286**(2): 119-133.

Kindle, K. L. (1990). "High-frequency nuclear transformation of Chlamydomonas reinhardtii." Proc Natl Acad Sci U S A **87**(3): 1228-1232.

King, S. M. and R. Kamiya (2009). Axonemal Dyneins: Assembly, Structure, and Force Generation. The *Chlamydomonas* Sourcebook. G. B. Witman. Oxford, UK, Academic Press. **3:** 131-208.

Kirschner, J. A. (2009). Mapping the deflagellation-defective *adf1* gene in *Chlamydomonas reinhardtii*. Department of Molecular Biology and Biochemistry. Burnaby, BC, Simon Fraser University. **Master of Science:** 118.

Knibbs, R. N., et al. (1989). "Structure of the major concanavalin A reactive oligosaccharides of the extracellular matrix component laminin." Biochemistry **28**(15): 6379-6392.

Kordulakova, J., et al. (2002). "Definition of the first mannosylation step in phosphatidylinositol mannoside synthesis. PimA is essential for growth of mycobacteria." J Biol Chem **277**(35): 31335-31344.

Kozminski, K. G., et al. (1995). "The Chlamydomonas kinesin-like protein FLA10 is involved in motility associated with the flagellar membrane." J Cell Biol **131**(6 Pt 1): 1517-1527.

Lal, M., et al. (2008). "Polycystin-1 C-terminal tail associates with beta-catenin and inhibits canonical Wnt signaling." Hum Mol Genet **17**(20): 3105-3117.

Lang, W. C. (1984). "Glycoprotein biosynthesis in Chlamydomonas. A mannolipid intermediate with the properties of a short-chain alpha-saturated polyprenyl monophosphate." Biochem J **220**(3): 747-754.

Langmead, B. and S. L. Salzberg (2012). "Fast gapped-read alignment with Bowtie 2." Nat Methods **9**(4): 357-359.

Lechtreck, K. F., et al. (2009). "The Chlamydomonas reinhardtii BBSome is an IFT cargo required for export of specific signaling proteins from flagella." J Cell Biol **187**(7): 1117-1132.

Lechtreck, K. F. and G. B. Witman (2007). "Chlamydomonas reinhardtii hydin is a central pair protein required for flagellar motility." J Cell Biol **176**(4): 473-482.

Lee, R. W. and R. F. Jones (1976). "Lethal and mutagenic effects of nitrosoguanidine on synchronized Chlamydomonas." Mol Gen Genet **147**(3): 283-289.

Lefebvre, P. A., et al. (1980). "Increased levels of mRNAs for tubulin and other flagellar proteins after amputation or shortening of Chlamydomonas flagella." Cell **20**(2): 469-477.

Lewin, R. A. and C. Burrascano (1983). "Another new kind of Chlamydomonas mutant, with impaired flagellar autotomy." Experientia **39**(12): 1397-1398.

Li, H., et al. (2009). "The Sequence Alignment/Map format and SAMtools." Bioinformatics **25**(16): 2078-2079.

Li, J. B., et al. (2004). "Comparative genomics identifies a flagellar and basal body proteome that includes the BBS5 human disease gene." Cell **117**(4): 541-552.

Li, Y., et al. (2010). "Chlamydomonas starchless mutant defective in ADP-glucose pyrophosphorylase hyper-accumulates triacylglycerol." Metab Eng **12**(4): 387-391.

Liang, Y. and J. Pan (2013). "Regulation of flagellar biogenesis by a calcium dependent protein kinase in Chlamydomonas reinhardtii." PLOS One **8**(7): e69902.

Ligon, L. A., et al. (2004). "A direct interaction between cytoplasmic dynein and kinesin I may coordinate motor activity." J Biol Chem **279**(18): 19201-19208.

Lin, H. and U. W. Goodenough (2007). "Gametogenesis in the Chlamydomonas reinhardtii minus mating type is controlled by two genes, MID and MTD1." Genetics **176**(2): 913-925.

Lin, H., et al. (2013). "Whole genome sequencing identifies a deletion in protein phosphatase 2A that affects its stability and localization in Chlamydomonas reinhardtii." PLoS Genet **9**(9): e1003841.

Lohret, T. A., et al. (1998). "A role for katanin-mediated axonemal severing during Chlamydomonas deflagellation." Mol Biol Cell **9**(5): 1195-1207.

Lohret, T. A., et al. (1999). "Cloning of Chlamydomonas p60 katanin and localization to the site of outer doublet severing during deflagellation." Cell Motil Cytoskeleton **43**(3): 221-231.

Loktev, A. V., et al. (2008). "A BBSome subunit links ciliogenesis, microtubule stability, and acetylation." Dev Cell **15**(6): 854-865.

Lopes, V. S., et al. (2010). "Dysfunction of heterotrimeric kinesin-2 in rod photoreceptor cells and the role of opsin mislocalization in rapid cell death." Mol Biol Cell **21**(23): 4076-4088.

Loppes, R. (1970). "Selection of arginine-requiring mutants in Chlamydomonas reinhardi after treatment with 3 mutagens." Experientia **26**(6): 660-661.

Luck, D., et al. (1977). "Flagellar mutants of Chlamydomonas: studies of radial spoke-defective strains by dikaryon and revertant analysis." Proc Natl Acad Sci U S A **74**(8): 3456-3460.

Ludwig, R. A. (1993). "Arabidopsis chloroplasts dissimilate L-arginine and L-citrulline for use as N source." Plant Physiol **101**(2): 429-434.

Lyman, K. A. and D. M. Chetkovich (2015). "Cortical Compass: EML1 Helps Point the Way in Neuronal Migration." Epilepsy Curr **15**(1): 43-44.

Ma, M., et al. (2013). "Loss of cilia suppresses cyst growth in genetic models of autosomal dominant polycystic kidney disease." Nat Genet **45**(9): 1004-1012.

Mahjoub, M. R., et al. (2002). "The FA2 gene of Chlamydomonas encodes a NIMA family kinase with roles in cell cycle progression and microtubule severing during deflagellation." J Cell Sci **115**(Pt 8): 1759-1768.

Mahjoub, M. R., et al. (2004). "A NIMA-related kinase, Fa2p, localizes to a novel site in the proximal cilia of Chlamydomonas and mouse kidney cells." Mol Biol Cell **15**(11): 5172-5186.

Mahjoub, M. R., et al. (2005). "NIMA-related kinases defective in murine models of polycystic kidney diseases localize to primary cilia and centrosomes." J Am Soc Nephrol **16**(12): 3485-3489.

Majerus, P. W., et al. (2010). "Expression of inositol 1,3,4-trisphosphate 5/6-kinase (ITPK1) and its role in neural tube defects." Adv Enzyme Regul **50**(1): 365-372.

Mandal, D. K. and C. F. Brewer (1992). "Interactions of concanavalin A with glycoproteins: formation of homogeneous glycoprotein-lectin cross-linked complexes in mixed precipitation systems." Biochemistry **31**(50): 12602-12609.

Marshall, W. F., et al. (2005). "Flagellar Length Control System: Testing a Simple Model Based on Intraflagellar Transport and Turnover." Mol Biol Cell **16**(1): 270-278.

Marshall, W. F. and J. L. Rosenbaum (2001). "Intraflagellar transport balances continuous turnover of outer doublet microtubules: implications for flagellar length control." J Cell Biol **155**(3): 405-414.

Mathieu-Rivet, E., et al. (2013). "Exploring the N-glycosylation pathway in Chlamydomonas reinhardtii unravels novel complex structures." Mol Cell Proteomics **12**(11): 3160-3183.

May, S. R., et al. (2005). "Loss of the retrograde motor for IFT disrupts localization of Smo to cilia and prevents the expression of both activator and repressor functions of Gli." Dev Biol **287**(2): 378-389.

McKenna, A., et al. (2010). "The Genome Analysis Toolkit: a MapReduce framework for analyzing next-generation DNA sequencing data." Genome Res **20**(9): 1297-1303.

McNally, F. J. and S. Thomas (1998). "Katanin is responsible for the M-phase microtubule-severing activity in Xenopus eggs." Mol Biol Cell **9**(7): 1847-1861.

Merchant, S. S., et al. (2012). "TAG, you're it! Chlamydomonas as a reference organism for understanding algal triacylglycerol accumulation." Curr Opin Biotechnol **23**(3): 352-363.

Molendijk, A. J. and R. F. Irvine (1998). "Inositide signalling in Chlamydomonas: characterization of a phosphatidylinositol 3-kinase gene." Plant Mol Biol **37**(1): 53-66.

Moyer, J. H., et al. (1994). "Candidate gene associated with a mutation causing recessive polycystic kidney disease in mice." Science **264**(5163): 1329-1333.

Msanne, J., et al. (2012). "Metabolic and gene expression changes triggered by nitrogen deprivation in the photoautotrophically grown microalgae Chlamydomonas reinhardtii and Coccomyxa sp. C-169." Phytochemistry **75**: 50-59.

Nachury, M. V., et al. (2007). "A Core Complex of BBS Proteins Cooperates with the GTPase Rab8 to Promote Ciliary Membrane Biogenesis." Cell **129**(6): 1201 - 1213.

Nagel, G., et al. (2002). "Channelrhodopsin-1: a light-gated proton channel in green algae." Science **296**(5577): 2395-2398.

Nagel, G., et al. (2003). "Channelrhodopsin-2, a directly light-gated cation-selective membrane channel." Proc Natl Acad Sci U S A **100**(24): 13940-13945.

Nilius, B. and G. Owsianik (2011). "The transient receptor potential family of ion channels." Genome Biol **12**(3): 218.

Nishikawa, A., et al. (2010). "Induction of deflagellation by various local anesthetics in Chlamydomonas reinhardtii Dangeard (Chlamydomonadales, Chlorophyceae)." Phycological Research **58**(2): 79-87.

Nultsch, W. (1977). "Effect of external factors on phototaxis of Chlamydomonas reinhardtii. II. Charbon dioxide, oxygen and pH." Arch Microbiol **112**(2): 179-185.

Numata, T., et al. (2011). Activation of TRP Channels in Mammalian Systems. TRP Channels. M. X. Zhu. Boca Raton (FL).

O'Connor, V., et al. (2004). "Eml5, a novel WD40 domain protein expressed in rat brain." Gene **336**(1): 127-137.

O'Toole, E. T., et al. (2003). "Three-dimensional organization of basal bodies from wild-type and delta-tubulin deletion strains of Chlamydomonas reinhardtii." Mol Biol Cell **14**(7): 2999-3012.

Osteryoung, K. W., et al. (1998). "Chloroplast division in higher plants requires members of two functionally divergent gene families with homology to bacterial ftsZ." Plant Cell **10**(12): 1991-2004.

Ou, G., et al. (2005). "Functional coordination of intraflagellar transport motors." Nature **436**(7050): 583-587.

Overgaard, C. E., et al. (2009). "Deciliation is associated with dramatic remodeling of epithelial cell junctions and surface domains." Mol Biol Cell **20**(1): 102-113.

Pan, J., et al. (2013). "The role of the cilium in normal and abnormal cell cycles: emphasis on renal cystic pathologies." Cell Mol Life Sci **70**(11): 1849-1874.

Pan, J. and W. J. Snell (2005). "Chlamydomonas shortens its flagella by activating axonemal disassembly, stimulating IFT particle trafficking, and blocking anterograde cargo loading." Dev Cell **9**(3): 431-438.

Pan, J., et al. (2004). "An aurora kinase is essential for flagellar disassembly in Chlamydomonas." Dev Cell **6**(3): 445-451.

Panteris, E., et al. (2011). "A role for katanin in plant cell division: microtubule organization in dividing root cells of fra2 and lue1Arabidopsis thaliana mutants." Cytoskeleton (Hoboken) **68**(7): 401-413.

Park, J. J., et al. (2015). "The response of Chlamydomonas reinhardtii to nitrogen deprivation: a systems biology analysis." Plant J **81**(4): 611-624.

Parker, J. D., et al. (2010). "Centrioles are freed from cilia by severing prior to mitosis." Cytoskeleton (Hoboken) **67**(7): 425-430.

Parker, J. D. K. (2008). Co-ordinate regulation of cilia and the cell cycle in Chlamydomonas reinhardtii.

Parker, J. D. K. and L. M. Quarmby (2003). "Chlamydomonas fla mutants reveal a link between deflagellation and intraflagellar transport." BMC Cell Biol **4**: 11.

Pasquale, S. M. and U. W. Goodenough (1987). "Cyclic AMP functions as a primary sexual signal in gametes of Chlamydomonas reinhardtii." J Cell Biol **105**(5): 2279-2292.

Pazour, G. J. (2004). "Comparative genomics: prediction of the ciliary and basal body proteome." Curr Biol **14**(14): R575-577.

Pazour, G. J., et al. (2000). "Chlamydomonas IFT88 and its mouse homologue, polycystic kidney disease gene tg737, are required for assembly of cilia and flagella." J Cell Biol **151**(3): 709-718.

Pazour, G. J. and J. L. Rosenbaum (2002). "Intraflagellar transport and cilia-dependent diseases." Trends Cell Biol **12**(12): 551-555.

Pazour, G. J., et al. (2002). "Polycystin-2 localizes to kidney cilia and the ciliary level is elevated in orpk mice with polycystic kidney disease." Curr Biol **12**(11): R378-380.

Pazour, G. J., et al. (1998). "A dynein light chain is essential for the retrograde particle movement of intraflagellar transport (IFT)." J Cell Biol **141**(4): 979-992.

Pedersen, L. B. and J. L. Rosenbaum (2008). "Intraflagellar transport (IFT) role in ciliary assembly, resorption and signalling." Curr Top Dev Biol **85**: 23-61.

Petrecca, K., et al. (1999). "N-linked glycosylation sites determine HERG channel surface membrane expression." J Physiol **515 (Pt 1)**: 41-48.

Philipps, G., et al. (2012). "Nitrogen deprivation results in photosynthetic hydrogen production in Chlamydomonas reinhardtii." Planta **235**(4): 729-745.

Piasecki, B. P. and C. D. Silflow (2009). "The UNI1 and UNI2 genes function in the transition of triplet to doublet microtubules between the centriole and cilium in Chlamydomonas." Mol Biol Cell **20**(1): 368-378.

Pike, J. C. R. (2013). Discovery of a Suppressor of ADF1 and the Mapping of a new ADF gene, ADF2, in Chlamydomonas reinhardtii. MBB. Burnaby, BC, Simon Fraser University. **Master of Science:** 99.

Plotnikova, O. V., et al. (2009). "Primary cilia and the cell cycle." Methods Cell Biol **94**: 137-160.

Pollmann, M., et al. (2006). "Human EML4, a novel member of the EMAP family, is essential for microtubule formation." Exp Cell Res **312**(17): 3241-3251.

Pugacheva, E. N., et al. (2007). "HEF1-dependent Aurora A activation induces disassembly of the primary cilium." Cell **129**(7): 1351-1363.

Pulver, S. R., et al. (2011). "Optogenetics in the teaching laboratory: using channelrhodopsin-2 to study the neural basis of behavior and synaptic physiology in Drosophila." Adv Physiol Educ **35**(1): 82-91.

Quarmby, L. M. (1994). "Signal transduction in the sexual life of Chlamydomonas." Plant Mol Biol **26**(5): 1271-1287.

Quarmby, L. M. (1996). "Ca2+ influx activated by low pH in Chlamydomonas." J Gen Physiol **108**(4): 351-361.

Quarmby, L. M. (2004). "Cellular deflagellation." Int Rev Cytol **233**: 47-91.

Quarmby, L. M. (2009). Deflagellation. The Chlamydomonas Sourcebook G. B. Witman. Oxford, UK, Academic Press. **3:** 43-69.

Quarmby, L. M. and H. C. Hartzell (1994). "Two distinct, calcium-mediated, signal transduction pathways can trigger deflagellation in Chlamydomonas reinhardtii." J Cell Biol **124**(5): 807-815.

Quarmby, L. M., et al. (1992). "Inositol phospholipid metabolism may trigger flagellar excision in Chlamydomonas reinhardtii." J Cell Biol **116**(3): 737-744.

Ramstrom, O., et al. (2004). "Dynamic combinatorial carbohydrate libraries: probing the binding site of the concanavalin A lectin." Chemistry **10**(7): 1711-1715.

Rash, J. E., et al. (1969). "Cilia in cardiac differentiation." J Ultrastruct Res **29**(5): 470-484.

Rasi, M. Q., et al. (2009). "Katanin Knockdown Supports a Role for Microtubule Severing in Release of Basal Bodies before Mitosis in Chlamydomonas." Mol Biol Cell **20**(1): 379-388.

Reaves, B. J. and A. J. Wolstenholme (2007). "The TRP channel superfamily: insights into how structure, protein-lipid interactions and localization influence function." Biochem Soc Trans **35**(Pt 1): 77-80.

Reiter, J. F., et al. (2012). "The base of the cilium: roles for transition fibres and the transition zone in ciliary formation, maintenance and compartmentalization." EMBO Rep.

Rieder, C. L., et al. (1979). "The resorption of primary cilia during mitosis in a vertebrate (PtK1) cell line." J Ultrastruct Res **68**(2): 173-185.

Ringo, D. L. (1967). "Flagellar motion and fine structure of the flagellar apparatus in Chlamydomonas." J Cell Biol **33**: 543-571.

Robert, A., et al. (2007). "The intraflagellar transport component IFT88/polaris is a centrosomal protein regulating G1-S transition in non-ciliated cells." J Cell Sci **120**(Pt 4): 628-637.

Rochaix, J. D., et al. (1998). The molecular biology of chloroplasts and mitochondria in Chlamydomonas. Dordrecht ; Boston, Kluwer Academic Publishers.

Rohatgi, R., et al. (2007). "Patched1 regulates hedgehog signaling at the primary cilium." Science **317**(5836): 372-376.

Rosenbaum, J. (2002). "Intraflagellar transport." Curr Biol **12**(4): R125.

Rosenbaum, J. L. and F. M. Child (1967). "Flagellar regeneration in protozoan flagellates." J Cell Biol **34**(1): 345-364.

Saiardi, A., et al. (1999). "Synthesis of diphosphoinositol pentakisphosphate by a newly identified family of higher inositol polyphosphate kinases." Curr Biol **9**(22): 1323-1326.

Sanders, M. A. and J. L. Salisbury (1989). "Centrin-mediated microtubule severing during flagellar excision in Chlamydomonas reinhardtii." J Cell Biol **108**(5): 1751-1760.

Santos, H. and M. S. Da Costa (2002). "Compatible solutes of organisms that live in hot saline environments." Environmental Microbiology **4**(9): 501-509.

Sarmah, B., et al. (2005). "Inositol polyphosphates regulate zebrafish left-right asymmetry." Dev Cell **9**(1): 133-145.

Sarmah, B., et al. (2007). "A role for the inositol kinase Ipk1 in ciliary beating and length maintenance." Proc Natl Acad Sci U S A **104**(50): 19843-19848.

Saso, L., et al. (1998). "Changes of glycosylation of serum proteins in psoriatic arthritis, studied by enzyme-linked lectin assay (ELLA), using concanavalin A." Biochem Mol Biol Int **46**(5): 867-875.

Satir, B., et al. (1976). "Membrane renewal after dibucaine deciliation of Tetrahymena. Freeze-fracture technique, cilia, membrane structure." Exp Cell Res **97**: 83-91.

Satir, P. and S. T. Christensen (2008). "Structure and function of mammalian cilia." Histochem Cell Biol **129**(6): 687-693.

Schermer, B., et al. (2006). "The von Hippel-Lindau tumor suppressor protein controls ciliogenesis by orienting microtubule growth." J Cell Biol **175**(4): 547-554.

Schloss, J. A., et al. (1984). "mRNA abundance changes during flagellar regeneration in Chlamydomonas reinhardtii." Mol Cell Biol **4**(3): 424-434.

Schmidt, J. A. and R. Eckert (1976). "Calcium couples flagellar reversal to photostimulation in Chlamydomonas reinhardtii." Nature **262**(5570): 713-715.

Schmollinger, S., et al. (2014). "Nitrogen-Sparing Mechanisms in Chlamydomonas Affect the Transcriptome, the Proteome, and Photosynthetic Metabolism." Plant Cell **26**(4): 1410-1435.

Schneider, L., et al. (2005). "PDGFRalphaalpha signaling is regulated through the primary cilium in fibroblasts." Curr Biol **15**(20): 1861-1866.

Scholey, J. M. (2012). "Kinesin-2 motors transport IFT-particles, dyneins and tubulin subunits to the tips of Caenorhabditis elegans sensory cilia: Relevance to vision research?" Vision Research **75**(0): 44 - 52.

Schrick, J. J., et al. (1995). "Characterization of the human homologue of the mouse Tg737 candidate polycystic kidney disease gene." Hum Mol Genet **4**(4): 559-567.

Scranton, M. A., et al. (2015). "Chlamydomonas as a model for biofuels and bio-products production." The Plant Journal **82**(3): 523-531.

Shears, S. B. (2009). "Molecular basis for the integration of inositol phosphate signaling pathways via human ITPK1." Adv Enzyme Regul **49**(1): 87-96.

Shih, S. M., et al. (2013). "Intraflagellar transport drives flagellar surface motility." Elife **2**: e00744.

Shiina, N., et al. (1995). "Microtubule-severing activity in M phase." Trends Cell Biol **5**(7): 283-286.

Shimogawara, K., et al. (1998). "High-efficiency transformation of Chlamydomonas reinhardtii by electroporation." Genetics **148**(4): 1821-1828.

Silflow, C. D. and J. L. Rosenbaum (1981). "Multiple alpha- and beta-tubulin genes in Chlamydomonas and regulation of tubulin mRNA levels after deflagellation." Cell **24**(1): 81-88.

Simpson, C. J. and A. Wise (1990). "Binding of zinc and calcium to inositol phosphates (phytate) in vitro." Br J Nutr **64**(1): 225-232.

Singh, P., et al. (2011). "Transcriptomic analysis in a Drosophila model identifies previously implicated and novel pathways in the therapeutic mechanism in neuropsychiatric disorders." Front Neurosci **5**: 161.

Sizova, I., et al. (2001). "A Streptomyces rimosus aphVIII gene coding for a new type phosphotransferase provides stable antibiotic resistance to Chlamydomonas reinhardtii." Gene **277**(1-2): 221-229.

Sjoblad, R. D. and P. H. Frederikse (1981). "Chemotactic responses of Chlamydomonas reinhardtii." Mol Cell Biol **1**(12): 1057-1060.

Smith, E. F. and P. A. Lefebvre (1996). "PF16 encodes a protein with armadillo repeats and localizes to a single microtubule of the central apparatus in Chlamydomonas flagella." J Cell Biol **132**(3): 359-370.

Snell, W. J., et al. (2004). "Cilia and flagella revealed: from flagellar assembly in Chlamydomonas to human obesity disorders." Cell **117**(6): 693-697.

Solonenko, S. A., et al. (2013). "Sequencing platform and library preparation choices impact viral metagenomes." BMC Genomics **14**: 320.

Stadtlander, C. T. (2006). "A model of the deciliation process caused by Mycoplasma fermentans strain incognitus on respiratory epithelium." Scanning **28**(4): 212-218.

Stirnimann, C. U., et al. (2010). "WD40 proteins propel cellular networks." Trends Biochem Sci **35**(10): 565-574.

Stolc, V., et al. (2005). "Genome-wide transcriptional analysis of flagellar regeneration in Chlamydomonas reinhardtii identifies orthologs of ciliary disease genes." Proc Natl Acad Sci U S A **102**(10): 3703-3707.

Stoppin-Mellet, V., et al. (2002). "Functional evidence for in vitro microtubule severing by the plant katanin homologue." Biochem J **365**(Pt 2): 337-342.

Strosser, J., et al. (2004). "Regulation of GlnK activity: modification, membrane sequestration and proteolysis as regulatory principles in the network of nitrogen control in Corynebacterium glutamicum." Mol Microbiol **54**(1): 132-147.

Su, D., et al. (2014). "Influence of high temperature during filling period on grain phytic acid and its relation to spikelet sterility and grain weight in non-lethal low phytic acid mutations in rice." Journal of Cereal Science **60**(2): 331-338.

Suprenant, K. A., et al. (2000). "Conservation of the WD-repeat, microtubule-binding protein, EMAP, in sea urchins, humans, and the nematode C. elegans." Dev Genes Evol **210**(1): 2-10.

Sussenbach, J. S. and P. J. Strijkert (1969). "Arginine metabolism in chlamydomonas reinhardi Arginine deiminase: The first enzyme of the catabolic pathway." FEBS Lett **3**(3): 166-168.

Sweetman, D., et al. (2007). "Arabidopsis thaliana inositol 1,3,4-trisphosphate 5/6-kinase 4 (AtITPK4) is an outlier to a family of ATP-grasp fold proteins from Arabidopsis." FEBS Lett **581**(22): 4165-4171.

Tegha-Dunghu, J., et al. (2008). "EML3 is a nuclear microtubule-binding protein required for the correct alignment of chromosomes in metaphase." J Cell Sci **121**(Pt 10): 1718-1726.

Terashima, M., et al. (2010). "Characterizing the anaerobic response of Chlamydomonas reinhardtii by quantitative proteomics." Mol Cell Proteomics **9**(7): 1514-1532.

Thomas, B., et al. (2010). "Ciliary dysfunction and ultrastructural abnormalities are features of severe asthma." J Allergy Clin Immunol **126**(4): 722-729 e722.

Thomas, J., et al. (2010). "Transcriptional control of genes involved in ciliogenesis: a first step in making cilia." Biol Cell **102**(9): 499-513.

Thorvaldsdottir, H., et al. (2013). "Integrative Genomics Viewer (IGV): high-performance genomics data visualization and exploration." Brief Bioinform **14**(2): 178-192.

Tillmann, U., et al. (1987). "Subcellular location of enzymes involved in the N-glycosylation and processing of asparagine-linked oligosaccharides in Saccharomyces cerevisiae." Eur J Biochem **162**(3): 635-642.

Tomita, H., et al. (2014). "Restoration of the majority of the visual spectrum by using modified Volvox channelrhodopsin-1." Mol Ther **22**(8): 1434-1440.

Ulvskov, P., et al. (2013). "Classification, naming and evolutionary history of glycosyltransferases from sequenced green and red algal genomes." PLOS One **8**(10): e76511.

Umen, J. G. and U. W. Goodenough (2001). "Control of cell division by a retinoblastoma protein homolog in Chlamydomonas." Genes Dev **15**(13): 1652-1661.

Valledor, L., et al. (2014). "System-level network analysis of nitrogen starvation and recovery in Chlamydomonas reinhardtii reveals potential new targets for increased lipid accumulation." Biotechnol Biofuels **7**: 171.

Varki, A. (2009). Essentials of glycobiology. Cold Spring Harbor, N.Y., Cold Spring Harbor Laboratory Press.

Vysotskaia, V. S., et al. (2001). "Development and characterization of genome-wide single nucleotide polymorphism markers in the green alga Chlamydomonas reinhardtii." Plant Physiol **127**(2): 386-389.

Walther, Z., et al. (1994). "The Chlamydomonas FLA10 gene encodes a novel kinesin-homologous protein." J Cell Biol **126**(1): 175-188.

Wang, S., et al. (2007). "Fibrocystin/polyductin, found in the same protein complex with polycystin-2, regulates calcium responses in kidney epithelia." Mol Cell Biol **27**(8): 3241-3252.

Wargo, M. J. and E. F. Smith (2003). "Asymmetry of the central apparatus defines the location of active microtubule sliding in Chlamydomonas flagella." Proc Natl Acad Sci U S A **100**(1): 137-142.

Watanabe, D., et al. (2003). "The left-right determinant Inversin is a component of node monocilia and other 9+0 cilia." Development **130**(9): 1725-1734.

Weiner, I. D., et al. (2015). "Urea and Ammonia Metabolism and the Control of Renal Nitrogen Excretion." Clin J Am Soc Nephrol **10**(8): 1444-1458.

Wheeler, G. L., et al. (2008). "Rapid spatiotemporal patterning of cytosolic Ca2+ underlies flagellar excision in Chlamydomonas reinhardtii." Plant J **53**(3): 401-413.

Wiens, C. J., et al. (2010). "Bardet-Biedl syndrome-associated small GTPase ARL6 (BBS3) functions at or near the ciliary gate and modulates Wnt signaling." J Biol Chem **285**(21): 16218-16230.

Wilson, N. F., et al. (2008). "Regulation of flagellar length in Chlamydomonas." Semin Cell Dev Biol **19**(6): 494-501.

Wirkner, K., et al. (2005). "Characterization of rat transient receptor potential vanilloid 1 receptors lacking the N-glycosylation site N604." Neuroreport **16**(9): 997-1001.

Witman, G. B. (1986). "Isolation of Chlamydomonas flagella and flagellar axonemes." Methods Enzymol **134**: 280-290.

Wormald, M. R. and R. A. Dwek (1999). "Glycoproteins: glycan presentation and protein-fold stability." Structure **7**(7): R155-160.

Xu, J., et al. (2010). "VHL inactivation induces HEF1 and Aurora kinase A." J Am Soc Nephrol **21**(12): 2041-2046.

Yagi, T., et al. (2009). "Identification of dyneins that localize exclusively to the proximal portion of Chlamydomonas flagella." J Cell Sci **122**(Pt 9): 1306-1314.

Yang, P., et al. (2004). "Flagellar radial spoke protein 2 is a calmodulin binding protein required for motility in Chlamydomonas reinhardtii." Eukaryot Cell **3**(1): 72-81.

Yoshimura, K. and R. Kamiya (2001). "The sensitivity of chlamydomonas photoreceptor is optimized for the frequency of cell body rotation." Plant Cell Physiol **42**(6): 665-672.

Yuan, S., et al. (2015). "Intraciliary calcium oscillations initiate vertebrate left-right asymmetry." Curr Biol **25**(5): 556-567.

Yuan, X., et al. (2015). "Function and regulation of primary cilia and intraflagellar transport proteins in the skeleton." Ann N Y Acad Sci **1335**: 78-99.

Yueh, Y. G. and R. C. Crain (1993). "Deflagellation of Chlamydomonas reinhardtii follows a rapid transitory accumulation of inositol 1,4,5-trisphosphate and requires Ca2+ entry." J Cell Biol **123**(4): 869-875.

Zaghloul, N. A. and N. Katsanis (2009). "Mechanistic insights into Bardet-Biedl syndrome, a model ciliopathy." J Clin Invest **119**(3): 428-437.

Zhang, Q., et al. (2013). "BBS7 is required for BBSome formation and its absence in mice results in Bardet-Biedl syndrome phenotypes and selective abnormalities in membrane protein trafficking." J Cell Sci **126**(Pt 11): 2372-2380.

Zhang, R., et al. (2014). "High-Throughput Genotyping of Green Algal Mutants Reveals Random Distribution of Mutagenic Insertion Sites and Endonucleolytic Cleavage of Transforming DNA." Plant Cell **26**(4): 1398-1409.